2012

MOLECULAR AND BIOCHEMICAL CHARACTERIZATION OF OLEATE- AND GLYCEROL-3-PHOSPHATE-REGULATED SIGNALING IN PLANTS

Mihir Kumar Mandal
University of Kentucky, mihir.biotech@gmail.com

STUDENT AGREEMENT:

I represent that my thesis or dissertation and abstract are my original work. Proper attribution has been given to all outside sources. I understand that I am solely responsible for obtaining any needed copyright permissions. I have obtained and attached hereto needed written permission statements(s) from the owner(s) of each third-party copyrighted matter to be included in my work, allowing electronic distribution (if such use is not permitted by the fair use doctrine).

I hereby grant to The University of Kentucky and its agents the non-exclusive license to archive and make accessible my work in whole or in part in all forms of media, now or hereafter known. I agree that the document mentioned above may be made available immediately for worldwide access unless a preapproved embargo applies.

I retain all other ownership rights to the copyright of my work. I also retain the right to use in future works (such as articles or books) all or part of my work. I understand that I am free to register the copyright to my work.

REVIEW, APPROVAL AND ACCEPTANCE

The document mentioned above has been reviewed and accepted by the student's advisor, on behalf of the advisory committee, and by the Director of Graduate Studies (DGS), on behalf of the program; we verify that this is the final, approved version of the student's dissertation including all changes required by the advisory committee. The undersigned agree to abide by the statements above.

Mihir Kumar Mandal, Student

Dr. Pradeep Kachroo, Major Professor

Dr. Lisa J Vaillancourt, Director of Graduate Studies

MOLECULAR AND BIOCHEMICAL CHARACTERIZATION OF OLEATE- AND GLYCEROL-3-PHOSPHATE-REGULATED SIGNALING IN PLANTS

DISSERTATION

A dissertation submitted in partial fulfillment of the requirements
for the degree of Doctor of Philosophy in the
College of Agriculture at the
University of Kentucky

By
MIHIR KUMAR MANDAL
Lexington, Kentucky

Director: Dr. Pradeep Kachroo, Associate Professor of Plant Pathology
Lexington, Kentucky
2012

ABSTRACT OF DISSERTATION

MOLECULAR AND BIOCHEMICAL CHARACTERIZATION OF OLEATE- AND GLYCEROL-3-PHOSPHATE-REGULATED SIGNALING IN PLANTS

Oleic acid (18:1), a monounsaturated fatty acid (FA), is synthesized upon desaturation of stearic acid (18:0) and this reaction is catalyzed by the plastidal enzyme stearoyl-acyl carrier protein-desaturase (SACPD). A mutation in the *SSI2*/*FAB2* encoded SACPD lowers 18:1 levels, which correlates with induction of various resistance (*R*) genes and increased resistance to pathogens. Genetic and molecular studies have identified several suppressors of *ssi2* which restore altered defense signaling either by normalizing 18:1 levels or by affecting function(s) of a downstream component. Characterization of one such *ssi2* suppressor mutant showed that it is required downstream of low 18:1-mediated constitutive signaling and partially restores altered defense signaling in the *ssi2* mutant. Molecular and genetic studies showed that the second site mutation was in the *Nitric Oxide Associated* (*NOA*) *1* gene, which is thought to participate in NO biosynthesis. Consistent with this result, *ssi2* plants accumulated high levels of NO and showed an altered transcriptional profile of NO-responsive genes. Interestingly, the partial defense phenotypes observed in *ssi2 noa1* plants were completely restored by an additional mutation in either of the two nitrate reductases *NIA1* or *NIA2*. This suggested that NOA1 and NIA proteins participated in NO biosynthesis in an additive manner. Biochemical studies showed that 18:1 physically bound NOA1, in turn leading to its degradation in a protease-dependent manner. In concurrence, overexpression of *NOA1* did not promote NO-derived defense signaling in wild-type plants unless 18:1 levels were lowered. Subcellular localization showed that NOA1 and the 18:1-synthesizing SSI2 were present in close proximity within the nucleoids of chloroplasts. Indeed, pathogen- or low 18:1-induced accumulation of NO was primarily detected in the chloroplasts and their

nucleoids. Together, these data suggested that 18:1 levels regulate NO synthesis and thereby NO-mediated retrograde signaling between the nucleoids and the nucleus.

Since cellular pools of glycerol-3-phosphate (G3P) regulate 18:1 levels, I next analyzed the relationship between G3P and 18:1. Interestingly, unlike 18:1, an increased G3P pool was associated with enhanced systemic immunity in Arabidopsis. This was consistent with G3P-mediated transcriptional reprogramming in the distal tissues. To determine mechanism(s) underlying G3P-conferred systemic immunity, I analyzed the interaction between G3P and a lipid transfer protein (LTP), DIR1. In addition, I monitored localization of DIR1 in both Arabidopsis as well as tobacco. Contrary to its predicted apoplastic localization, DIR1 localized to endoplasmic reticulum and plasmodesmata. The symplastic localization of DIR1 was confirmed using several different assays, including co-localization with plasmodesmatal-localizing protein, plasmolysis and protoplast-based assays. Translocation assays showed that G3P increased DIR1 levels and translocated DIR1 to distal tissues. Together, these results showed that G3P and DIR1 are present in the symplast and their coordinated transport into distal tissues is likely essential for systemic immunity.

In conclusion, this work showed that low 18:1-mediated signaling is mediated via NO, synthesis of which is likely initiated in the plastidal nucleoids. In addition, my work shows that G3P functions as an independent signal during systemic signaling by mediating translocation of the lipid transfer protein, DIR1.

Key words: Oleic acid, Glycerol 3 phosphate, Nitric oxide, Nucleoid, Lipid transfer protein.

MIHIR KUMAR MANDAL
March 15, 2012

MOLECULAR AND BIOCHEMICAL CHARACTERIZATION OF OLEATE- AND GLYCEROL-3-PHOSPHATE-REGULATED SIGNALING IN PLANTS

By

MIHIR KUMAR MANDAL

Pradeep Kachroo

Director of Dissertation

Lisa J Vaillancourt

Director of Graduate Studies

March 15, 2012

Date

ACKNOWLEDGEMENTS

First of all I would like to express my deep sense of gratitude and indebtedness to my major advisor Dr. Pradeep Kachroo for his illuminating guidance, constant encouragement, active support and valuable suggestions throughout the course of my research program, helping me understand the subject and in successful completion of my thesis. I would also like to appreciate him for providing me an opportunity to work in his lab and providing me the best platform for a successful career ahead. My deepest gratitude is due to Dr. Aardra Kachroo for her valuable suggestions and ideas for the successful accomplishment of my thesis. Her critical thinking helped me in designing experiments for which I will always remain indebted to her. Words fail to express my heartfelt gratitude to Dr. Ludmila Lapchyk for her untiring help, support and inspiration throughout my PhD. My sincere thanks to Drs. Keshun Yu, Chandra-Shekara, Srivathsa Venugopal, Rae-Dong Jeong, Shifeng Zhu, Devarshi Selote, Mr. Qing-Ming Gao and Ms. Bidisha Chanda for their valuable help during my research. I would like to provide my sincere thanks to Ms. Amy Crume for maintaining our plant growth facility and green house plants. I would also like to thank Mr. John Johnson for analyzing our fatty acid samples. I would like to acknowledge the cooperation extended by the previous and present members of Dr. Kachroo's lab and for creating a friendly atmosphere in the lab. My sincere thanks to Ester and Maria for useful scientific discussions and Sladna for helping me with the thesis formatting.

I would like to express my sincere thanks to all my committee members, Drs. David Smith, Mark Farman, David Hildebrand and Aardra Kachroo for their valuable suggestions during the committee meetings. I would like to thank Drs. David Smith and Lisa Vaillancourt for updating me about various academic fellowships and job vacancies.

I would like to thank Dr. Duroy Navarre for salicylic acid analysis, Dr. Michael Goodin for pSITE vectors, RFP-ER, RFP-H2B plants, Dr. Lynnette Dirk for her valuable suggestions in NOA1 and DIR1 protein expression and allowing me to use the Fast Protein Liquid Chromatography (FPLC) system, Dr. Nigel Crawford for *noa1* seeds, Dr. Zach Adam for anti-ClpP and-ClpC antibodies, Dr. Brain Crane for GsYqeH clone and Arabidopsis Biological Resource Center (ABRC) for *nia1* and *nia2* seeds. I would like to

thank Dr. Marciel Stadnik for help with NO estimations, Dr. Arnold Stromberg, Dr. Matthew Hersh and Yanling Hu for statistical analysis. I would also like to thank UK Microarray Core Facility for final processing and providing the raw data of microarray samples, Advanced Genetic Technologies Center (AGTC) for sequencing.

I am very grateful to Dr. Daniel Klessig, Boyce Thompson Institute for plant research for agreeing as an external examiner and taking out his valuable time for my defense seminar. I would like to thank my previous advisors Dr. Anil Kumar and Dr. Subhra Chakraborty for infusing and introducing me into the field of molecular biology and host-pathogen biology.

Finally, I would like to thank the Department of Plant Pathology and all the Faculty and staff members for timely help during my research work.

TABLE OF CONTENTS

LIST OF TABLES

LIST OF FIGURES

CHAPTER 1

INTRODUCTION

Plants activate defense against pathogens by eliciting a response against pathogen-encoded factors. These involve immunity against pathogen- or microbe-associated molecular patterns (PAMPs or MAMPs; also known as basal resistance or pathogen-triggered immunity) or direct/indirect recognition of pathogen-encoded effector protein(s) by the host encoded resistance (R) protein [also known as effector-triggered immunity (ETI)] (Boller et al. 2009; Clay et al. 2009). The R proteins have been classified into five classes based on their structure. The R proteins containing nucleotide-binding site (NBS) and leucine-rich repeat (LRR) domains represent one of the major categories of R proteins (Martin et al. 2003; Kachroo et al. 2009). In most cases R proteins do not interact directly with their cognate avirulence (avr) proteins but, rather, each guards a host protein, which is targeted by the avr protein. In this "guard model", resistance signaling is initiated in response to avr-mediated changes to the guardee protein (Van der Biezen et al. 1998; Axtell et al. 2003; Kim et al. 2005). For example, R proteins RPM1 and RPS2 guard RIN4 and are activated upon avr-mediated phosphorylation or proteolysis of RIN4, respectively (Axtell and Staskawicz. 2003; Mackey et. al. 2003).

R protein-mediated activation of defense often involves one or more phytohormones including salicylic acid (SA), a phenolic derived from the Shikimate pathway (Kachroo et al. 2009, Shah et al. 1999). The key enzymes involved in SA biosynthesis include chloroplast-localized isochorismate synthase (encoded by *SID2*), which catalyzes the conversion of chorismate to isochorismate (Wildermuth et al. 2001). A mutation in *sid2* compromises SA biosynthesis and impairs defense against pathogens (Wildermuth et al. 2001; Nawrath et al. 1999; Dempsey et al. 1999; Dong et al. 2001). The *sid2* mutation also compromises systemic acquired resistance (SAR), a form of broad-spectrum defense induced in the uninoculated parts of the plant in response to local infections. Mutation in other genes, including *EDS1* (*Enhanced Disease Susceptibility 1*), *PAD4* (*Phytoalexin*

Deficient 4) and *EDS5* also compromise SA levels and/or signaling and thereby compromise defense against pathogens. Interestingly, SA and EDS1 function redundantly and mutations in both are required to compromise certain R-mediated pathways (Venugopal et al. 2009). Furthermore, SA and EDS1 also act redundantly downstream of the oleate (18:1)-regulated pathway (Venugopal et al. 2009), suggesting a role for fatty acid(s) (FA) in plant defense.

In plants *de novo* fatty acid biosynthesis takes place in chloroplasts and leads to the synthesis of palmitic acid (16:0), which is elongated to stearic acid (18:0) (Kachroo and Kachroo 2009). Stearoyl-ACP desaturase (SACPD), which catalyzes the desaturation of stearic acid (18:0) to oleic acid (18:1), is one of the important soluble chloroplastic enzymes that regulates the generation of mono-unsaturated FA in plant cells (Shanklin and Cahoon 1998; Kachroo et al. 2007). The Arabidopsis genome contains seven isoforms of SACPD (Kachroo et al. 2007) and a mutation in the *SSI2*-encoded SACPD results in the constitutive activation of defense responses (Chandra-Shekara et al. 2007; Kachroo et al. 2001, 2003a, 2003b; 2004, 2005, 2007; Venugopal et al. 2009; Xia et al. 2009), which is not compensated by endogenous expression of the other isoforms. A reduction in 18:1 levels causes induction of *R* genes and results in increased resistance to pathogens (Chandra-Shekara et al. 2007; Kachroo et al. 2001, 2003a, 2003b; 2004, 2005, 2007; Venugopal et al. 2009; Xia et al. 2009). Genetic and molecular studies have identified several factors that can normalize 18:1 levels, thereby restoring *R* gene-mediated signaling (Kachroo et al. 2004; Venugopal et al. 2009; Xia et al. 2009). A mutation in *GLY1*-encoded glycerol-3-phosphate (G3P) dehydrogenase (G3Pdh) restores the low 18:1-mediated signaling (Kachroo et al. 2004) by reducing the G3P pool which in turn increases endogenous 18:1 levels (Fig. 1). G3P is a precursor for the biosynthesis of glycerolipids and can also be synthesized via phosphorylation of glycerol (Kachroo et al. 2009). G3P also modulates defense independent of its effect on 18:1. For example, G3P levels modulate basal resistance to the hemibiotrophic fungal pathogen *Colletotrichum higginsianum* (Chanda et al. 2008).

Objectives:

Previous studies showed that a decrease in chloroplastic 18:1 levels regulates expression of *R* genes via an unknown mechanism. It was hypothesized that a reduction in 18:1 levels induced the formation/accumulation of an intermediate signaling component(s) that directly or indirectly triggered the expression of nuclear *R* genes. In this study, I demonstrate that nitric oxide likely acts as one of the downstream components required for low 18:1-mediated induction of *R* genes. In addition, I characterized relationship between 18:1 and G3P by analyzing their roles in SAR. The objectives of my work were:

i) Molecular, genetic and biochemical analysis of *ssi2* suppressor mutant compromised in low 18:1-mediated signaling

ii) Role of G3P in systemic acquired resistance

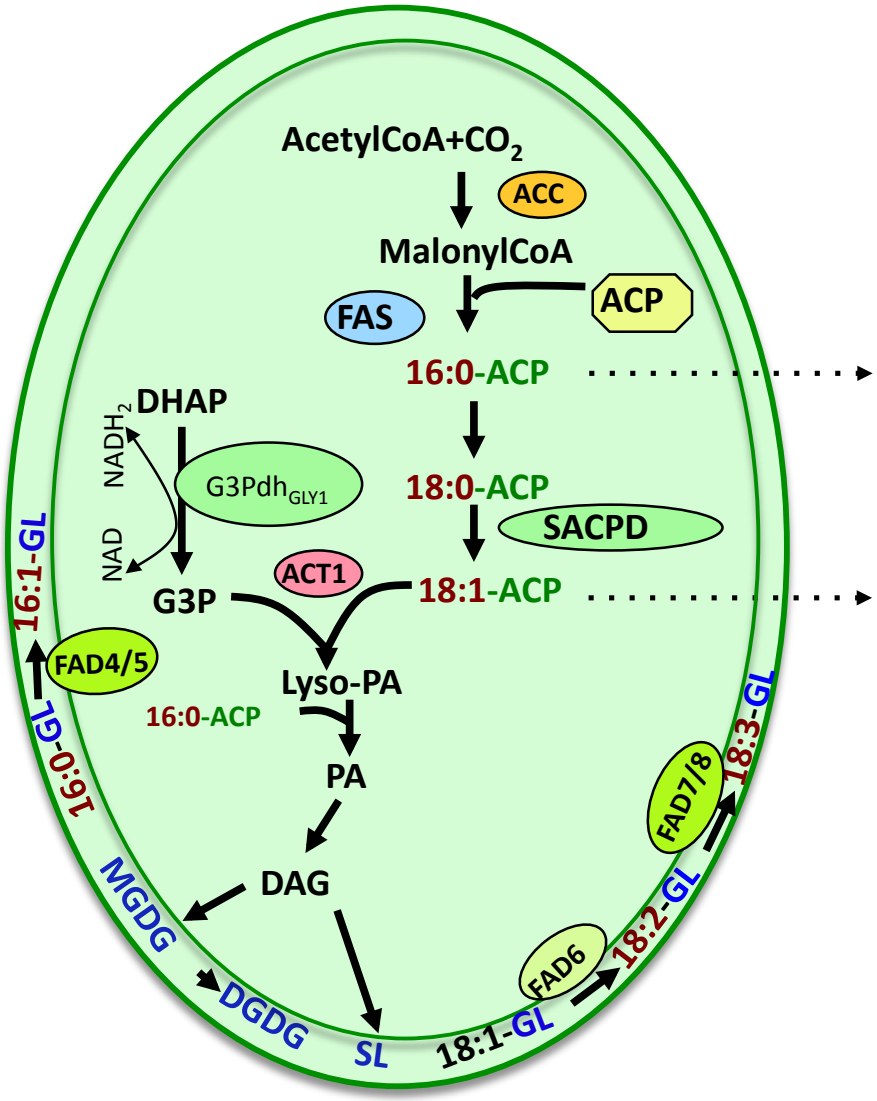

Figure 1. A condensed scheme of plastid fatty acid biosynthesis in plants. The acylation of G3P is catalyzed by the ACT1-encoded G3P acyltransferase. Abbreviations used are: ACC, AcetylCoA carboxylase; ACP, Acyl carrier protein; PA, phosphatidic acid; PG, phosphatidylglycerol; MGDG, monogalactosyldiacylglycerol; DGDG, digalactosyldiacylglycerol; SL, sulfolipid; DAG, diacylglycerol, FAD, fatty acid desaturase; GK, glycerolipid, G3Pdh, glycerophosphate dehydrogenase; Dotted line indicates export of thesefatty acids. (Kachroo et al. 2009).

CHAPTER 2

MATERIALS AND METHODS

Plant growth conditions and genetic analysis

The seeds were sown on steam-sterilized soil and subjected to overnight cold treatment to achieve synchronized germination. The seedlings were transplanted after germination and covered with transparent plastic domes for 2-3 days and placed in MTPS 144 (Conviron, Winnigen, MN, Canada) walk-in chambers at 22^{o}C, 65% relative humidity and 14 h photoperiod. These chambers were equipped with cool white fluorescent bulbs (Sylvania, F096/841/ XP / ECO). The photon flux density (PFD) of the day period was 106.9 μmoles m^{-2} s^{-1} (measured using a digital light meter, Phytotronic Inc, MO). Genotypes used in this study are listed in Table 2.1. Crosses were performed by pollinating emasculated flowers of recipient plants with pollen from donor plants. The wild-type and mutant alleles were identified by PCR, cleaved amplified polymorphic sequence (CAPS) (Konieczny and Ausubel, 1993), derived (d)- CAPS (Neff et al. 1998) analysis and/ or based on the fatty acid (FA) profile. The primers used for this screen are listed in Table 2.2.

Arabidopsis transformation

A single colony of *Agrobacterium tumefaciens* was grown overnight in 5mL LB at 29 ^{o}C. Next day, this suspension was inoculated into 500 mL LB and bacteria were cultured overnight at 29 ^{o}C . The culture was centrifuged for 10 min at 5,000 rpm to pellet the cells. The pellet was washed with water and dissolved in transformation solution (1 litre contained 2.15 g Murashige and Skoog [MS] basal salt mixture, 30 g sucrose (3%), 0.5 mL of Silwett –77, and the solution was adjusted to pH 5.7 with 1 M KOH). The transformation solution was dispensed into square containers and plants were immersed (pot upside-down) into the transformation solution. Two pots/container were placed inside a dessicator and infiltrated under vacuum. After 4 min infiltration, the pots were removed and plants were rinsed gently under tap water. The treated plants were placed under a dome for 12- 24 h, after which the plants were allowed to set seeds.

The seeds from transformed plants were collected after ~4-6 weeks, surface-sterilized with 70% ethanol for 1 min, washed with 5% bleach for ~20-30 min in a rotary shaker and finally washed 2-3 times with sterile water. The transgenic plants were screened by plating seeds on the Murashige and Skoog media (MS) medium containing appropriate antibiotic or on soil sprayed with herbicide 1.19% BASTA (4-(hydroxyl (methyl) phosphonoyl) butanoic acid.

Bacterial transformation

Escherichia coli transformation was carried out using heat shock and/or electroporation methods. For heat-shock, a single isolated colony of DH5α strain (Invitrogen) was grown overnight in 5 mL LB broth at 37^{o}C. A 1% inoculum from this was transferred into 100 mL LB broth, grown to an OD of 0.5 (A_{600}) and chilled on ice for 15 min. The cells were centrifuged at 3,000 rpm for 10 min at 4^{o}C, and the pellet was suspended in 50 mL ice-cold transformation buffer 1 [Tfb1] containing 30 mM Potassium acetate [CH3CO2K] pH 5.8, 100 mM $RbCl_2$, 10 mM $CaCl_2$ and 15% glycerol. After a 30 min incubation on ice, cells were again centrifuged at 3,000 rpm for 10 min and the pellet was resuspended in 5 mL of ice-cold transformation buffer 2 [Tfb II] (10 mM MOPS pH 6.5, 75 mM $CaCl_2$ 10 mM $RbCl_2$, 15% glycerol). After a 15 min incubation on ice, these cells were dispensed as 100 μL aliquots in 1.5 mL microfuge tubes and stored at -80^{o}C till further use. For transformation, ~50-100 ng of DNA was mixed with 100 μL of competent cells, incubated on ice for 30 min, followed by heat shock at 42^{o}C for 90 Sec. The cells were chilled on ice for 5 min, mixed with 1 mL of LB broth and incubated at 37^{o}C for 30 min.

For electroporation, a single isolated colony of DH5α, or *Agrobacterium* strains MP90, and LBA4404 were grown overnight in 5 mL LB at 37^{o}C or 29^{o}C, respectively. A 1% inoculum from each overnight-grown culture was transferred into 100 mL LB broth, grown to an OD of 0.5 (A_{600}) and chilled on ice for 15 min. The cells were centrifuged at 3,000 rpm for 10 min at 4^{o}C, and the pellet was suspended in ice-cold solution of 8.0% glycerol. After a 15 min incubation on ice, these cells were dispensed as 20 μL aliquots in 1.5 mL microfuge tubes and stored at -80^{o}C till further use. For transformation ~50-100 ng of DNA was mixed with 20 μL of competent cells, placed in a pre-chilled cuvet

and electroporated using 25 μ F capacitance, 200 Ω resistance and 2 volts pulse. The electroporated cells were mixed with 1 mL of LB broth and incubated at 37°C or 29°C for 30 min. The transformed cells were plated on LB-agar plates containing appropriate antibiotic and incubated overnight at 37°C (*Escherichia coli*) or 29°C (*Agrobacterium*).

Sequencing

The sequencing reaction was carried out in 10 μL total volume containing 50-100 ng of PCR- or gel- purified-DNA (Qiagen, CA-USA), 1 μL of 5 μM primer and 0.5 μL of BigDye Terminator V3.1 (Applied Biosystems, CA-USA). The reaction product was precipitated, washed with 70% alcohol and air-dried before submitting the Advanced Genetic Technologies Center (AGTC) sequencing facility, University of Kentucky.

Complementation and overexpression

For complementation of *ssi2 noa1*, a SalI-KpnI-linkered genomic fragment spanning the *NOA1* promoter, open reading frame and terminator was amplified from the Col-0 plants and cloned into pCAMBIA-2301 binary vector. After confirmation of the DNA sequence, the binary vector was transformed into *ssi2 noa1* plants using the floral dip method. The transgenic plants were selected on MS plates containing hygromycin.

For overexpression, a XhoI-XbaI-linkered cDNA was amplified from the Col-0 plants and cloned downstream of the 35S-CaMV promoter in pRTL-GUS. After confirmation of the DNA sequence, the HindIII fragment from this recombinant vector was transferred to pBAR1. For NOA1-HIS overexpression, a HIS tag was added at the C-terminal end and the PCR fragment was cloned into the pSITE vector using Gateway technology (Invitrogen, CA-USA).

For overexpression of DIR1, full-length, PCR-amplified cDNA from DIR1 was cloned into the pSITE vector containing a GFP tag. The construct was introduced into *Agrobacterium tumefaciens* MP90 by electroporation and transformed into *Arabidopsis thaliana* wild-type Col-0 plants using the floral dip method. The transgenic plants were

selected on MS plates containing Kanamycin antibiotic. The overexpressed transgenic plants were confirmed by Kanamycin and specific primers listed in Table 2.2.

Chemical and hormone treatments

Glycerol, Glycerol-3-Phosphate, Salicylic acid analog [BTH, Benzothiadiazole] and Nitric oxide donor [SNP, Sodium Nitro Prusside] treatments

Three-four-week-old plants were treated with glycerol (50 mM; VWR or Invitrogen CA-USA), G3P (25 or 50 mM; Sigma, St. Louis, MO-USA), SA (500 μM; Sigma, St. Louis, MO-USA) and BTH (100 μM; CIBA-GEIGY Ltd), SNP (100-1000 μM; Sigma, St. Louis, MO-USA) were prepared in water. Applications were carried out using spray and soil drenching (BTH), spray (glycerol, SNP) and injection of G3P.

Trypan-blue staining

The leaves were vacuum-infiltrated with trypan-blue stain prepared in 10 mL acidic phenol, 10 mL glycerol, and 20 mL sterile water with 10 mg of trypan blue. The samples were placed in a heated water bath (90^{o}C) for 2 min and incubated at room temperature for 2-12 h. The samples were destained using chloral hydrate (25 g/10 mL sterile water; Sigma, St. Louis, MO-USA), mounted on slides and observed for cell death under a compound microscope. The samples were photographed using AxioCam camera (Zeiss, Germany) and images were analyzed using Openlab 3.5.2 (Improvision) software.

Pathogen infection

Pseudomonas syringae Pv. *tomato*:

Inoculations of *Pseudomonas syringae* DC 3000 or *avrRpt2/avrRps4* were conducted as described before (Kachroo et al., 2005). A single bacterial colony was grown overnight in 10 mL King's B medium containing antibiotics rifampicin and kanamycin (Sigma, St. Louis, MO-USA) at 29^{o}C (for 1 liter broth, 20 g Peptone, 10 mL Glycerol, 1.5 g K_2HPO_4, 1.5 g $MgSO_4.7H_20$, P^H=7.5; for plate, 15 g agarose was added). The bacterial cells were harvested by centrifugating at 3,000 rpm for 10 min, then washed and suspended in 10 mM $MgCl_2$ twice. The cell density was quantifed using a spectrophotometer (A_{600}) and the cells were diluted to a final density of 10^5 to 10^7/mL. The bacterial suspension was

injected into the abaxial surface of the leaf using a needle-less syringe. Three leaf discs from the inoculated leaves were taken at 0 and 3 days post inoculation (dpi). The leaf discs were ground and homogenized in 10 mM $MgCl_2$, diluted 10^3 or 10^4 fold and plated on King's B plates. The plates were kept at 29^{o}C for 2 days and the colonies were counted using a colony counter.

NOA1 expression and purification

NOA1 cDNA lacking the N-terminal 37 and 101 amino acids were amplified as a NheI-XhoI- linkered fragment from Col-0 and cloned into the pET28a vector. The primers used for PCR are listed in Table S2. NOA1-HIS protein was purified using an HiTrap Chelating HP column (GE Healthcare, PA-USA) on a FPLC system. The purified protein was dialyzed using 25 mM Tris-HCl buffer and quantified using Bradford reagent (Bio-RAD, CA-USA).

Protein extraction, immunoblot analysis, antibody generation

Proteins were extracted in buffer containing 50mM Tris-HCl, pH7.5, 10% glycerol, 150mM NaCl, 10mM MgCl2, 5mM EDTA, 5 mM DTT, and 1 X protease inhibitor cocktail (Sigma-Aldrich, St. Louis, MO-USA). Protein concentration was measured by the Bio-RAD protein assay (Bio-Rad, CA-USA).

For Ponceau-S staining, PVDF membranes were incubated 1 in Ponceau-S solution (40% methanol [v/v], 15% acetic acid [v/v], 0.25% Ponceau-S). The membranes were destained using deionized water. Proteins (30-50 μg) were fractionated on a 7-10% SDS-PAGE gel and subjected to immunoblot analysis using ∝-NOA1, ∝-HIS or ∝-GFP (Sigma-Aldrich, St. Louis, MO-USA) antibody. Immunoblots were developed using ECL detection kit (Roche) or alkaline phosphatase-based color detection. Rabbit anti-NOA1 polyclonal antibodies were generated against $NOA1^{\Delta 37}$ protein (Cocalico Biologicals, PA-USA).

Expression of DIR1 protein and purification

DIR1 cDNA lacking the region corresponding to the N-terminal 25 amino acids was amplified as a NdeI-XhoI linkered fragment from Col-0 and cloned into the pET28

vector. The primers used for PCR are listed in Table 2.2. The protein was purified using a HiTrap Chelating HP column (GE Healthcare, PA) on a FPLC system. The purified protein was dialyzed using 25 mM Tris-HCl buffer and quantified using Bradford reagent (Bio-RAD, CA).

GTPase assay

For GTPase assay, 10 μM protein was incubated with 50-100 μM GTP, 50 mM Tris-HCl pH 7.5, 2 mM $MgCl_2$, 150 mM NaCl, 10% glycerol, and 2 mM dithiothreitol at 37 °C overnight. Samples were boiled for 5 min to stop the reaction, centrifuged and the supernatant was analyzed by reverse phase high performance liquid chromatography (HPLC) using a C_{18} 5 μm (4.6 × 250-mm) column (Dionex Inc., IL). Nucleotides were separated under isocratic conditions at 1 ml/min of 100 mM potassium di-hydrogen phosphate [KH_2PO_4], pH 6.5, 10 mM tetrabutylammonium bromide, 0.2 mM sodium azide [NaN_3], and 7.5% acetonitrile.

Binding assays

Binding assays were carried out as described earlier (Rasmussen et al., 1990). Briefly, 1-8 μM of ^{14}C 18:1 (specific activity 58.2 Ci/mmol; Perkin Elmer Inc.) was incubated at 37°C with 1-20 μM of NOA1 protein in a 200 μl reaction volume containing 10 mM-potassium phosphate buffer pH 7.4. After 1 h the reaction was placed on ice for 15 min, mixed with 400 ml of ice-cold Lipidex-1000 and incubated on ice for 20 min. The reaction was centrifuged at 10,000 g for 5 minutes at 4°C and the radiolabel in the supernatant was measured using a scintillation counter.

Oleate agarose affinity chromatography

Oleic acid sepharose was kindly provided by Dr. Shifeng Zhu. Oleic acid (Sigma-Aldrich) was coupled to EAH-Sepharose (GE Healthcare, PA) using 1-ethyl-3-(3-dimethylaminopropyl)-carbodiimide (Fisher Scientific) as described earlier (Kim et al.,

2005; Peters et al., 1973). Briefly, 18:1 was coupled by stirring the EAH-Sepharose in 1.5 volumes of 0.1 M sodium oleate at pH 10 in presence of the 1-ethyl- 3-(3-dimethylaminopropyl)-carbodiimide (50 mg/ ml of Sepharose) for 3 days at 37^{o}C. The matrix was washed extensively at 37^{o}C with 50% (v/v) ethanol followed by washes with 100% ethanol, 0.075 M sodium phosphate (1:1) pH 2.4, and finally with ethanol-0.05N sodium hydroxide [NaOH] (1:1). Unreacted amino groups were blocked by acetylation with acetic anhydride at pH 7.0 at 0^{o}C for 1 h. Oleic acid coupling was verified by carrying out binding assays with 18:1 binding protein, bovine serum albumin. Mock-Sepharose was prepared from EAH-Sepharose by blocking ligand with 1 M acetic acid.

Chloroplast and nucleoid purifications

For chloroplast isolation, leaves from wt and mutant plants were harvested at the end of the night period. Five grams fresh weight of leaves were homogenized and the chloroplasts were isolated as described earlier (Aronsson et al. 2002).

Nucleoid isolation from chloroplasts was carried out as described earlier (Jeong et al., 2003). Briefly, intact chloroplasts from 20 g of leaves were pelleted and resuspended in 30 ml of nucleoid extraction buffer containing 17% (w/v) sucrose, 20 mM Tris-HCl, 0.5 mM EDTA, 1.2 mM spermidine, 7 mM 2-mercaptoethanol, and 1x protease-inhibitor cocktail. A 1/20 volume of 20% (v/v) Nonidet P-40 was added and stirred at 4°C for 30 min. The solution was centrifuged for 10 min at 3,000 g at 4°C and the supernatant was re-centrifuged at 48,000 g for 40 min at 4°C. The pellet was washed twice with nucleoid extraction buffer and resuspended in 100 µl of nucleoid extraction buffer.

NO staining and quantification

For NO staining, the adaxial sides of leaves were infiltrated with 4 µM 4-amino-5-methylamino-2′,7′-difluorofluorescein diacetate (DAF-FM DA) and, after 5 min incubation in dark, leaves were observed under an Olympus FV1000 laser-scanning confocal microscope using 488 nm laser. For nucleoid staining, nucleoids were incubated in 1 µM DAF-FM DA for 5 min prior to confocal microscopy. For NO quantification, ~300 mg of leaf tissue was homogenized in 50 mM phosphate buffer pH 7.0 in the dark.

The supernatant was incubated with DAF-FM DA for 30 min with constant shaking and the fluorescence was measured at 495 and 515 nm using a fluorimeter (Molecular Devices, CA-USA). NO quantification using the Greiss method was carried out using reagents assay system from Promega (WI). Briefly, ~300 mg of leaf tissue was homogenized in 50 mM phosphate buffer pH 7.0 in dark. The supernatant was incubated with sulfanilamide solution for 10 minute in the dark. To this 50 μL of the N-(1-Naphthyl) ethylendiamine dihydrochloride solution was added followed by another 10 min incubation in the dark. The absorbance was measured at 520 nm using a DTX 880, multimode detector (Beckman Coulter).

DNA extraction

DNA extraction was usually carried out from leaves harvested from 3-4-weeks-old Arabidopsis plants. Each leaf sample was frozen in liquid nitrogen and ground using disposable pestle (Fisher Scientific, USA). The extract was suspended in 150 μL of DNA extraction buffer containing 200 mM Tris, 25 mM EDTA, 1% SDS and 250 mM NaCl. The homogenate was extracted with 100 μL of phenol: chloroform: isoamyl alcohol (25:24:1), centrifuged for 10 min at 12,000 rpm at room temperature and the supernatant was precipitated with 100 μL of isopropanol. Samples were centrifuged immediately for 10 min at 12,000 rpm at room temperature and the DNA pellet was air dried and suspended in 50-75 μL Tris:EDTA (10:1, pH 8.0) or sterile water.

RNA extraction, reverse transcriptase-polymerase chain reaction and northern analysis

The total RNA was extracted using Trizol reagent (Invitrogen CA-USA). Two or three Arabidopsis leaves were frozen in liquid nitrogen, ground using disposable pestles and suspended in 1,000 μL of Trizol. To this, 200 μL of chloroform was added and the samples were centrifuged at 12000 rpm at room temperature for 15 min. The supernatant was precipitated with 0.5 mL of isopropanol. The RNA precipitate was washed with 75% alcohol, air-dried and suspended in 15-20 μL of DEPC-treated water. The RNA was quantified spectrophotometrically (A_{260}) and ~7 μg of total RNA was electrophoresed on 1.5% agarose gel containing 3% formaldehyde and 1X MOPS. MOPS buffer was

prepared by mixing 4.18 g MOPS, 680 mg NaOAc, 37 mg EDTA in 1 L sterile water and adjusted to pH 7.0. Before loading, RNA was mixed with 39 μg/mL ethidium bromide, 0.39 X MOPS, 13.7% formaldehyde and 39% formamide, denatured at 65^{o}C for 15 min, chilled on ice for 15 min and mixed with 2μL of RNA loading dye (50% glycerol, 1mM EDTA, 0.4% bromophenol blue and 0.4% xylene cyanol).

For cDNA synthesis, ~5-7μg of RNA was denatured at 65^{o}C and annealed with oligo dT_{17}. The reaction mixture was supplemented with 1 μL reverse transcriptase (200U/μL), 1 μL RNAase inhibitor (40U/μL), 0.5 mM dNTPs and 10 mM DTT and incubated at 42^{o}C for 1 h. The reaction was stopped by incubating the tubes at 65^{o}C for 15 min and subsequently used for RT-PCR.

For northern analysis, RNA was transferred onto Hybond^{TM}-NX (Amersham Biosciences, NJ-USA) nylon membrane. After overnight wet-transfer, RNA was fixed under UV for 0.9 min in a CL-1000 ultraviolet Cross-linker. The membrane was washed in 2xSSC, dried at 65^{o}C and used for hybridization. The membrane was hybridized in sodium phosphate buffer (pH 7.0) containing sheared salmon sperm DNA (100 μg/mL), 7% SDS and 1.25 mM EDTA.

Real-time Quantitative PCR

Real-time quantitative PCR (RT-qPCR) was carried out using the Power SYBR® Green PCR Master Mix (2x) reagent kit (Applied Biosystems, CA-USA) in 96-well PCR plates on a Fast Real-Time PCR system PRISM 7900HT instrument (Applied Biosystems, CA-USA) with cycling conditions 95°C for 10 min, followed by 40 cycles of 95°C for 15 sec, 60°C for 1 min, and finally a dissociation stage with temperature regime of 95°C for 15 sec, 60°C for 15 sec, and 95°C for 15 sec. The primers were supplied and designed using IDT (Integrated DNA Tech., IA). The primer design parameters were according to real-time PCR conditions. The optimum settings of primer size were set to 24 nt, primer Tm 60 °C, primer GC % of 50 %, product size 100-200 bp. The cDNA (5 μl) was then used in a 20-μl reaction containing 10 μl SYBR® Green PCR Master Mix (2x) and 0.2

μM each of forward and reverse primers. Each sample was run in triplicate on a plate for obtaining standard curves, and as triplicates for relative quantification of the transcript. Levels of target gene and the endogenous control gene (*Actin*) were analyzed on the same plate to avoid plate-to-plate variations. Ct (cycle threshold) values were automatically calculated by the SDS 2.3 software (PRISM 7900HT), and the default baseline setting (cycles 3-15) was used. Expression of all tested genes was calculated with the relative comparative Ct method (Δ ΔCt = normalized Ct as ΔCt – calibrator, where ΔCt = Ct of *target gene* – Ct of *Actin*, and calibrator = median of ΔCt), using *Actin* as the reference gene for normalization. The relative level of gene expression was then converted into fold-difference relative to the calibrator as $2^{-\Delta\Delta Ct}$.

Synthesis of probe and hybridization

DNA fragments were labeled using DNA polymerase I Klenow fragment. DNA fragments used for labeling were PCR- or gel-purified (Qiagen, MD-USA), denatured and mixed with Klenow enzyme (NEB, 2,000U/mL), hexanucleotide primers, dATP, dGTP, dTTP, BSA and 25 μCi α-^{32}P-dCTP (Perkin Elmer, USA). The reaction was incubated at 37^{o}C for 1 h and the reaction probe was purified using a MicroSpin G-50 sephadex column (GE Healthcare, NJ-USA). The labeled DNA was denatured using one-tenth volume of 2N NaOH, neutralized with 1M Tris pH 7.5 and added to the hybridization buffer. Hybridization was routinely carried out overnight. The hybridized membrane was washed once at room temperature with 2xSSC, 0.5% SDS, twice at 65^{o}C with 2xSSC, 0.5% SDS and once at 65^{o}C with 1xSSC, 0.1%SDS solutions. The membrane was exposed using a Storage Phosphor Screen (Amersham Biosciences, CA-USA) and scanned on a Typhoon 9400 Variable Mode Imager (GE Healthcare, NJ-USA). The signal intensity was quantified using ImageQuant TL V2005 software.

Transcriptional Profiling

Total RNA was isolated from four-week-old plants using TRIZOL as outlined above. The experiment was carried out in triplicate and a separate group of plants was used for each set. RNA was processed and hybridized to the Affymetric Arabidopsis ATH1 genome array GeneChip following the manufacturer's instructions

(http://www.affymetrix.com/Auth/support/downloads/manuals/expression_analysis_technical_manual.pdf). All probe sets on the Genechips were assigned hybridization signal above background using Affymetrix Expression Console Software v1.0 (http://www.affymetrix.com/Auth/support/downloads/manuals/expression_console_userguide.pdf). Data were analyzed by one-way Anova followed by post hoc two sample t-tests. The P values were calculated individually and in pair-wise combination for each probe set.

Confocal microscopy

For confocal imaging, samples were scanned on an Olympus FV1000 microscope (Olympus America, Melville, NY). GFP, CFP and RFP was excited using 488, 440, and 543 nm laser lines, respectively. The various constructs were transformed to *A. tumefaciens* strain LBA4404. Agrobacterium strains carrying various proteins were infiltrated into *Nicotiana. benthamiana* plants expressing RFP- or CFP-tagged nuclear protein H2B, RFP-ER or wild-type *Nicotiana benthamiana* plants (Martin et al., 2009). After 48 h, water-mounted sections of leaf tissue were examined by confocal microscopy using a water immersion PLAPO60XWLSM 2 (NA 1.0) objective on a FV1000 point-scanning/point-detection laser scanning confocal 3 microscope (Olympus) equipped with lasers spanning the spectral range of 405–633 nm. RFP, CFP and GFP overlay images (40X magnification) were acquired at a scan rate of 10 ms/pixel. For nucleoid staining, leaves were infiltrated with 1 mg/ml solution of 4, 6-diamidino-2-phenylindole (DAPI) ~5 min prior to microscopy. Isolated nucleoids were stained with 0.5mg/ml solution of DAPI. Olympus FLUOVIEW 1.5 was used to control the microscope, image acquisition and the export of TIFF files.

Fatty acid profiling

FA extraction was carried out by placing leaf tissue in 2 ml of 3% H_2SO_4 in methanol containing 0.001% butylated hydroxytoluene (BHT). After 30 min incubation at 80^{o}C, 1 ml of hexane with 0.001% BHT was added. The hexane phase was then transferred to vials for gas chromatography (GC). One-microliter samples were analyzed by GC on a Varian FAME 0.25 mm x 50 m column and quantified with flame ionization detection.

For quantification of FAs, leaves (~50 mg) were extracted together with the 17:0 FA internal standard and the relative levels were calculated based on flame ionization detector peak areas. The identities of the peaks were determined by comparing the retention time with known FA standards. Mole values were calculated by dividing peak area by molecular weight of the FA.

Lipid profiling

For lipid extraction, six to eight leaves were incubated at 75^{o}C in isopropanol containing 0.001% BHT for ~15 min. To this, 1.5 ml chloroform and 0.6 ml water was added and the samples were agitated at room temperature for 1h. The lipids were re-extracted in chloroform: methanol (2:1, v/v) until the leaves were bleached. The aqueous content was removed by partitioning with 1M KCl and water. The lipid extract was dried under a gentle stream of nitrogen gas and re-dissolved in 0.5 ml of chloroform. Lipid analysis and acyl group identification was carried out using the Automated Electrospray Ionization-tandem Mass Spectrometry facility at Kansas Lipidomics Research Center.

Extraction and quantification of salicylic acid and SA glucoside (SAG)

SA and SAG were extracted from ~300 mg of leaves using anisic acid as internal standard. Samples were analyzed on an Agilent 1100 (Agilent Technologies, Palo Alto, CA-USA) with diode-array detector and fluorescence-array detector detection, using a Novapak C18 column (Waters, Milford, MA, USA). Sample extraction and analysis was carried out by Dr. Duroy Navarre (USDA-ARS, Prosser, Washington).

Binding assay of G3P with DIR1

G3P binding assays were carried out by using 250 µg of DIR1 protein equilibrated in a dialysis bag (3.5 kD cutoff) at 4 °C in 10 mM Tris-HCl, pH 7.5, containing 1 mM sodium azide and 3 µM ^{14}C-G3P (American Radiolabel Co.). After overnight equilibration, the dialysis bag was immersed in 10 mM Tris-HCl, pH 7.5, and 10 µl aliquots were removed from the bag after 24 h and quantified using a liquid scintillation analyzer (1900-TR, Thermo Scientific).

Protein extraction and immunoblot analysis

Total proteins were extracted in buffer containing 50 mM Tris-HCl, pH 7.5, 10 mM $MgCl_2$, 10% glycerol, 150 mM NaCl, 5 mM DTT, 5 mM EDTA, and 1X protease inhibitor mixture (Sigma, St. Louis, MO-USA). Protein concentrations were determined by using the Bio-Rad protein assay kit. For Ponceau-S staining, PVDF membranes were incubated in Ponceau-S solution [40% methanol (vol/vol), 15% acetic acid (vol/vol), 0.25% Ponceau-S] The membranes were destained using deionized water. Proteins (30–50 μg) were fractionated on an 8–15% SDS/PAGE gel and subjected to immunoblot analysis using GFP specific antibodies. Immunoblots were developed using ECL detection kit (Thermo-Fisher Sci.) or alkaline phosphatase-based color detection.

For soluble and pellet fractionations, proteins were ex-tracted in buffer containing 50 mM Tris-MES, pH 8.0, 0.5 M sucrose, 1 mM $MgCl_2$, 10 mM EDTA, 10 mM EGTA, 10 mM ascorbic acid, 5 mM DTT, and 1X protease inhibitor mixture (Sigma St. Louis, MO-USA). Total protein extract was centrifuged at 10,000 X g followed by a second centrifugation at 45,000 X g for 60 min. The pellet fraction was suspended in a buffer containing 5 mM potassium phosphate pH 7.8, 2 mM DTT and 1X protease inhibitor mixture and supplemented either with 2 M urea or 1% Triton X-100 to release peripheral membrane proteins. Protein concentration was measured by the Bio-Rad protein assay (Bio-Rad).

Protoplast isolation

The protoplast isolation was carried out as described earlier (Wu et al., 2009). Leaves from three to four-week-old plants were washed with deionized water to remove any surface soil and dried on Kimwipes. The upper epidermal surface was stabilized by affixing a strip of Time tape while the lower epidermal surface was affixed to a strip of Magic tape. The Magic tape was pulled away from the Time tape, peeling away the lower epidermal surface cell layer. The peeled leaves were transferred to a Petri dish containing 10 mL of enzyme solution (1% cellulase 'Onozuka' R10, 0.25% macerozyme 'Onozuka' R10, 0.4 M mannitol, 10 mM $CaCl_2$, 20 mM KCl, 0.1% BSA and 20 mM MES, pH 5.7). The samples with solution were shaken for one hour until the protoplasts were released into the solution. The protoplasts were centrifuged at 100 X g for 3 min in glass

centrifuge tube, washed twice with 25 mL of pre-chilled modified W5 solution (154 mM NaCl, 125 mM $CaCl_2$, 5 mM KCl, 5 mM glucose, and 2 mM MES, pH 5.7) and incubated on ice for 30 min. Employing hemocytometer the protoplasts were counted using a light microscope and then scanned by using confocal Olympus FV1000 microscope (Olympus America, Melville, NY-USA). GFP and RFP were excited using 488 and 543 nm laser lines, respectively.

Table 2.1. **Seed materials used in the study.**

Sl No.	Mutants and transgenic seeds	References
1	Columbia-0 (Col-0)	Kachroo et al., 2003
2	Nössen (Nö)	Kachroo et al., 2001
3	*act1*	Kunst et al., 1988; Kachroo et al., 2003
4	*ssi2*	Kachroo et al., 2001
5	*ssi2 act1*	Kachroo et al., 2003 b
6	*ssi2 sid2*	Kachroo et al., 2005
7	*noa1*	Kachroo et al., 2004
8	*nia1 nia2*	Mandal et al., 2012
9	*noa1 nia1*	Mandal et al., 2012
10	*noa1 nia2*	Mandal et al., 2012
11	*ssi2 noa1 nia1*	Mandal et al., 2012
12	*ssi2 noa1 nia2*	Mandal et al., 2012
13	*nia1*	Crawford et al., 1993
14	*nia2*	Crawford et al., 1993
15	*ssi2 noa1: NOA1*	Mandal et al., 2012
16	35S-*NOA1*-HIS	Mandal et al., 2012
17	*nai ssi2*	Mandal et al., 2012
18	*nia2 ssi2*	Mandal et al., 2012
19	*cpr5 noa1*	Mandal et al., 2012
20	*cpr5*	Dong et al. (1997)
21	35S-*DIR1*-GFP	Mandal et al., 2012
22	35S-*AtNOA1*-GFP	Mandal et al., 2012

Table 2.2. **List of primers used in this study**. The name, sequence and the purpose for which the primers were used are listed. The enzymes used for dCAPS or CAPS markers are mentioned in parenthesis.

Name	Primer
NPT (Kan) Fwd-Rev (Genotyping)	CAA GAT GGA TTG CAC GCA GGT GCT CTT CAG CAA TAT CAC GGG
HPT (Hyg) Fwd-Rev (Genotyping)	ACC TAT TGC ATC TCC CGC CGT CCG GAT GCC TCC GCT CGA AGT
Lbb1 (Genotyping)	GCGTGGACCGCTTGCTGCAACT
PDF1.2 Fwd-Rev (PCR)	AAT GAG CTC TCA TGG CTA AGT TTG CT AAT CCA TGG AAT ACA CAC GAT TTA GC
SSI4 Fwd-Rev (PCR)	CTC AAG AGA GTA TGC TTC TCT TTC CAT AAC CC CTG GTT TGG TCT TCA TGA GAC TCC ATGAG
RPS2 Fwd-Rev (RT-PCR)	ATG GAT TTC ATC TCA TCT CTT TAT AAT CTC CGC GAG CCG GCG
RPM1 Fwd-Rev (RT-PCR)	GCA TAC ATG GGA CCT AGG TTG CGT TTT GCA CAA GGGCC TTG GCC GCC TAA GAT GAG AGG CTC AC
SNC1 Fwd-Rev (RT-PCR)	ATG GAG ATA GCT TCT TCT TCT ATC AGG TGG AGA GTC TTT CCC
RPP1	GTG GAG CTC CCC GCT ATC GAG AAT GCG AC

Fwd-Rev (RT-PCR)	GCA AGG GAA TCT GGA AGT TGG GGG AGT GAT ACC
NOA1-Xho1 Fwd *NOA1*-Xba1 Rev	CAG CCT CGA GAT GGC GCT ACG AAC ACT CTC TGC ATC TAG ATC AAA AGT ACC ATT TGG GTC T
NOA1- SalI Fwd *NOA1*- KpnI Rev	CAA GTC GAC CCC CAT AAA CCC TAG AAA TGG AAA CCC ACC GGT ACC CTG TTT CAT TTG TTG AAT TGT TGA TGT AG
NIA2-KO-LP *NIA2*-KO-RP	TGG CAT ATT CCT TCT TGA TGC AGT CAC AAA TGG TCC CAT ACG
ssi2-dCAPS-NsiI Fwd-Rev	TTG GTG GGG GAC ATG ATC ACA GAA GAT GCA AAG TAG GAC TAG CAC CTG TTT CAT CCC TAA
cpr5-dCAPS-BsmFI	GCG GTG TAT CGG GTA AAT TGT GTG TGC AAC GAA TTG CAA AAG GCA AAA CAC GTC
NOA1-Localization attB1 Fwd-Rev	AAA AAG CAG GCT TAA TGG CGC TAC GAA CAC TCT CA AGA AAG CTG GGT AAA AGT ACC ATT TGG GTC TTA C
NOA1-HIS Fwd-Rev overexpression	AAA AAG CAG GCT TAA TGG CGC TAC GAA CAC TCT CA AGA AAG CTG GGT ATC AGT GGT GGT GGT GGT GGT GGT GGT GGT GGT GAA AGT ACC ATT TGG GTC TTA C

Name	Primer
NOA1-NheI Fwd (del37) NOA1-Xho1 Rev E. coli expression	AGG GCT AGC ATG TGT AAA TCA ATA GCT AAT TCA GCG CTC GAG AAA GTA CCA TTT GGG TCT TAC
NOA1-NheI Fwd (del101) NOA1-Xho1 Rev E. coli expression	AGG GCT AGC GAT ACC TCA GTC TCA TGT TGT GCG CTC GAG AAA GTA CCA TTT GGG TCT TAC
NIA1-Localization-attBI Fwd-Rev	AAA AAG CAG GCT TAA TGG CGA CCT CCG TCG ATA AC AGA AAG CTG GGT AGA AGA TTA AGA GAT CCT CCT TCA C
NIA2-Localization-attBI Fwd-Rev	AAA AAG CAG GCT TAA TGG CGG CCT CTG TAG ATA AT AGA AAG CTG GGT AGA ATA TCA AGA AAT CCT CCT TGA T
NIA1-Localization-attBI Fwd-Rev	AAA AAG CAG GCT TAA TGG CGA CCT CCG TCG ATA AC AGA AAG CTG GGT AGA AGA TTA AGA GAT CCT CCT TCA C
NIA2-Localization-attBI Fwd -Rev	AAA AAG CAG GCT TAA TGG CGG CCT CTG TAG ATA AT AGA AAG CTG GGT AGA ATA TCA AGA AAT CCT CCT TGA T
SSI2 localization-attBI Fwd-Rev	AAA AAG CAG GCT TAA TGG CTC TAA AGT TTA ACC C AGA AAG CTG GGT AGA GCT GCA CTT CTC TGT
β-Tubulin Fwd-Rev	CGT GGA TCA CAG CAA TAC AGA GCC CCT CCT GCA CTT CCA CTT CGT CTT
SNC1 (RT) At4g16890	AAC AGA CCG GCG AAT TTG GAA AGG GCA AGC TCT TCA ATC ATG GCT GCT

Name	Primer
RPS2 (RT) At4g26090 Fwd -Rev	TCT TAT CGT TGG CTG TGC TCA GGT ACG TAT GGC CTT CAA GTC ACC GAT
SSI4 (RT) Fwd-Rev	TCT TAC GGG TGT TGC TGA CCA TGA TGT AGC CTT TCT CGT ATT GCG CCT
Actin(RT) At3g18780 Fwd-Rev	ACA CTG TGC CAA TCT ACG AGG GTT ACA ATT TCC CGC TCT GCT GTT GTG
DIR1 NdeI del25-Fwd *DIR1* Xho1 Rev	CCG CAT ATG GCG ATA GAT CTC TGC GGC ATG AGC CCG CTC GAG CAC ACG TAT ACA GAG TCT TTT AAC
DIR1attB1 FL Fwd DIR1attB1 Rev	AAA AAG CAG GCT TAA TGG CGA GCA AGA AAG CAG CT AGA AAG CTG GGT AAC AAG TTG GGG CGT TGG CTA GAC C
ACT1 attB1 Fwd ACT1 attB1 Rev	AAA AAG CAG GCT TAA TGA CTC TCA CGT TTT CCT CCT CC AGAAAGCTGGGTAATTCCAAGGTTGTGACAAAGAGACCCT
EGFP XhoI Fwd EGFP NcoI Rev	CCG CTC GAG ATG GTG AGC AAG GGC GAG GAG GCG CCA TGG CAG ATC TGA GTC CGG ACT TGT ACA G

CHAPTER 3

Oleic acid-dependent modulation of NITRIC OXIDE ASSOCATED 1 protein levels regulate nitric oxide-mediated signaling in plant defense

Introduction

Fatty acids (FAs) are important signaling components regulating various biological processes in plants and animals. They also serve as important structural components of cell membranes in plants and animals. FAs also function as reserve energy storage and regulate various inflammatory and metabolic responses (Hotamisligil, 2006; Denys et al. 2001). Unsaturated FAs in membrane lipids are reported to provide tolerance to low temperature to various organisms including the cyanobacterium *Synechocystis* (Gombos et al. 1992). Fatty acids are also involved in regulating developmental and reproductive biology in mycotoxic *Aspergillus spp.* (Calvo et al. 1999; Wilson et al. 2004). In plants, various fatty acids are involved in defense signaling and modulate resistance or susceptibility to various pathogens (Kachroo et al. 2003, 2004; Ongena et al.2004; Trepanier et al. 2005). FAs also act as effectors in regulating abiotic stress responses (Guerzoni et al. 2001).

De novo FA biosynthesis occurs exclusively in the plastids of all plant cells and leads to the synthesis of palmitic acid (16:0) and oleic acid (18:1) (Kachroo and Kachroo 2009). Stearoyl-ACP desaturase (SACPD), which catalyzes the desaturation of stearic acid (18:0) to oleic acid (18:1), is one of the important soluble chloroplastic enzymes that regulates the generation of mono-unsaturated FA in plant cells (Shanklin and Cahoon 1998; Kachroo et al. 2007). The Arabidopsis genome encodes seven isoforms of SACPD.

The results shown in this chapter was published in the following journal:

Mandal MK, Chandra-Shekara AC, Jeong RD, Yu K, Zhu S, Chanda B, Navarre D, Kachroo A, Kachroo P. 2012. Oleic acid-dependent modulation of NITRIC OXIDE ASSOCATED 1 protein levels regulate nitric oxide-mediated signaling in plant defense. *Plant cell*.

(Kachroo et al. 2007). Yet, a mutation in the *SSI2*-encoded SACPD results in the constitutive activation of defense responses (Chandra-Shekara et al. 2007; Kachroo et al. 2001, 2003a, 2003b; 2004, 2005, 2007; Venugopal et al. 2009; Xia et al. 2009) and is not compensated by endogenous expression of the other isoforms. Mutations in two other SACPD isoforms do not induce defense signaling, suggesting a specific role for the *SSI2* encoded activity in regulating defense signaling (Kachroo et al. 2007). Detailed characterization has shown that the constitutive defense in *ssi2* plants is due to their inability to accumulate chloroplastic 18:1 (Chandra-Shekara et al. 2007; Kachroo et al. 2001, 2003a, 2003b; 2004, 2005, 2007; Venugopal et al. 2009; Xia et al. 2009) which via an unknown mechanism induces the expression of multiple nuclear-encoded resistance (*R*) genes (Chandra-Shekara et al. 2007; Venugopal et al. 2009; Xia et al. 2009). Restoration of 18:1 levels via second site mutations in the chloroplast-targeted glycerol-3-phosphate (G3P) acyltransferase (ACT1; (Kachroo et al. 2003a)), G3P dehydrogenase (GLY1; (Kachroo et al. 2004)) or acyl carrier protein 4 (Xia et al. 2009), normalizes *R* gene expression and thereby the altered defense phenotypes of *ssi2* plants. In wild-type (wt) plants, 18:1 levels can be reduced by the exogenous application of glycerol, which increases ACT1 catalysis and, thereby, 18:1 utilization (Kachroo et al. 2004; Kachroo et al. 2005).

Like 18:1, nitric oxide is a conserved signaling molecule common between plants and animals (Besson-Bard et al. 2008; Wendehenne et al. 2001). In plants, NO is known to participate in several responses, including germination, flowering, stomatal closure and pathogen defense (Besson-Bard et al. 2008; Delladonne et al. 1998; Durner et al. 1998; He et al. 2004; Wilson et al. 2008). NO biosynthesis in plants is thought to occur via the nitrate reductase (NR) and nitric oxide-associated (NOA) 1 catalyzed reactions (Besson-Bard et al. 2008; Desikan et al. 2002; Guo et al. 2003; Wendehenne et al. 2001). NR is a cytosolic enzyme which catalyzes NAD(P)H-dependent reduction of nitrate to nitrite (Besson-Bard et al. 2008; Moreau et al. 2008). NOA1 was earlier thought to function similarly to mammalian NO synthases (Guo et al. 2003), but was recently shown to have GTPase rather than NO synthase activity (Moreau et al. 2008). At present the relationship between GTPase activity and its role in NO biosynthesis/ accumulation or relative contributions of NR and NOA1 pathways to total NO levels in plants remains unclear.

Furthermore, the regulation of NO synthesis and how NO exerts its effects in various signaling processes remain largely unclear.

In this study, I have evaluated the relationship between low 18:1- and NO-mediated defense signaling pathways. I show that 18:1 synthesized within the chloroplast nucleoids regulates the activity and stability of NOA1 and, thereby, NO biosynthesis/ accumulation. Reduction in 18:1 levels led to increased levels of NOA1 protein, which in turn increased biosynthesis of NO. This triggered transcriptional upregulation of NO-responsive nuclear genes, thereby activating disease resistance. My results suggest that 18:1-regulated NO biosynthesis triggers retrograde signaling between chloroplasts and the nucleus.

Results

The *ssi2* plants accumulate high levels of chloroplastic NO

Like the *ssi2* mutation, application of glycerol induces expression of various nuclear-encoded *R* genes in wild-type plants in an ACT1-dependent manner (Chandra-Shekara et al. 2007; Kachroo et al. 2004; Venugopal et al. 2009; Xia et al. 2009). These observations suggest that changes in chloroplastic 18:1 levels can induce nuclear gene expression. I hypothesized that 18:1 levels might regulate key molecules that are involved in retrograde signaling between the chloroplast and the nucleus. One possibility was that reduction in 18:1 levels induced the formation/accumulation of an intermediate signaling component(s) that directly or indirectly triggered the expression of nuclear genes. To test this hypothesis, I first compared the transcriptional profile of *ssi2* plants with wild-type plants exposed to various biotic and abiotic treatments (obtained from the NCBI database). Strikingly, the transcription activation profile of *ssi2* plants remarkably overlapped with that of NO-treated wild-type plants; of 261 genes induced by 1 mM of the NO donor, sodium nitroprusside (SNP; Parani et al. 2004), 104 were upregulated in *ssi2* plants (Table 3.1). Notably, only 81 genes were upregulated when SNP was applied at lower concentrations (0.1 mM; Parani et al. 2004), suggesting that NO modulates gene expression in a concentration-dependent manner. Of the 104 NO inducible genes upregulated in *ssi2* plants, 68 were also induced in the *ssi2 sid2* plants, which exhibit

ssi2-like phenotypes due to their low 18:1 levels but contain reduced levels of SA (Table 3.1). In contrast, a majority of the NO-responsive genes were expressed at wild-type-like levels in *ssi2 act1* plants, which are restored in 18:1 levels and exhibit wild-type-like defense responses (Kachroo et al. 2003a) (Table S1). Together, these results suggest a correlation between the *ssi2* phenotypes and increased expression of NO responsive genes.

I tested if *ssi2* plants accumulated increased NO by staining wild-type and *ssi2* plants with the NO-sensitive dye, 4-amino-5-methylamino-2,7-difluorofluorescein diacetate [DAF-FM DA; (Balcerczyk et al. 2005)]. Interestingly, DAF-FM DA-stained *ssi2* leaves showed increased fluorescence compared to wild-type plants and accumulated higher levels of NO (Fig. 3.1A, 3.2A). This was further reconfirmed using the Griess reaction assay, which is based on the spontaneous oxidation of NO to nitrite under physiological conditions (Sun et al. 2003) (Fig. 3.2B). Furthermore, the *ssi2* plants also showed typical phenotypes associated with increased NO, including delayed flowering and shorter roots (He et al. 2004) (Fig. 3.2C, 3.2E, 3.2F). The delayed flowering in *ssi2* plants correlated with increased expression of *FLC* (Flowering Locus C), a repressor of flowering, and reduced expression of *CO* (Constans), a transcription factor that negatively regulates FLC expression to promote flowering (Fig. 3.2D) (Parcy 2005). Consistent with their transcriptional profiles and defense phenotypes, *ssi2 sid2* plants showed increased DAF-FM DA fluorescence, but *ssi2 act1* plants did not (Fig. 3.1A).

I used confocal microscopy to determine the subcellular location of the increased NO in *ssi2* plants. NO was primarily detected in the chloroplasts (Fig. 3.1B). Likewise, glycerol application, which lowered 18:1 levels, also induced NO accumulation in the chloroplasts of wild-type Arabidopsis and *Nicotiana benthamiana* plants (Fig. 3.1B, 3.3A). NO accumulation in response to low 18:1 mimicked pathogen-induced accumulation of NO; inoculations with *Pseudomonas syringae* expressing *avrRpt2* resulted in NO accumulation in the chloroplasts within 12 h post inoculation (hpi) (Fig. 3.1C). Notably, pathogen induced NO-accumulation preceded the increase in salicylic acid (SA) levels (Fig. 3.3B), which was consistent with the result that exogenous NO induces SA biosynthetic genes and thereby SA levels (Durner et al. 1998).

NOA1 derived NO contributes to defense phenotypes in *ssi2* plants

Increased accumulation of NO in the chloroplasts of *ssi2* plants and the fact that the chloroplastic *NOA1* contributes to elicitor-mediated accumulation of NO (Guo et al. 2003; Zeidler et al. 2004; Gas et al. 2008), prompted us to test the role of *NOA1* in *ssi2*-mediated signaling. We crossed *ssi2* plants with *noa1* and analyzed F2 progeny for *ssi2*-like phenotypes. Consistent with digenic segregation, approximately one of sixteen plants showed wild-type-like morphology (Fig. 3.4A); 10 of 147 plants contained the *ssi2* mutation, but showed wild-type-like phenotypes ($\chi 2$=0.08, *P*=0.77). In comparison to *ssi2*, the *ssi2 noa1* plants accumulated much lower levels of NO (Fig. 3.1A, 3.5A, 3.5B) and showed no visible or microscopic cell death (Fig. 3.4A, 3.4B). To confirm that the restoration of morphological and defense phenotypes in *ssi2 noa1* was due to the *noa1* mutation, we transformed a wild-type genomic copy of *NOA1* into *ssi2 noa1* plants and scored phenotypes in T1 and T2 generations (Fig. 3.6). The *ssi2 noa1* plants containing the *NOA1* transgene showed *ssi2*-like morphology (Fig. 3.6A), constitutive cell death (Fig. 3.6B) and *PR-1* expression (Fig. 3.6C), thus confirming a role for *NOA1* in *ssi2*-triggered phenotypes. In contrast to the *ssi2* mutation, *noa1* did not abolish the constitutive defense phenotypes in another mutant, *cpr5* (Fig. 3.7A, 3.7B, 3.7C, 3.7D). Like *ssi2*, the *cpr5* plants are constitutively activated in defense signaling, but this is not due to changes in 18:1 levels (Fig. 3.7E). Together, these results suggested that NOA1 specifically participates in low 18:1-derived signaling.

The *ssi2 noa1* plants accumulated *ssi2*-like levels of 18:1 (Fig. 3.4C), suggesting that NOA1 functions downstream of 18:1. Consistent with their wild-type-like morphology, levels of total lipids were significantly higher in *ssi2 noa1* compared to *ssi2* (Fig. 3.4D) and this correlated with a significant increase in the levels of monogalactosyl- and digalactosyl-diacylglycerol lipids in comparison to *ssi2* plants (Fig. 3.8). The *noa1* mutation by itself did not affect the FA or lipid profile in the wild-type background (Fig. 3.1C, 3.1D, 3.8). I next evaluated the various defense phenotypes in *ssi2 noa1* plants to determine if the reduction in NO levels restored *ssi2*-triggered defense signaling. In comparison to *ssi2*, the *ssi2 noa1* plants showed wild-type-like levels of *PR-1* and a significant reduction in *PR-2* transcript (Fig. 3.4E) and wild-type-like levels of SA (Fig.

3.4F) and H_2O_2 (Fig. 3.4G). However, *ssi2 noa1* plants expressed higher than wild-type levels of *R* genes, even though these were significantly lower than in *ssi2* plants (Fig. 3.4H). Consistent with their *R* gene expression levels, the resistance of *ssi2 noa1* to *avrRps4 P. syringae* was intermediate to *ssi2* and *noa1* plants (Fig. 3.4I). Together, these results suggested that *ssi2 noa1* plants were not completely restored in *R* gene expression or pathogen response.

NOA1, NIA1 and NIA2 contribute additively to NO accumulation in *ssi2* plants

The *ssi2 noa1* plants were not completely restored in *R* gene expression or pathogen response, suggesting that additional factor(s) contributed to a nominal increase in *R* gene expression. It was possible that residual NO levels in *ssi2 noa1* plants were sufficient to trigger a low level increase in *R* gene expression. To test this, I assayed *R* gene expression levels in plants treated with 0.1 mM SNP. Indeed, 0.1 mM SNP was sufficient to induce *R* gene expression in wild-type plants (Fig. 3.9A). This result prompted us to investigate the role of nitrate reductases in *ssi2*-triggered phenotypes, since NO is also generated as a byproduct of the nitrate reductase (encoded by *NIA1* and *NIA2* in Arabidopsis)-catalyzed reactions (Besson-Bard et al. 2008; Desikan et al. 2002). To determine if *NIA1* and/or *NIA2* contributed to the accumulation of NO in *ssi2* plants, I first evaluated the expression of *NIA1* and *NIA2* transcripts in wild-type, *ssi2*, *ssi2 sid2*, and *ssi2 act1* plants. Notably, *NIA1* and *NIA2* expression correlated with *ssi2* phenotypes; the *NIA1* and *NIA2* transcript levels were elevated in *ssi2* and *ssi2 sid2*, but not in *ssi2 act1* plants (Fig. 3.10). Exogenous NO or SA did not induce expression of *NIA1* and *NIA2* genes (data not shown, also see Table 3.2), suggesting that their induction was specific to low 18:1 levels. Consistent with this result, expression of *NIA1* and *NIA2* was also upregulated in *ssi2 noa1* plants (Fig. 3.9B). In contrast to *NIA*, *NOA1* expression was not upregulated in the *ssi2* plants (data not shown). Together, these results suggested that reduction in 18:1 levels resulted in NO accumulation via the upregulation of the *NIA1* and *NIA2* transcripts and the post-transcriptional alteration of NOA1.

To determine if the increased expression of *NIA1* and *NIA2* contributed to the NO-derived phenotypes in *ssi2* plants, I generated *ssi2 nia1* and *ssi2 nia2* plants. Both *ssi2*

nia1 and *ssi2 nia2* plants showed improved morphology (Fig. 3.9B), which correlated with an increase in total lipid and MGDG levels (Fig. 3.11A, 3.11B). The *ssi2 nia1* and *ssi2 nia2* plants accumulated reduced NO (Fig. 3.10C) or SA (Fig. 3.11C), and displayed reduced cell death and *PR* expression (Fig. 3.10D, 3.10E). Interestingly, the *ssi2 nia2* plants showed more pronounced reduction in cell death and *PR* expression than the *ssi2 nia1* plants which, in turn, correlated with the downregulation of *NIA1* expression in *ssi2 nia2* plants (Fig. 3.9B). Together, these results suggested that the increased expression of *NIA1* and *NIA2* in *ssi2* plants might also contribute to the increased NO production and defense phenotypes. Intriguingly, even though NIA1 and NIA2 localized to the extra-chloroplastic compartment (Fig. 3.12A), mutations in these lowered chloroplastic NO levels in *ssi2* plants (Fig. 3.12B). This suggests that NO synthesis and/or accumulation likely involve feedback regulation between NOA1 and NIA1/NIA2.

To determine if the relative contributions of NOA1 and NIA1/NIA2 resulted in additive effects, I generated and evaluated defense phenotypes in *ssi2 noa1 nia1* and *ssi2 noa1 nia2* plants. Interestingly, the *ssi2 noa1 nia1* and *ssi2 noa1 nia2* showed basal level expression of *R* genes and compromised resistance to avirulent pathogens (Fig. 3.13A, 3.13B). Consistent with this result, pathogen-treated *noa1 nia2* plants showed greater reduction in NO levels compared to single-mutant plants (Fig. 3.14A, 3.14B). I next assayed glycerol- triggered phenotypes in the *noa1*, *nia1*, *nia2*, single mutant plants and the *noa1 nia1* and *noa1 nia2* double-mutant plants. As shown earlier, exogenous application of glycerol reduced 18:1 levels in wild-type plants (Fig. 3.15), resulting in the induction of cell death and *PR-1* expression (Fig. 3.13C, 3.13D). Glycerol application also lowered 18:1 levels in all mutant genotypes (Fig. 3.15). However, glycerol application only induced *PR-1* expression and cell death in the *noa1*, *nia1*, *nia2* single mutants but not in the *noa1 nia1* and *noa1 nia2* double mutants (Fig. 3.13C, 3.13D). Glycerol-mediated depletion of 18:1 also inhibited root growth in wild-type and single mutants but not the double mutant plants (Fig. 3.13E, 3.13F). Together, these results suggest that the combined loss of *NOA1* with *NIA1* or *NIA2* is essential to completely abolish the increased *R* expression and altered defense phenotypes under low 18:1 conditions.

NOA1 localizes to the chloroplastic nucleoids

The accumulation of NO in chloroplasts correlated well with the plastidial localization of NOA1-GFP (Fig. 3.16A). Intriguingly, NOA1-GFP localized in a punctate pattern within the chloroplasts, unlike other chloroplastic proteins like GLY1, which was uniformly distributed in the chloroplast (Fig. 3.16A). DAPI (4',6-diamidino-2-phenylindole) staining identified the punctate structures as nucleoids, which are nucleus-like bodies that contain genetic material (Fig. 3.16B). The nucleoid-specific localization of NOA1 was further confirmed by protein blot analysis using NOA1-specific antibodies (Figure 3.16C). NOA1 protein was not detected in the *noa1* plants, as these contain a T-DNA insertion within the first exon (Guo et al. 2003). These results suggested that perhaps NO synthesis/accumulation was initiated in the chloroplastic nucleoids. Indeed, NO staining did show intensely stained areas within the chloroplasts of *ssi2* and pathogen-inoculated wild-type plants (Fig. 3.17). Furthermore, both pathogen infection and glycerol treatment increased DAF-FM staining of purified nucleoids (Fig. 3.16D, 3.16E). NOA1 has been shown to possess GTPase activity (Moreau et al. 2008). I investigated whether increased NO accumulation in the nucleoids also correlated with increased GTPase activity. Interestingly, both pathogen infection and glycerol treatment significantly increased nucleoid-associated GTPase activity in wild-type, but not in *noa1,* plants (Fig. 3.16F). Thus, the increased NO and GTPase activity in the nucleoids also correlated with the localization of NOA1 in these suborganelles.

Interestingly, increased GTPase activity in the pathogen inoculated plants correlated well with an increase in the NOA1 protein levels (Fig. 3.18A), although the *NOA1* transcript levels remained unchanged (Table 3.2). Similarly, glycerol treatment also increased NOA1 levels in the wild-type plants (Fig. 3.18B), even though there was no increase in the *NOA1* transcript under low 18:1 levels (Fig. 3.18C). This suggested that pathogen infection and 18:1 levels regulate the stability of NOA1 at the post-transcriptional level. Consistent with this notion, increased levels of NOA1 protein was detected in *ssi2*, *ssi2 nia1* and *ssi2 nia2* plants (Fig. 3.18B). A mutation in *ssi2* did not increase the levels of three other chloroplastic proteins, suggesting that its effect on NOA1 was a specific phenotype (Fig. 3.19). I next tested if the overexpression of *NOA1* in wild-type plants

could relieve the 18:1-mediated repression of NOA1. Notably, 35S-*NOA1* plants showed normal phenotype and near basal levels of defense gene expression. However, 35S-*NOA1* plants showed increased sensitivity to glycerol; exogenous application of glycerol induced higher levels of *PR-1* expression, NO levels, and cell death phenotypes in 35S-*NOA1* plants, compared to wild-type (Fig. 3.18C-3.18E). These results suggested that, while increased expression of *NOA1* in wild-type plants was unable to relieve 18:1-mediated repression, it did potentiate defense phenotypes under low 18:1 conditions.

NOA1 is an 18:1 binding protein

Because exogenous glycerol increased NOA1 levels, I considered the possibility that 18:1 levels regulated the stability of NOA1 by binding to it. Indeed, sequence analysis detected homology to mammalian FA-binding domains in the NOA1 protein and these domains were highly conserved in NOA1-like proteins from other plants (Furuhashi et al. 2008; Fig. 3.20A, 3.20B). To determine if NOA1 bound 18:1, it was important to use a biologically functional form of the protein. Database analysis showed that the transit peptide in NOA1 corresponds to the N-terminal 37 amino acids (aa). However, earlier studies showing GTPase activity associated with NOA1 were carried out with the $NOA1^{\Delta 101}$ protein lacking the N-terminal 101 aa (Moreau et al. 2008). I therefore compared the GTPase activity of *E. coli* purified $NOA1^{\Delta 37}$ with that of $NOA1^{\Delta 101}$ (Fig. 3.21A). Interestingly, $NOA1^{\Delta 37}$ showed significantly higher GTPase activity compared to $NOA1^{\Delta 101}$ (Fig. 3.21B), suggesting that the N-terminal 37-101 aa contributed significantly to the GTPase activity. All binding assays were therefore performed with $NOA1^{\Delta 37}$ protein. Six different preparations of $NOA1^{\Delta 37}$ bound 18:1 with similar efficiencies (Fig. 3.22A). The binding of $NOA1^{\Delta 37}$ to 18:1 saturated at ~20 μM ^{14}C-18:1 and competition assays using cold 18:1 showed a proportionate decrease in the retention of ^{14}C-18:1, indicating saturable binding between 18:1 and $NOA1^{\Delta 37}$ (Fig. 3.22B, 3.22C). Unlike 18:1, cold 18:0 did not compete with (^{14}C)-18:1 for binding with $NOA1^{\Delta 37}$ (Fig. 3.22C). To confirm the 18:1-NOA1 binding, I carried out 18:1-affinity chromatography where *E. coli*-purified NOA1 protein was applied to an 18:1-sepharose column. Indeed, NOA1 was specifically retained on the 18:1-sepharose matrix, but not on unconjugated

sepharose (Fig. 3.22C). I next generated transgenic plants that overexpressed the *NOA1-HIS* transgene and total plant protein extracted from these was applied to 18:1-sepharose column. As with the *E. coli* expressed NOA1, the NOA1-HIS protein from plant extracts was also retained on 18:1-sepharose, but not on-unconjugated sepharose (Fig. 3.22D). While these results confirmed binding between 18:1 and NOA, it suggested that the 18:1-binding site of NOA1 was not completely saturated with 18:1 *in planta*. Alternatively, it is possible that the 18:1 bound to NOA1 was dissociated during extraction or that the bound 18:1 was exchanged by the 18:1 present on the sepharose, which is known to occur in certain FA-binding proteins (Smith et al. 1992).

If low 18:1 were regulating the stability of the nucleoid-localized NOA1, then it might be expected that the 18:1-synthesizing SSI2 was in close proximity to NOA1. Indeed, SSI2 colocalized with NOA1, in the chloroplast nucleoids (Fig. 3.22E) and not exclusively in the stroma as presumed earlier (Shanklin and Somerville, 1991). Unlike SSI2, ACT1, which catalyzes the acylation of 18:1 on G3P (Kunst et al. 1988), was distributed throughout the chloroplasts (Fig. 3.23A). FA analysis showed that the nucleoids contained higher levels of 18:1 compared to chloroplasts (Fig. 3.22F). Nucleoids also contained other chloroplastic FAs, although their relative levels were different in chloroplast versus nucleoids (Fig. 3.23B). For instance, 16:0 was the most abundant FA in the nucleoids as opposed to 18:3 in the chloroplasts. The nucleoids also contained higher levels of 18:0, which serves as a substrate for the SSI2-catalyzed reaction. As predicted, exogenous application of glycerol lowered 18:1 levels in the nucleoids (Fig. 3.23C), which is consistent with the low 18:1-mediated increase in NOA1 and subsequent induction of NO levels and defense responses. The close proximity and the same suborganellar localization of SSI2 and NOA1 suggest that in the wild-type plants NOA1 is present in an 18:1-rich environment within nucleoids, which subjects it to degradation.

Discussion

The results indicate that the 18:1 in wild-type plants regulates the stability of NOA1. Reduction of 18:1, via a genetic mutation in the 18:1-synthesizing *SSI2* or exogenous application of glycerol, led to increased accumulation of NOA1 and an increase in the

chloroplastic NO. Reduction of 18:1 also increased *NIA1* and *NIA2* gene expression which, in turn, contributed to the increased NO in the chloroplasts of *ssi2* plants. Notably, both NIA1 and NIA2 are localized outside chloroplasts. This, together with the fact that *ssi2* phenotypes are fully restored in plants lacking *NOA1* and one of the nitrate reductases (*NIA1* or *NIA2*), suggests that cooperative interaction between NOA1- and NIA1/NIA2-triggered pathways is required for NO accumulation and/or NO-mediated signaling (Fig. 3.24). Interestingly, although NO was primarily detected in the chloroplasts of *ssi2* or pathogen-/glycerol-treated wild-type plants, it led to the transcriptional upregulation of multiple nuclear genes. Inability to detect NO in the nucleus suggests that nuclear *R* gene expression is likely mediated via one or more intermediates whose synthesis/ activation/localization is dependent on NO levels. However, at this stage I cannot rule out the possibility that diffusion of low levels of NO and its rapid metabolism in the nucleus results in the altered nuclear gene expression. The fact that tobacco cells treated with the fungal elicitor cryptogein accumulate NO in the chloroplasts as well as nucleus supports the possibility that NO can localize to the nucleus (Foissner et al., 2000). Furthermore, studies in animals systems have suggested that the diffusion of NO through 4-15 μm cellular radius is a rapid process that takes 2-30 msec (Lancaster, 1996). Thus, cellular diffusion of NO, which is thought to be a highly random process, and the ability of NO to react with various cellular components, are two key factors that likely govern NO-derived signaling.

In addition to its role in NO synthesis, / accumulation an allele of *NOA1* (*RIF1*) was recently identified in a screen for mutants affected in the methylerythritol phosphate (MEP) pathway (Gas et al. 2008), raising the possibility that *NOA1* might affect *ssi2*-mediated signaling by altering the MEP pathway. However, posttranscriptional upregulation of MEP pathway enzymes in *rif1* cannot be restored by exogenous application of NO, suggesting that the regulation of the MEP pathway by NOA1 is unrelated to its role in NO biosynthesis. The MEP pathway functions in the biosynthesis of carotenoids, mono- and di-terpenoids, plastoquinones, and the prenyl group of chlorophylls in plant plastids (Rodriguez-Concepcion 2004). Therefore *ssi2*, *ssi2 noa1* and *noa1* plants were tested for their levels of carotenoids and chlorophyll, which are derived from the MEP pathway. Results show that the changes in these metabolites do

not correlate with the resoration of wild-type-like phenotypes in *ssi2 noa1* plants (Figure 3.25). For example, *noa1* contained normal levels of chlorophyll, but both *ssi2* and *ssi2 noa1* contained reduced chlorophyll. Reduced chlorophyll levels seen in the *ssi2* plants correlate well with their altered structure of chloroplasts (Lightner et al. 1994). In contrast, a reduction in NO levels in *ssi2 noa1* plants correlated well with their wild-type-like morphology. Thus, the restoration of a majority of phenotypes in *ssi2 noa1* are associated with altered NO levels rather than changes in the MEP pathway.

A recent study suggested that the reduced accumulation of NO in the *noa1* plants was due to their inability to accumulate the carbon reserve, sucrose (Ree et al. 2011). Consistent with the earlier report (Ree et al. 2011), *noa1* accumulated reduced levels of sucrose compared to the wild-type plants (Fig. 3.26A). However, this was also the case for *ssi2* and *ssi2 noa1* plants. Furthermore, very similar cell death phenotype and NO-specific staining of roots was observed in *ssi2* and *ssi2 noa1* plants when grown with or without sucrose (Fig. 3.26B, 3.26C). Together, these results suggest that sucrose levels do not contribute to the *noa1*-mediated restoration of the *ssi2*-triggered defense phenotypes.

Increased accumulation of NO under low 18:1 conditions suggest that 18:1 is an important signal that regulates retrograde signaling between the chloroplast nucleoids and the nucleus by controlling NO synthesis. Sub-organellar compartmentalization of 18:1 biosynthesis and its utilization suggests that 18:1 likely shuttles in and out of the nucleoids. Consistent with this notion, pathogen inoculation did not alter 18:1 levels, suggesting that 18:1 flux between stroma and nucleoids or a transient change in 18:1 may play an important role in regulating NOA1. In addition to destabilizing NOA1, binding of 18:1 might also regulate its GTPase activity. Indeed, a marked reduction in GTPase activity in the presence of 18:1 was observed (Fig. 3.27). However, 250 and 500 μM of 18:1 was required to inhibit the GTPase activity by 33 and 90% respectively (data not shown). These concentrations are higher than the biological levels of 18:1 (~250 μM of total 18:1), much of which is conjugated to the membrane lipids. One possibility is that other cellular factors may be required for 18:1-mediated inhibition of GTPase activity at lower concentrations. Interestingly, 18:1 also inhibits NO synthase activity in humans (Davda et al. 1995), suggesting that plants and humans use conserved mechanism(s) to regulate NO levels even though they differ in their biosynthetic processes. The fact that

NOA1-like proteins are present in the genomes of all metazoans (Zemojtel et al. 2004) suggests that 18:1-mediated regulation of NOA1-like proteins might contribute to regulation of NO in other non-plant systems. As yet the link between NOA1-derived NO synthesis and its GTPase activity remains unknown. It is possible that NOA1 serves as an important catalytic component of a larger complex that facilitates NO production in plants. An alternate possibility is that GTPase activity of NOA1 regulates synthesis of enzyme(s) required for the biosynthesis/ accumulation of NO. Further work on the compartmentalization of 18:1 and its flux within the chloroplast may provide novel insights into the complex sub-organellar regulation of NOA1.

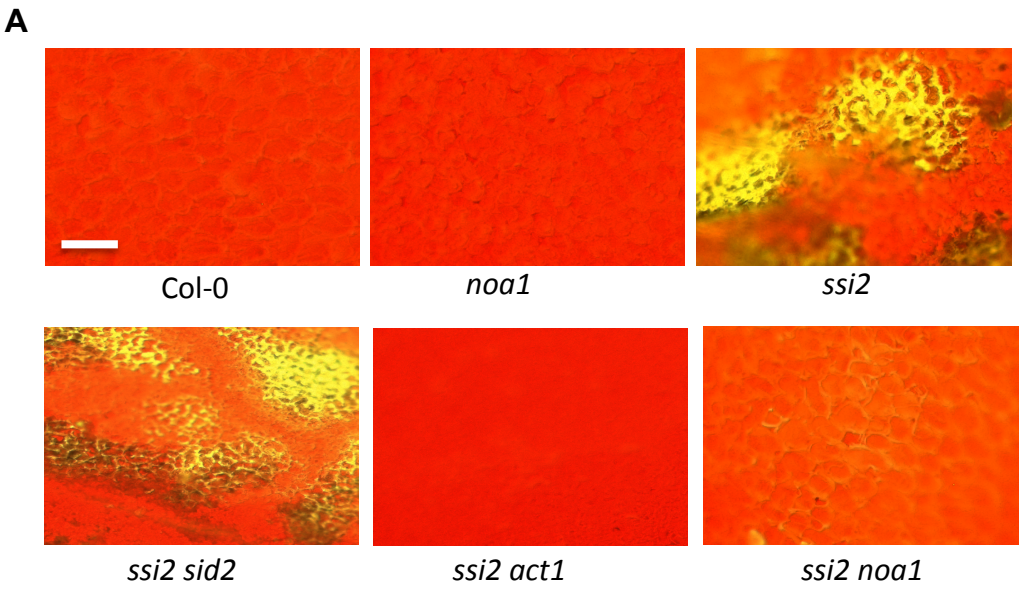
A
Col-0
noa1
ssi2
ssi2 sid2
ssi2 act1
ssi2 noa1

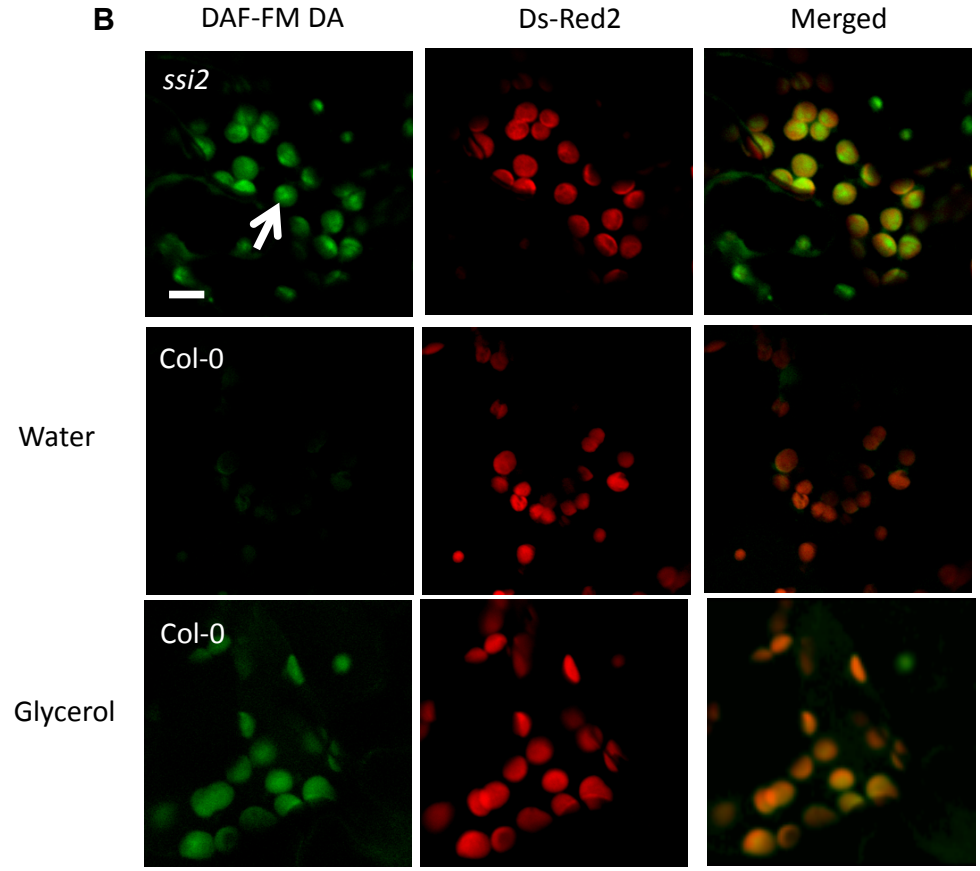
B
DAF-FM DA
Ds-Red2
Merged
ssi2
Water
Col-0
Glycerol
Col-0

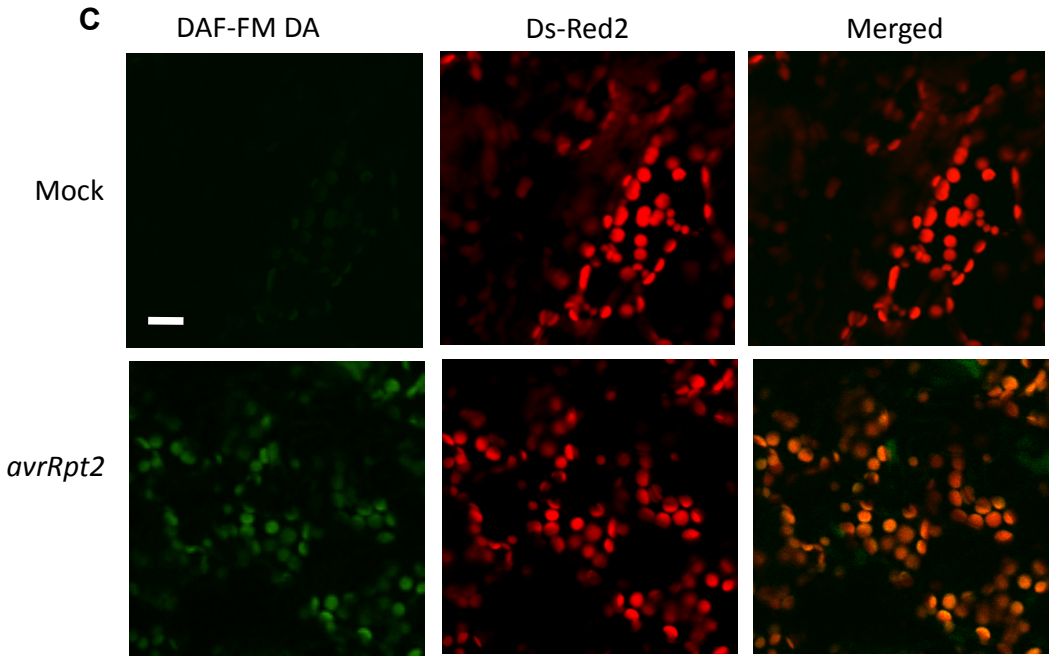

Figure 3.1. The *ssi2* plants accumulate high levels of chloroplastic NO. (A) Fluorescence microscopy of DAF-FM-DA infiltrated leaves using an epifluorescent microscope. Scale bars, 270 microns. (B) Confocal micrograph of DAF-FM DA-stained leaves showing subcellular location of NO in *ssi2* and water- or glycerol-treated wild-type (Col-0) plants. Scale bar, 5 µm. (C) Confocal micrograph showing pathogen-induced NO accumulation in Col-0 plants at indicated hours post inoculation (hpi). Plants were inoculated with $MgCl_2$ (mock) or *avrRpt2 Pseudomonas syringae*. Scale bar, 20 µm.

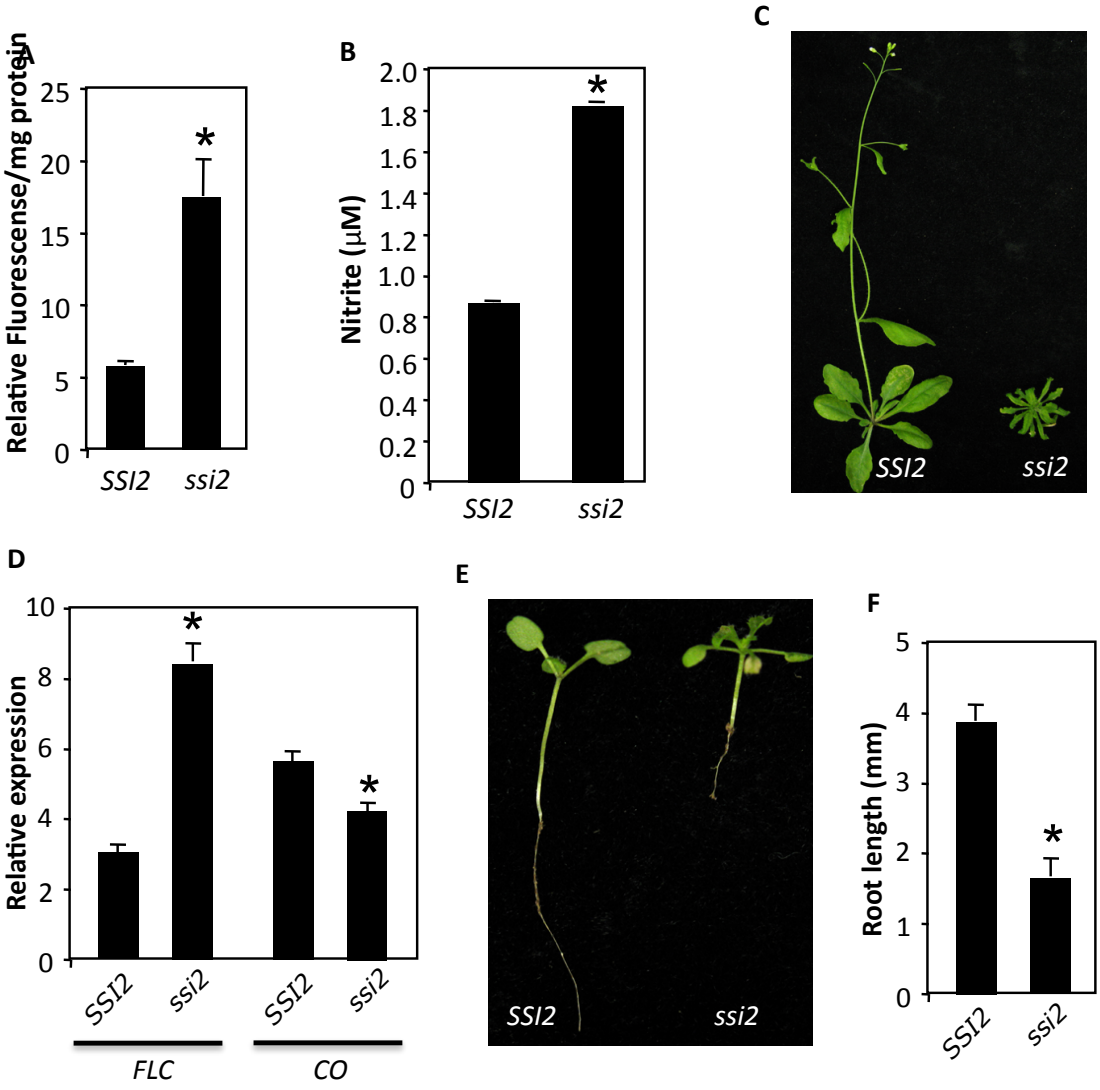

Figure 3.2. *SSI2* plants show delayed flowering and reduced root growth.

Figure 3.2. *SSI2* plants show delayed flowering and reduced root growth. (A) Relative fluorescence in DAF-FM-DA treated wild-type (*SSI2*) and *ssi2* plants quantified using a fluorimeter. The error bars represent SD. Asterisks denote a significant difference with wild-type (*t* test, $P<0.05$, n=4). (B) Levels of nitrite in the soil-grown four-week-old plants. The nitrite levels were estimated using Griess assay. The error bars represent SD. Asterisks denote a significant difference with wild-type (*t* test, $P<0.05$, n=4). (C) Delayed flowering in *ssi2* plants. The wild-type (*SSI2*) and *ssi2* plants were grown in soil and photographed after 28 days of growth at 14 h light/ 10 h dark photocycles. (D) Quantitative RT-PCR analysis showing relative levels of flowering locus C (*FLC*) and constans (*CO*) genes in wild-type and *ssi2* plants. The error bars represent SD. Asterisks denote a significant difference with wild-type (*t* test, $P<0.05$, n=3). (E) The root growth phenotype of *ssi2* plants. (F) Relative root lengths of four-week-old soil-grown wild-type and *ssi2* plants. Asterisks denote a significant difference with wild-type (*t* test, $P<0.05$, n=15).

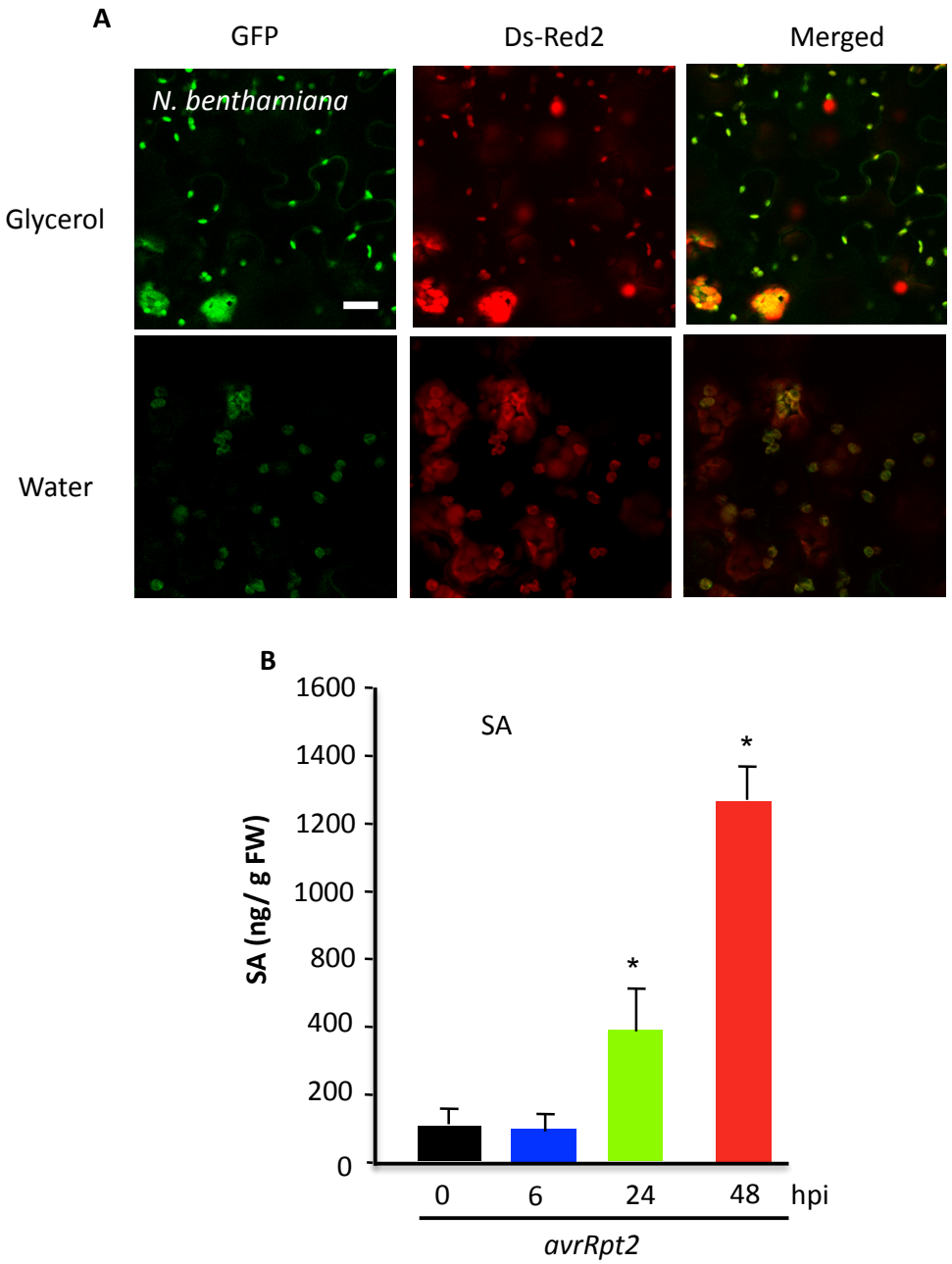

Figure 3.3. NO and SA levels in glycerol- and pathogen-treated plants, respectively. (A) Confocal micrograph of DAF-FM DA-stained leaves showing subcellular location of NO in glycerol-treated *Nicotiana benthamiana* plants. Scale bar, 10 µm. (B) A time course showing SA levels in pathogen-inoculated wild-type Col-0 plants. Plants were inoculated with *avrRpt2 Pseudomonas syringae* and SA was measured from the inoculated leaves at indicated hours post inoculation (hpi). Asterisks denote a significant difference with wild-type (*t* test, $P<0.05$, n=4).

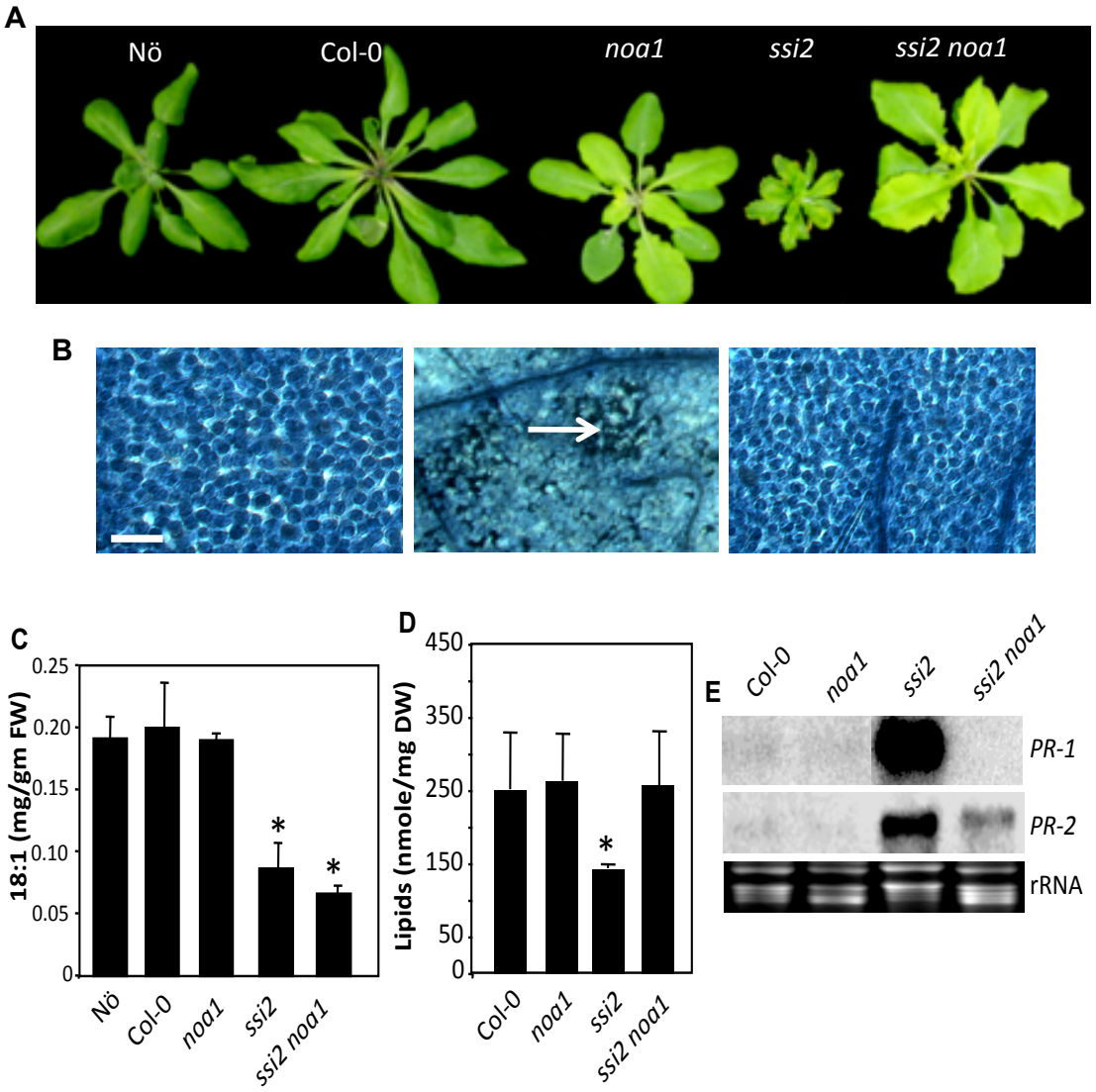
A
Nö
Col-0
noa1
ssi2
ssi2 noa1
B
C
18:1 (mg/gm FW)
0.25
0.20
0.15
0.10
0.05
0
Nö
Col-0
noa1
ssi2
ssi2 noa1
D
Lipids (nmole/mg DW)
450
350
250
150
50
0
Col-0
noa1
ssi2
ssi2 noa1
E
Col-0
noa1
ssi2
ssi2 noa1
PR-1
PR-2
rRNA

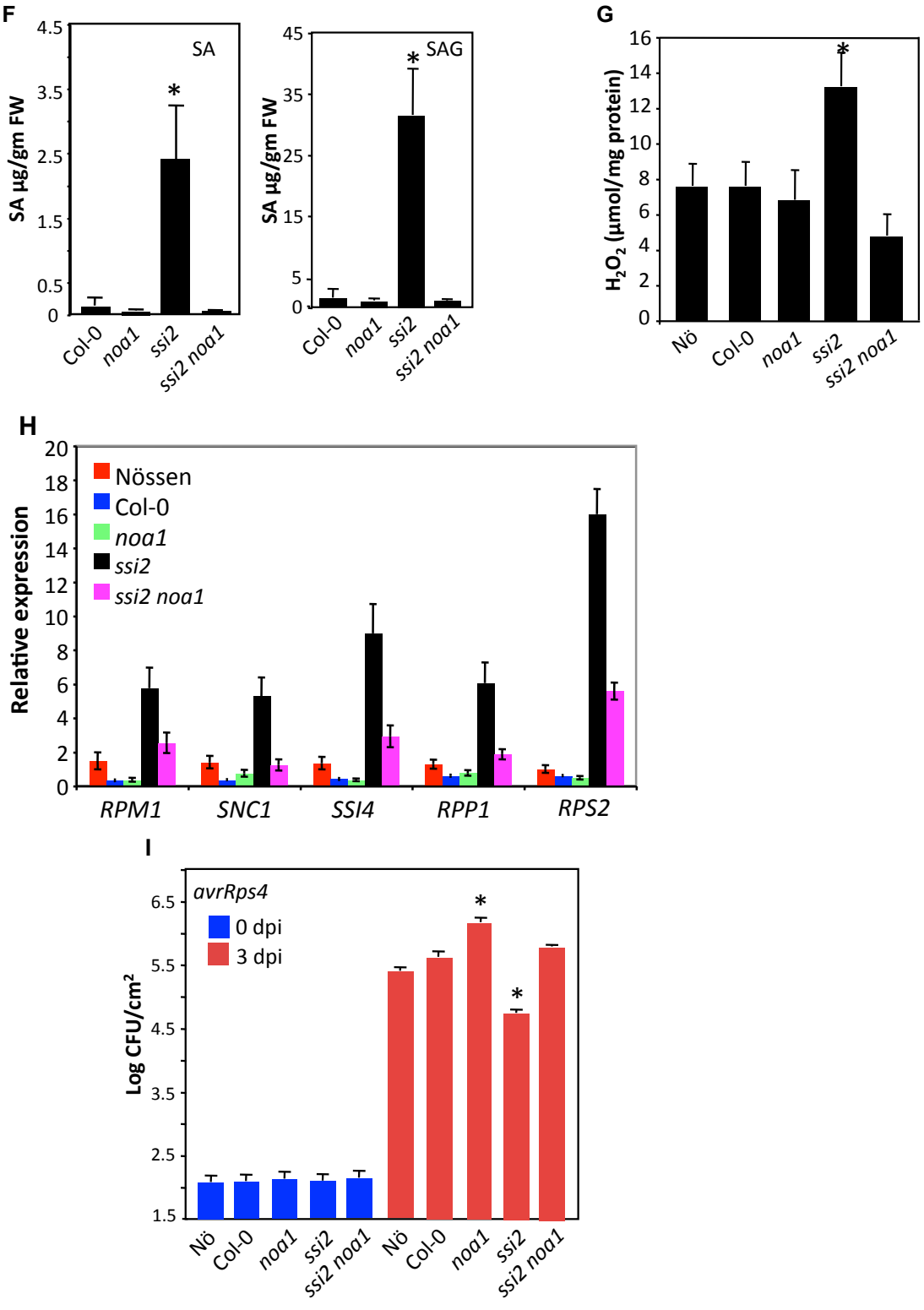
F
SA
SAG
SA µg/gm FW
Col-0
noa1
ssi2
ssi2 noa1
G
H2O2 (µmol/mg protein)
Nö
H
Relative expression
Nössen
Col-0
noa1
ssi2
ssi2 noa1
RPM1
SNC1
SSI4
RPP1
RPS2
I
avrRps4
0 dpi
3 dpi
Log CFU/cm²

Figure 3.4. NOA1-derived NO contributes to defense phenotypes in *ssi2* plants. (A) Morphological phenotype of three-week-old plants. Scale bar, 0.5 cm. (B) Microscopy of trypan blue-stained leaves. Scale bar, 270 microns. Arrow indicates dead cells. (C) Levels of FAs in four-week-old plants. The error bars represent SD. Asterisks denote significant differences with wild-type plants (*t* test, $P<0.05$). (D) Total lipid levels in indicated genotypes. DW indicates dry weight. The error bars represent SD. Asterisks denote significant differences with wild-type plants (*t* test, $P<0.05$). (E) RNA gel blot showing transript levels of *PR-1* and *PR-2* genes. Ethidium bromide staining of rRNA was used as the loading control. (F) SA and SAG levels in indicated genotypes. The error bars represent SD. Asterisks denote significant differences with wild-type plants (*t* test, $P<0.05$). (G) H_2O_2 levels in indicated genotypes. The error bars represent SD. Asterisks denote a significant difference with wild-type (*t* test, $P<0.05$). (H) Quantitative RT-PCR analysis showing relative levels of indicated *R* genes. The error bars represent SD. (I) Growth of *avrRps4* bacteria in indicated genotypes. The error bars indicate SD. Asterisks indicate data statistically significant from wild-type (Col-0, $P<0.05$ n=4).

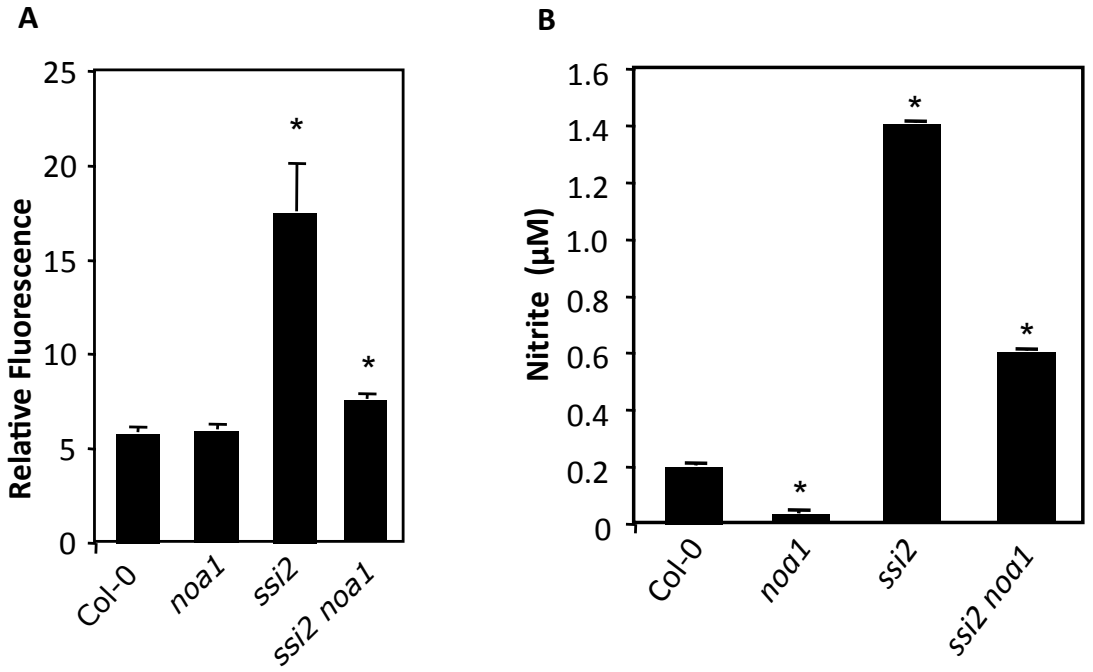

Figure 3.5. NO levels in four-week-old soil-grown Col-0, *noa1*, *ssi2* and *ssi2 noa1* plants. (A) Relative fluorescence in DAF-FM DA-treated plants quantified using a fluorimeter. Asterisks denote a significant difference with wild-type Col-0 (*t* test, $P<0.05$, n=4). (B) Levels of nitrite in the soil-grown four-week-old plants. The nitrite levels were estimated using Griess assay. The error bars represent SD. Asterisks denote a significant difference with wild-type (*t* test, $P<0.05$, n=4).

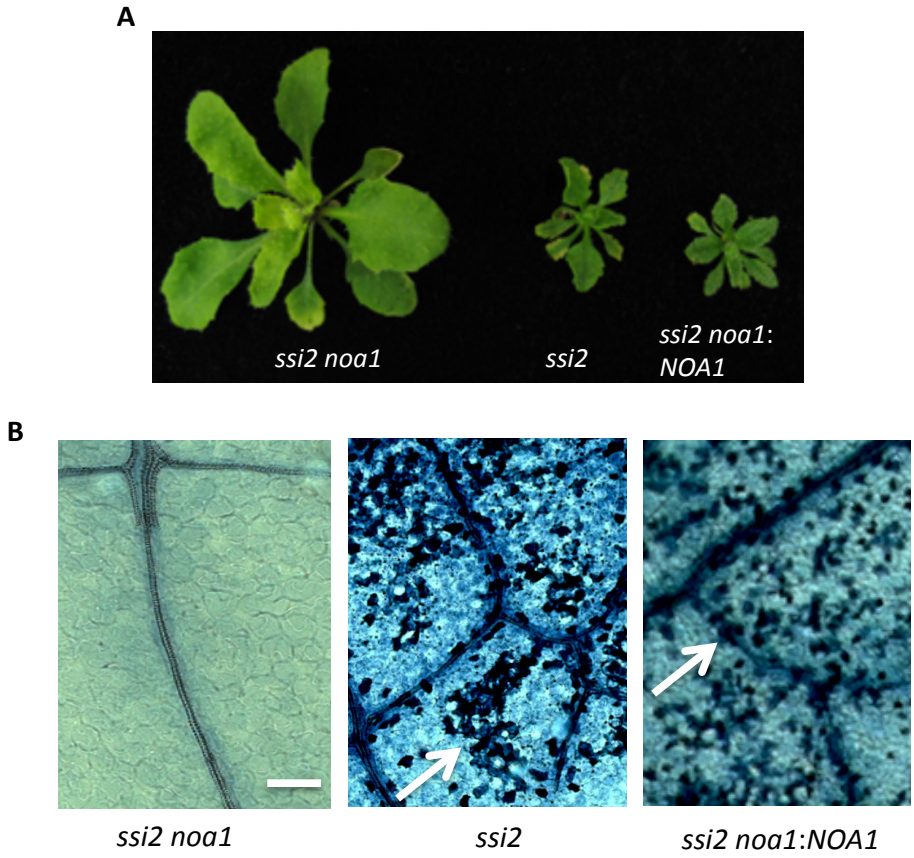

Figure 3.6. Transgenic expression of *NOA1* restores *ssi2*-like phenotypes in *ssi2 noa1* plants. (A) Morphological phenotype of four-week-old soil-grown plants. (B) Microscopy of trypan blue stained-leaves. Scale bars, 270 microns. Arrows indicate dead cells. (C) RNA gel blot showing transript levels of *PR-1* gene. Ethidium bromide staining of rRNA was used as the loading control.

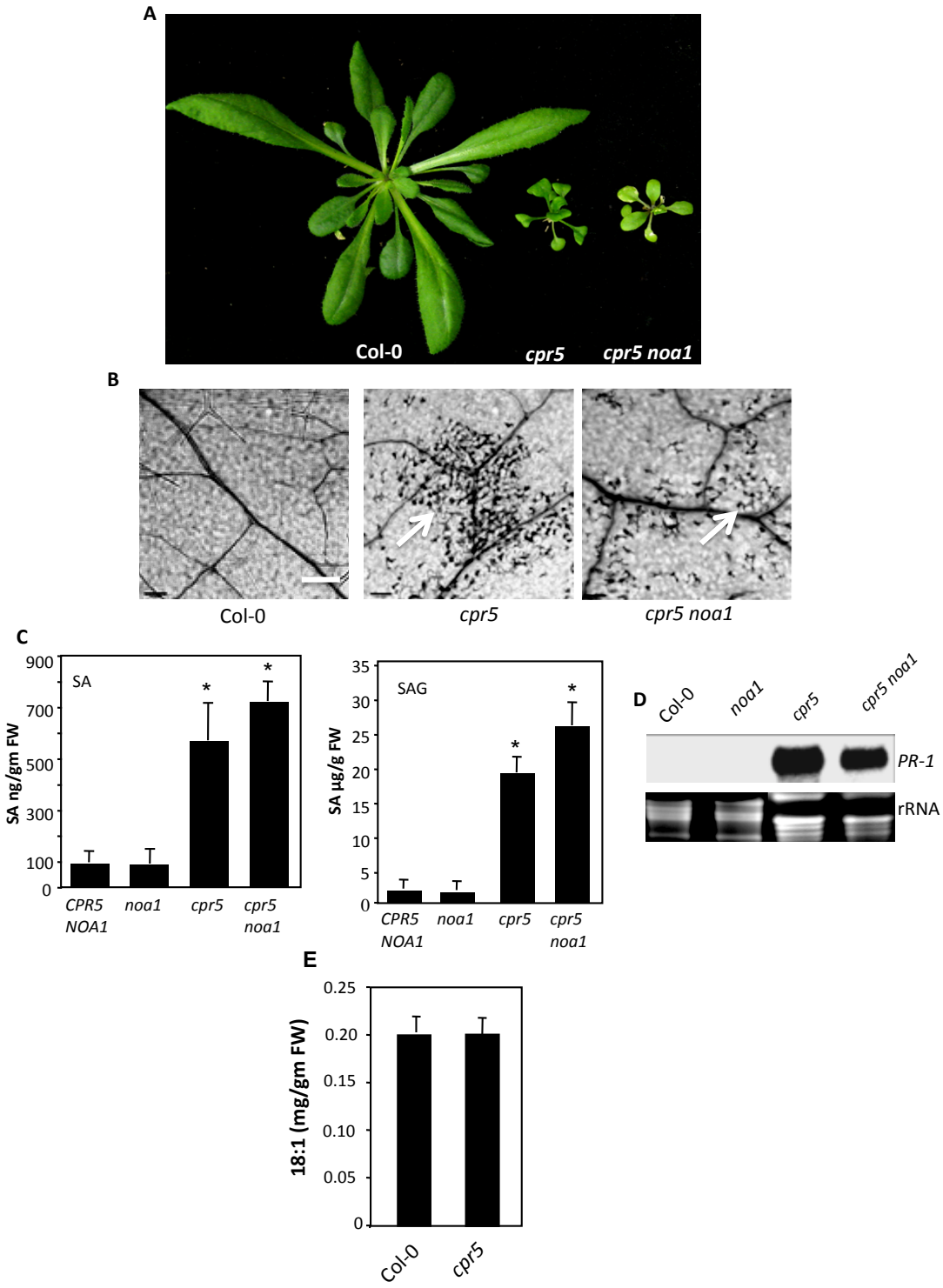

Figure 3.7. A mutation in *NOA1* does not restore constitutive defense phenotypes

Figure 3.7. A mutation in *NOA1* does not restore constitutive defense phenotypes in *cpr5* plants. (A) Morphological phenotype of four-week-old plants. (B) Microscopy of trypan blue-stained leaves. Scale bars, 270 microns. Arrows indicate dead cells. (C) SA and SAG levels in indicated genotypes. The error bars represent SD (n=3). Asterisks denote a significant difference with wild-type (*t* test, $P<0.05$). (D) RNA gel blot showing transript levels of *PR-1* gene. Ethidium bromide staining of rRNA was used as the loading control. (E) 18:1 levels in wild-type Col-0 and *cpr5* plants. The error bars represent SD (n=6).

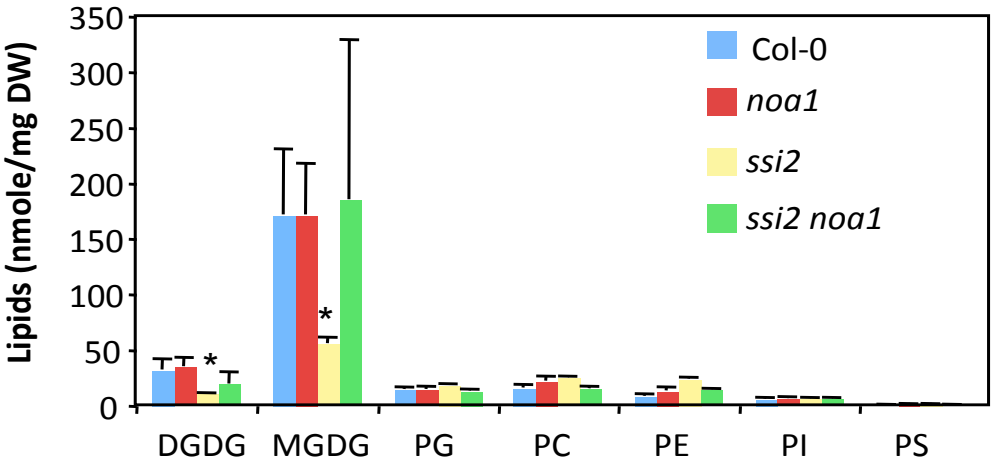

Figure 3.8. Profile of total lipids extracted from wild-type (Col-0), *noa1*, *ssi2* and *ssi2 noa1* plants. The values are presented as an average of 5 replicates. The error bars represent SD. Asterisks denote a significant difference with wild-type (*t* test, $P<0.05$, n=5). Symbols for various components are: DGDG, digalactosyldiacylglycerol; MGDG, monogalactosyldiacylglycerol; PG, phosphatidylglycerol; PC, phosphatidylcholine; PE, phosphatidylethaloamine; PI, phosphatidylinositol; PS, phosphatidylserine.

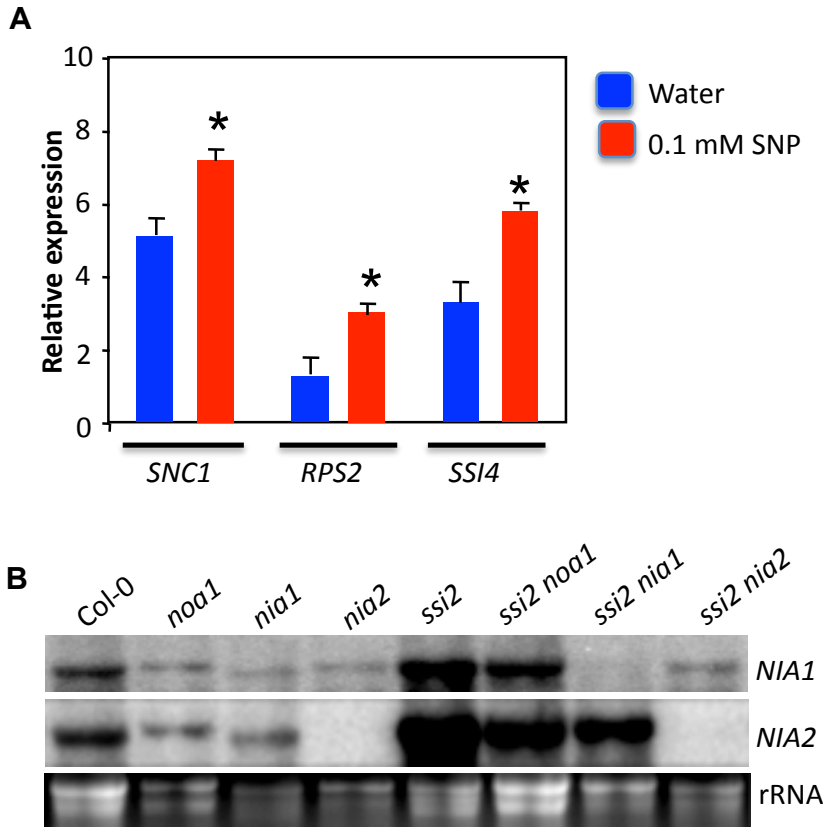

Figure 3.9. Expression of *R* and the *NIA1/NIA2* genes is induced by NO and low 18:1 conditions, respectively. (A) Quantitative RT-PCR analysis showing relative levels of *SNC1*, *RPS2* and *SSI4* genes in wild-type Col-0 plants treated with water or 0.1 mM SNP. Leaves were sampled 12 h post treatments. Asterisks denote a significant difference with wild-type (*t* test, $P<0.05$, n=3). The error bars represent SD. (B) RNA gel blot showing transcript levels of *NIA1* and *NIA2* genes in indicated genotypes. Ethidium bromide staining of rRNA was used as the loading control.

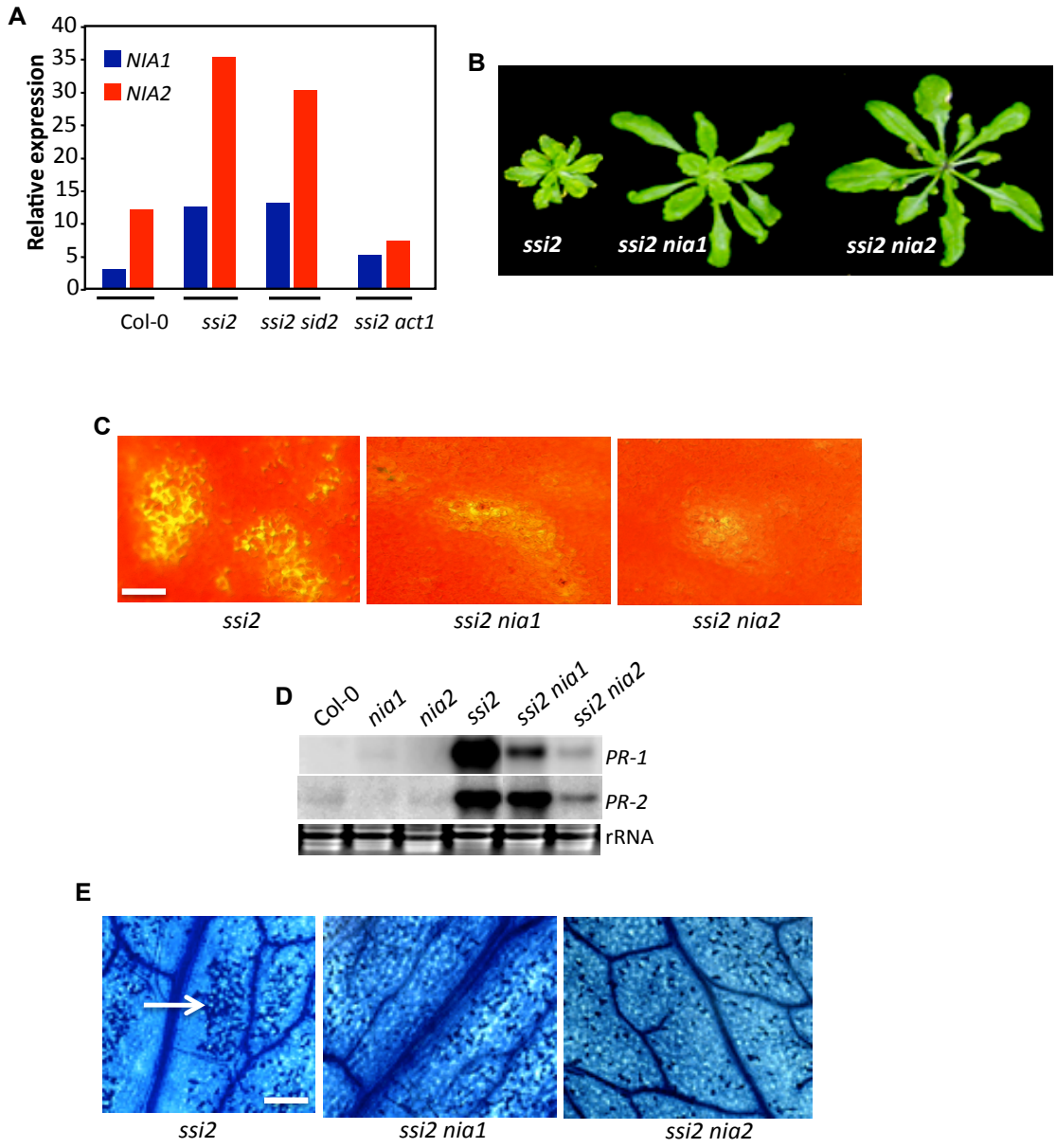

Figure 3.10. NIA1 and NIA2 contribute to NO accumulation in *ssi2* plants. (A) Quantitative RT-PCR analysis showing relative levels of indicated genes. (**B**) Morphological phenotypes of three-week-old plants. (**C**) Fluorescence microscopy of DAF-FM DA-infiltrated leaves using an epifluorescent microscope. Scale bar, 270 microns. (**D**) RNA gel blot showing transript levels of *PR-1* and *PR-2* genes. Ethidium bromide staining of rRNA was used as the loading control. (**E**) Trypan blue stained-leaves showing microscopic cell death phenotype on indicated genotypes.

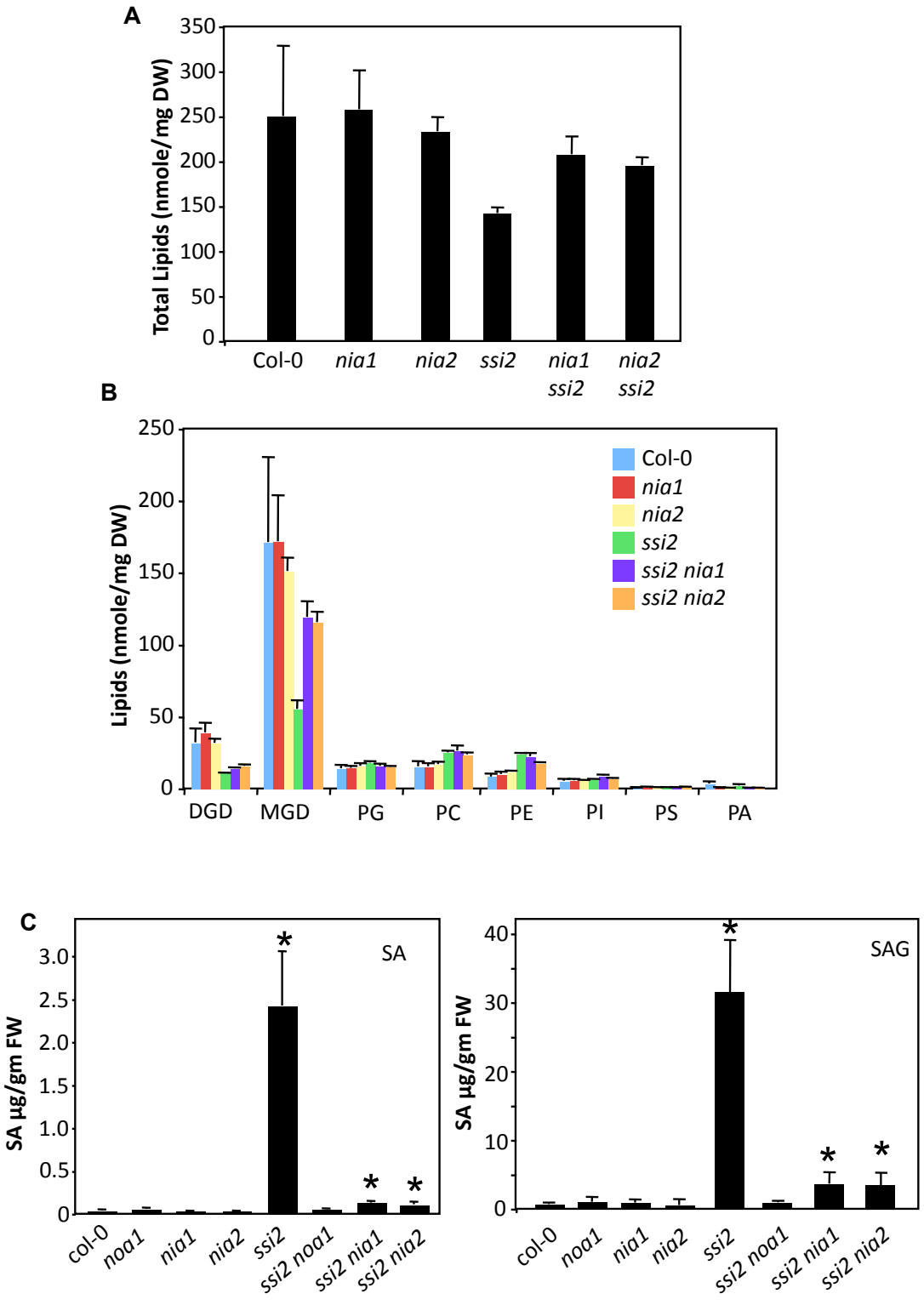

Figure 3.11. Mutations in *NIA1* and *NIA2* partially restore *ssi2* phenotypes.

Figure 3.11. Mutations in *NIA1* and *NIA2* partially restore *ssi2* phenotypes. (A) Total lipid levels in indicated genotypes. DW indicates dry weight. The error bars represent SD. (B) Profile of total lipids extracted from wild-type (Col-0), *nia1*, *nia2*, *ssi2*, *ssi2 nia1* and *ssi2 nia2* plants. The values are presented as an average of 5 replicates. The error bars represent SD. (C) SA and SAG levels in indicated genotypes. The error bars represent SD (n=3). Asterisks denote a significant difference with wild-type (*t* test, $P<0.05$).

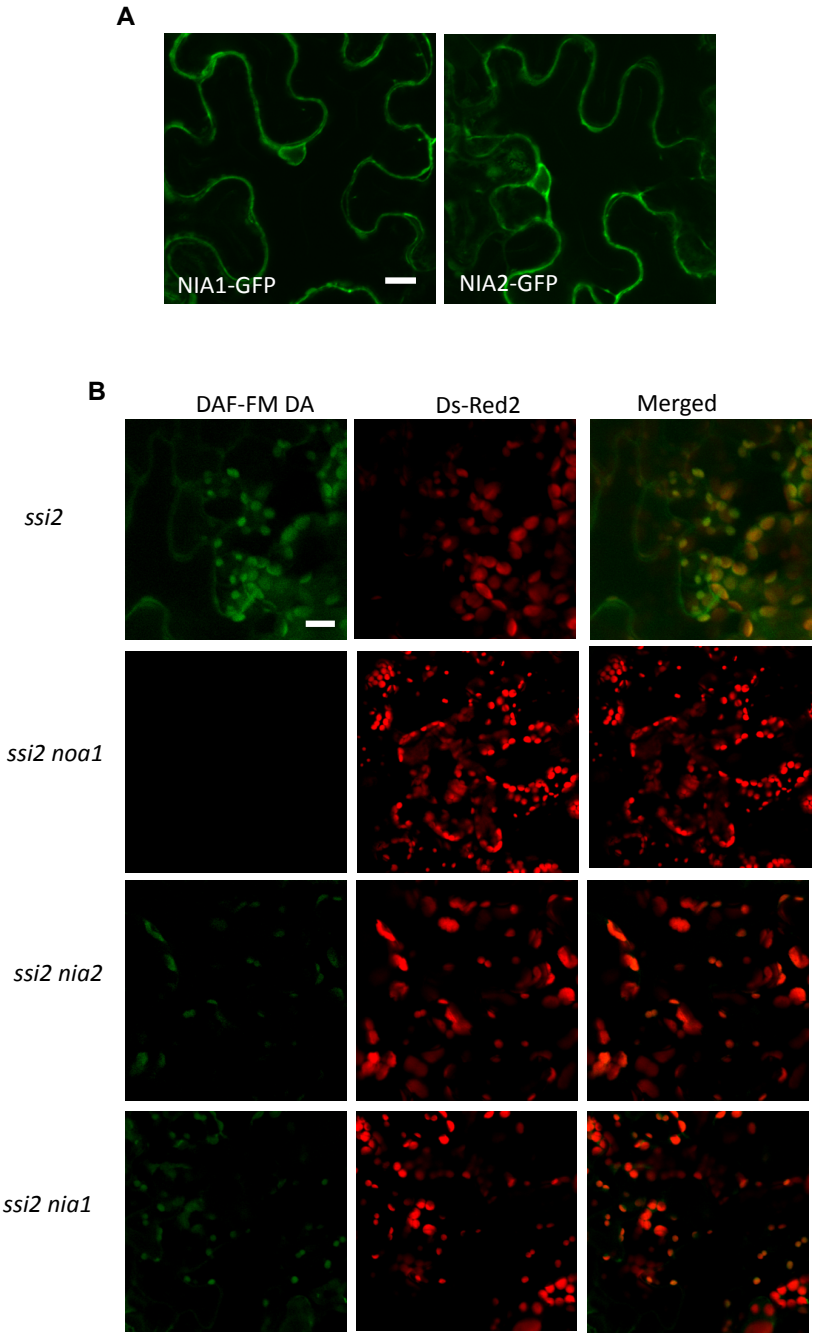

Figure 3.12. NIA1 and NIA2 are extrachloroplastic proteins required for chloroplastic NO accumulation in *ssi2* plants. (A) Confocal micrograph showing localization of NIA1-GFP and NIA2-GFP protein in *Nicotiana. benthamiana*. Scale bar, 5 µm (B) Confocal micrograph of DAF-FM DA-stained leaves showing subcellular location of NO in indicated genotypes. Scale bar, 10 µm.

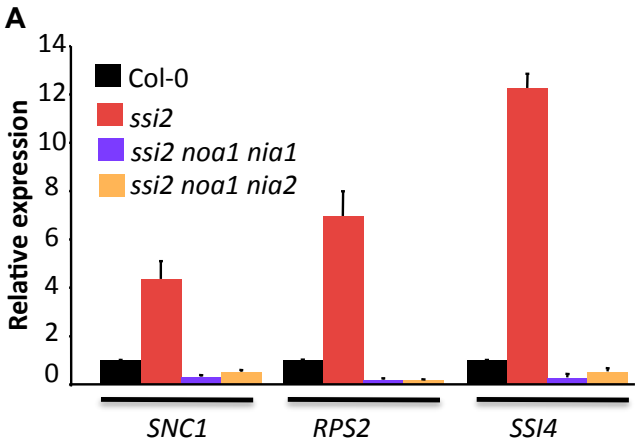
A
Relative expression
14
12
10
8
6
4
2
0
Col-0
ssi2
ssi2 noa1 nia1
ssi2 noa1 nia2
SNC1
RPS2
SSI4

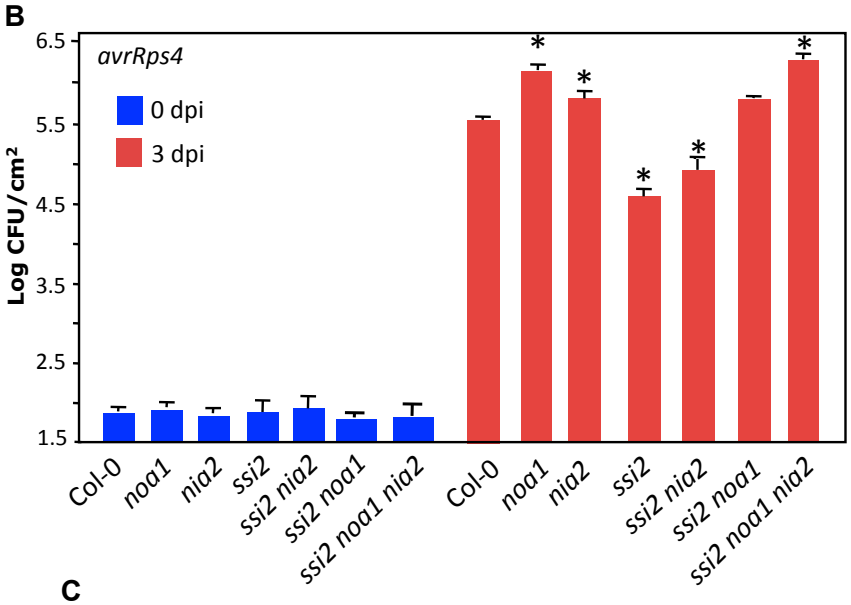
B
avrRps4
0 dpi
3 dpi
Log CFU/cm²
6.5
5.5
4.5
3.5
2.5
1.5
Col-0
noa1
nia2
ssi2
ssi2 nia2
ssi2 noa1
ssi2 noa1 nia2
Col-0
noa1
nia2
ssi2
ssi2 nia2
ssi2 noa1
ssi2 noa1 nia2

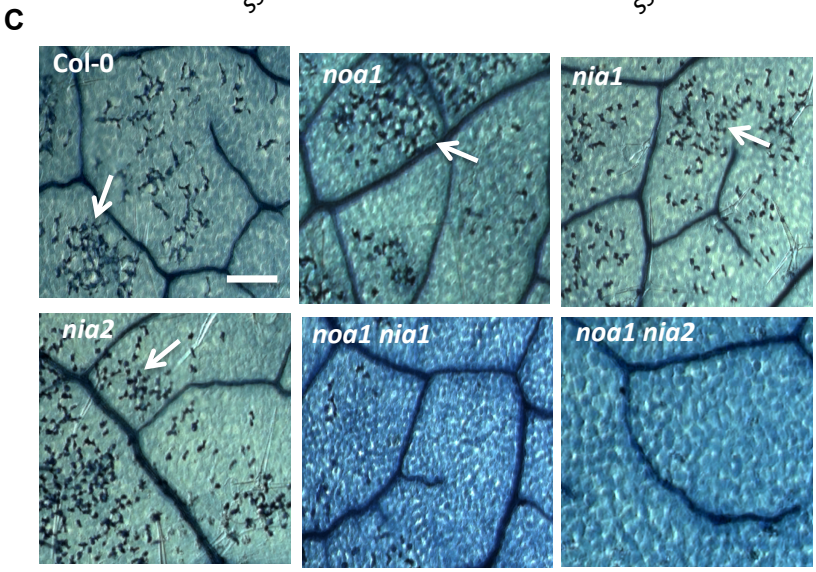
C
Col-0
noa1
nia1
nia2
noa1 nia1
noa1 nia2

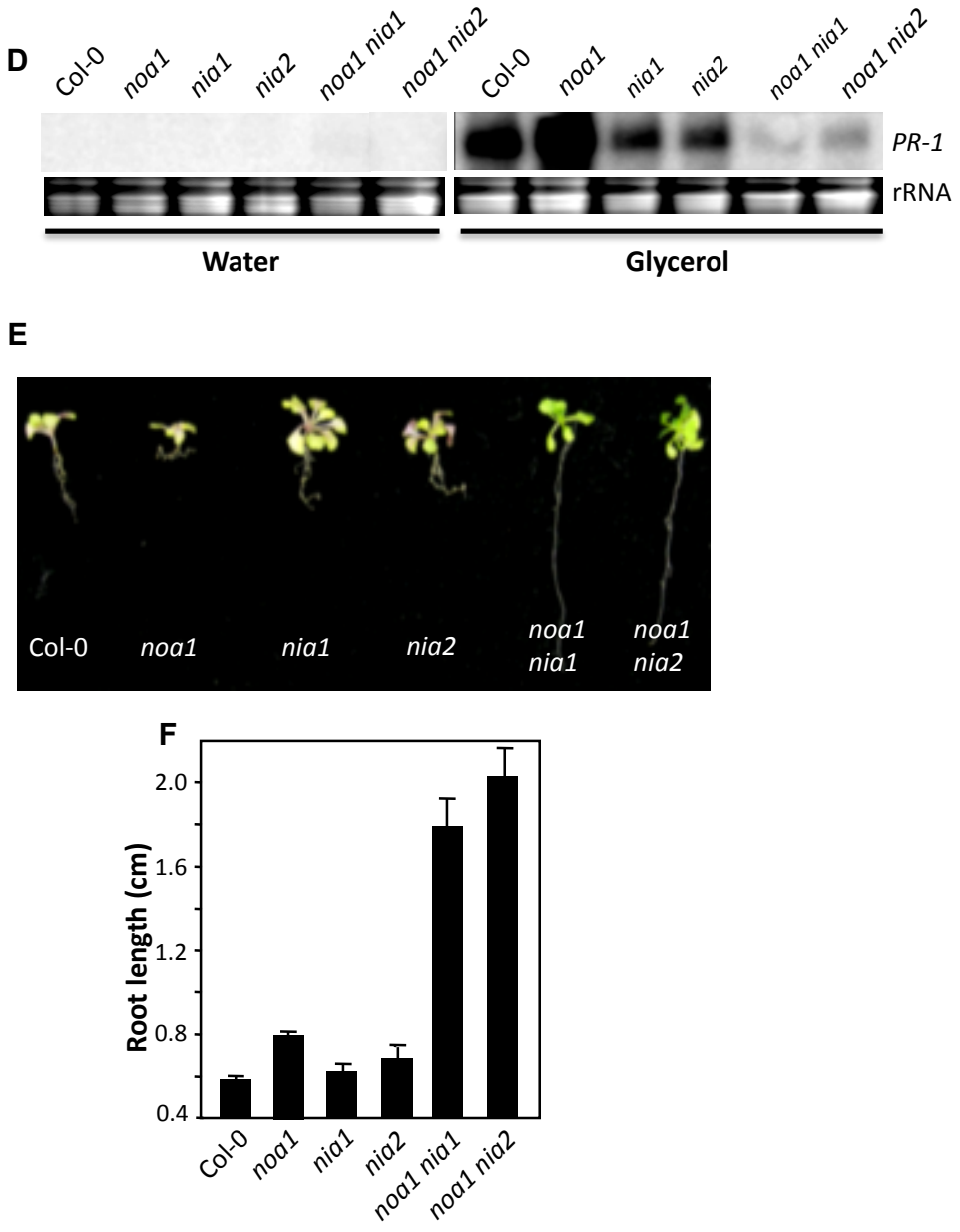

Figure 3.13. NOA1, NIA1 and NIA2 contribute additively to NO accumulation in *ssi2* plants.

Figure 3.13. NOA1, NIA1 and NIA2 contribute additively to NO accumulation in *ssi2* plants. (A) Quantitative RT-PCR analysis showing relative levels of indicated *R* genes. (B) Growth of *avrRps4* bacteria in indicated genotypes. The error bars indicate SD. Asterisks indicate data statistically significant from wild-type (Col-0, $P<0.05$ n=4). (C) Microscopy of trypan blue stained-leaves. Scale bar, 270 microns. Arrows indicate dead cells. (D) RNA gel blot showing transript levels of *PR-1* gene in water- and glycerol- treated plants. Ethidium bromide staining of rRNA was used as the loading control. (E) Morphology and root length of plants grown on MS medium containing 0.2% glycerol. (F) Relative root length of plants grown on MS medium containing 0.2% glycerol. The error bars represent SD.

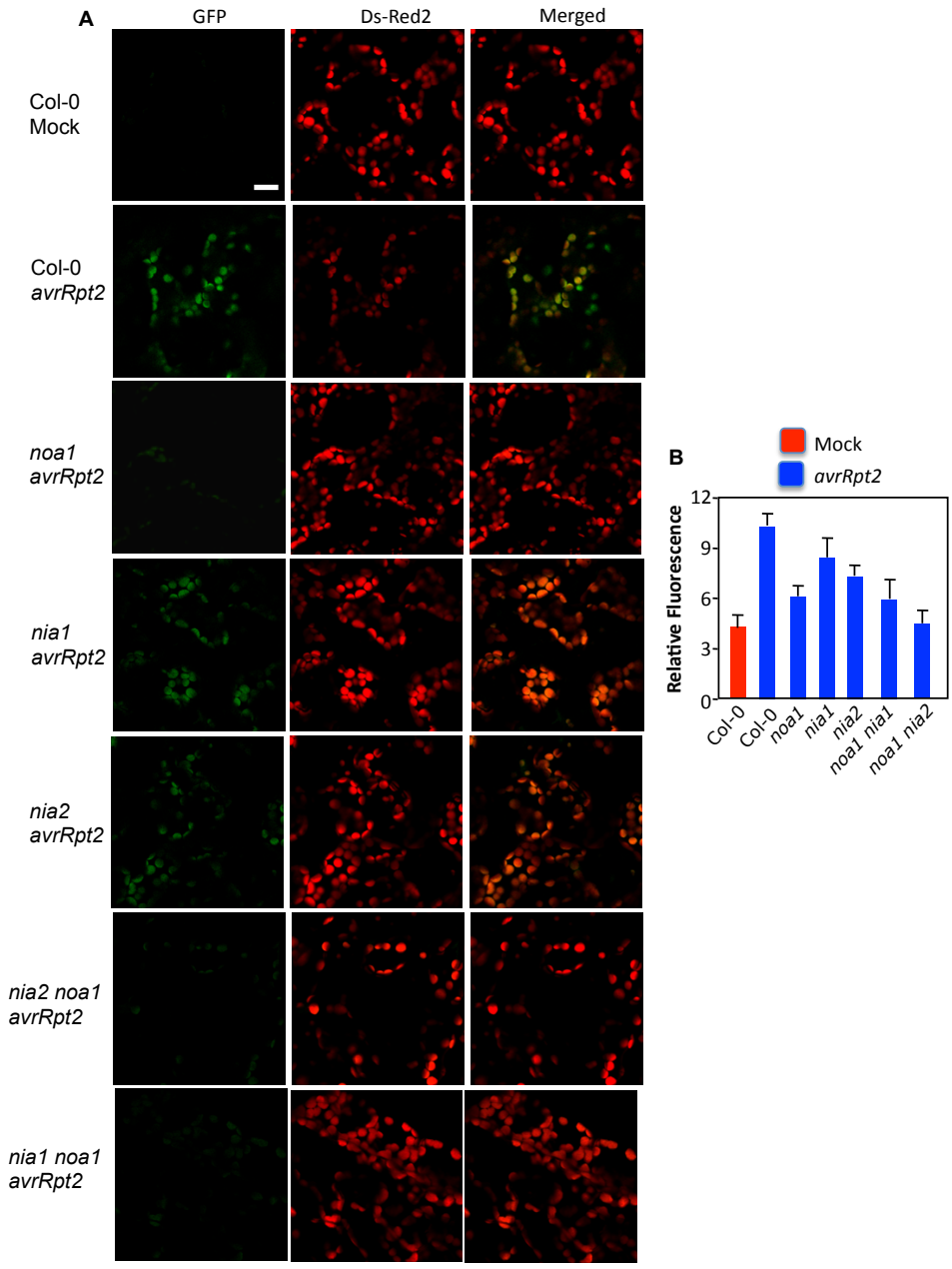

Figure 3.14. The *noa1 nia* plants are compromised in pathogen-induced NO accumulation. (A) Confocal micrograph showing pathogen-induced NO accumulation in indicated genotypes. Plants were inoculated with $MgCl_2$ (mock) or *avrRpt2* expressing *P. syringae*. Scale bar, 20 µm. (B) Relative fluorescence in $MgCl_2$- treated or pathogen-inoculated leaves quantified using a fluorimeter. The relative fluorescence in mock-inoculated *noa1*, *nia1*, *nia2*, *noa1 nia1* and *noa1 nia2* were similar to the mock-inoculated Col-0 plants.

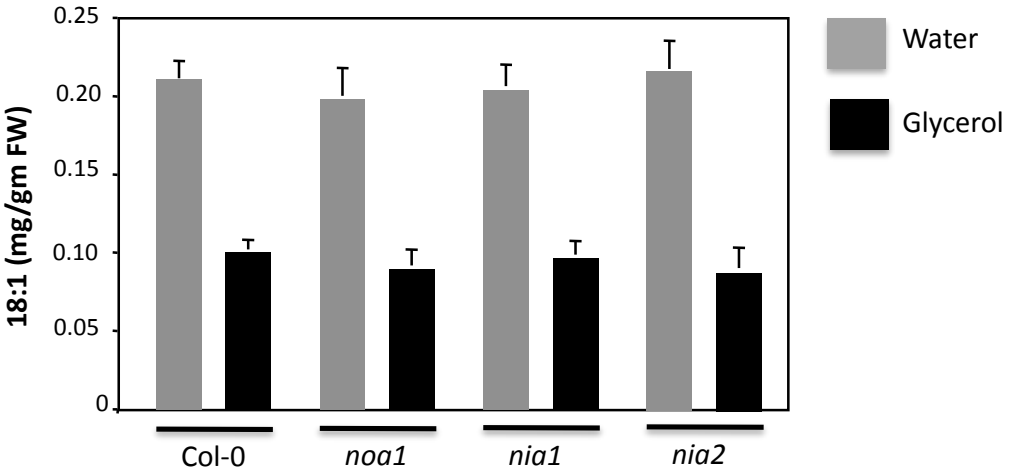

Figure 3.15. The glycerol-treated Col-0, *noa1*, *nia1* and *nia2* plants show similar decrease in their total 18:1 levels. 18:1 levels in water- and glycerol-treated plants. Error bars represent SD.

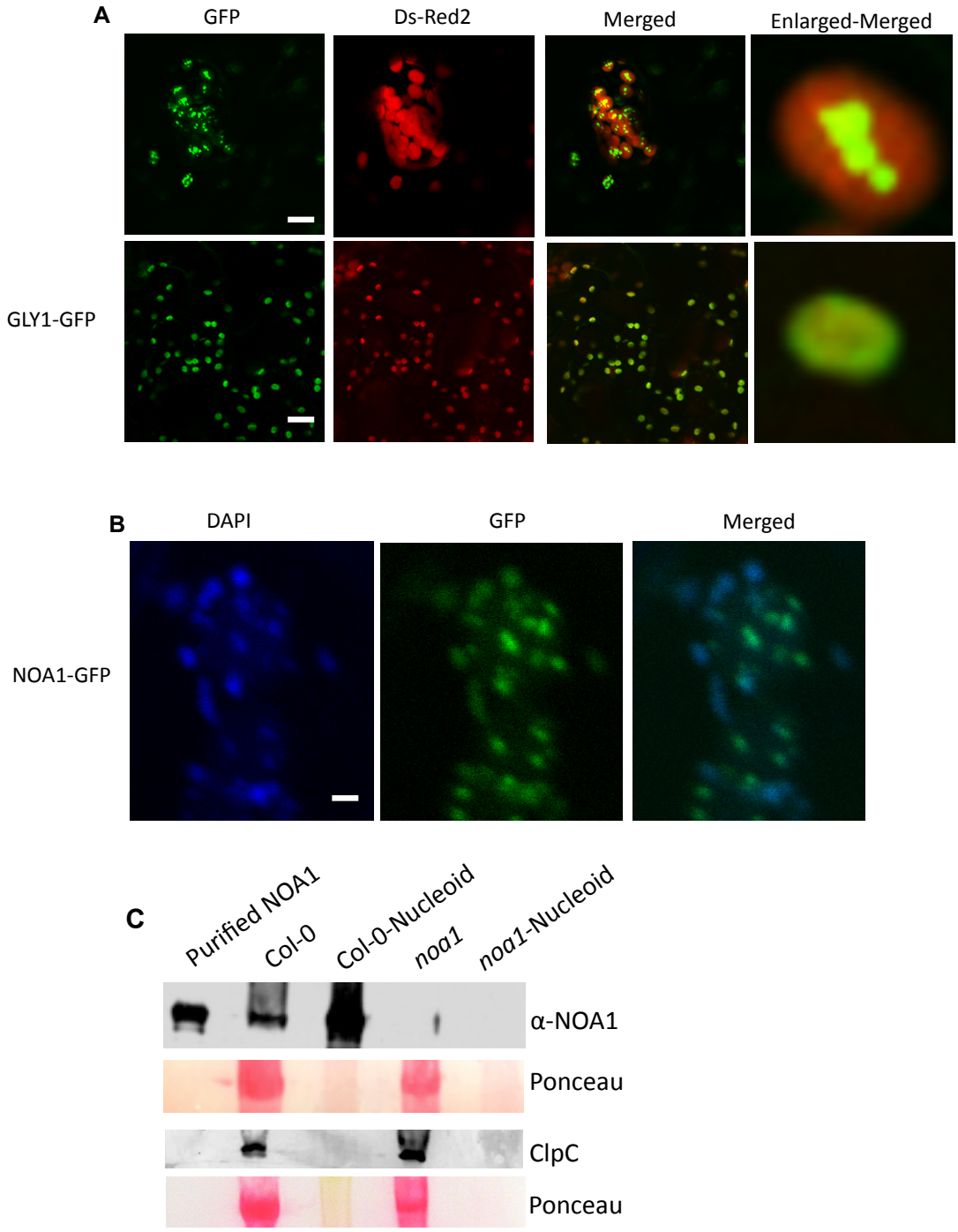
A
GFP
Ds-Red2
Merged
Enlarged-Merged
GLY1-GFP
B
DAPI
GFP
Merged
NOA1-GFP
C
Purified NOA1
Col-0
Col-0-Nucleoid
noa1
noa1-Nucleoid
α-NOA1
Ponceau
ClpC
Ponceau

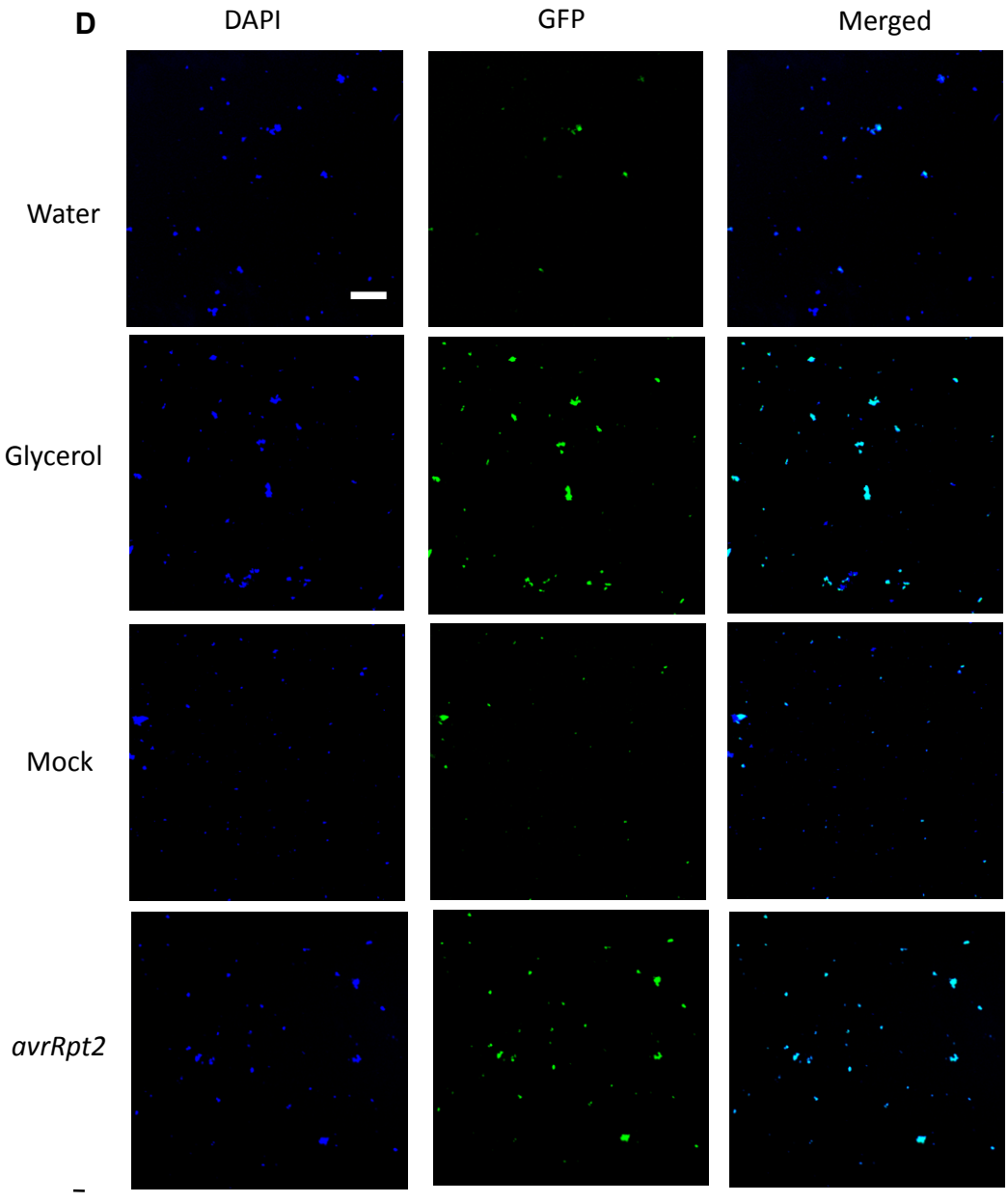
D
DAPI
GFP
Merged
Water
Glycerol
Mock
avrRpt2
-

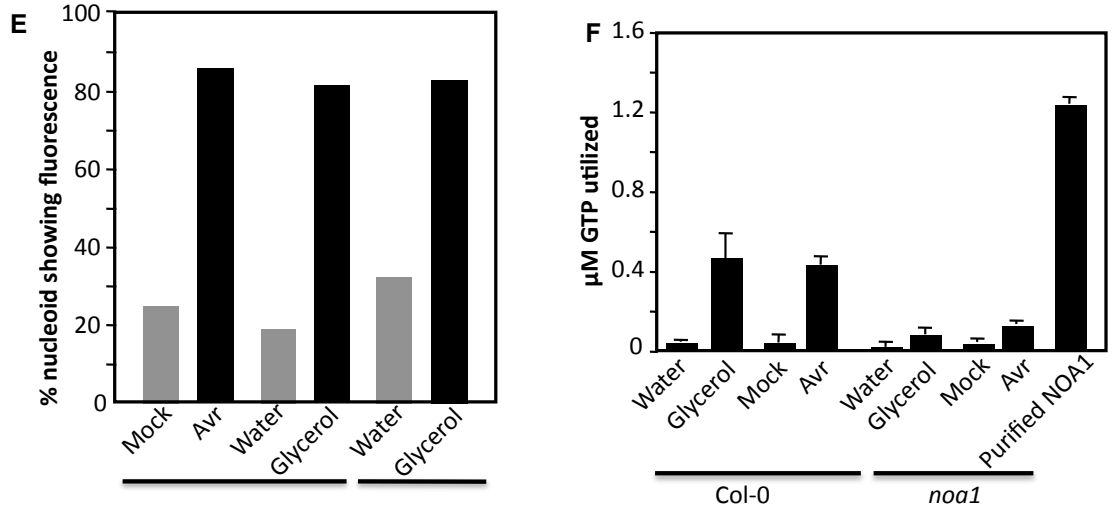

Figure 3.16. GTPase activity of the nucleoid-localizing NOA1 correlates with NO accumulation. (A) Confocal micrograph showing localization of NOA1-GFP and GLY1-GFP proteins. Agroinfiltration was used to express proteins in *Nicotiana benthamiana*. Scale bar, 5 µm (upper panel) and 10 µm (lower panel). Right panel shows enlarged micrographs of individual chloroplasts. (B) Confocal micrograph showing nucleoid-specific localization of NOA1. Agroinfiltration was used to express NOA1-GFP in *Nicotiana. benthamiana* and the leaves were stained with DAPI prior to microscopy. Scale bar, 2 µM. (C) Western blot showing NOA1 levels in the protein extracted from the leaves or the purified nuceloids. *Escherichia coli* purified NOA1 protein was used as a positive control and ClpC as stromal protein control. Ponceau-S staining of the Western blot was used as the loading control. (D) Confocal micrograph showing DAF-FM DA- and DAPI-stained nucleoids. Scale bar, 20 µM. (E) Percentage nucleoids showing fluorescence in water-, glycerol- or pathogen-treated plants. Nucleoids were purified from treated plants and assayed for fluorescence under a confocal microscope. (F) GTPase activity associated with nucleoids purified from water, glycerol or pathogen treated plants at 12 hpi. Protein was extracted from 1 x 10^8 nucleoids and *Escherichia coli* purified NOA1 protein was used as a positive control.

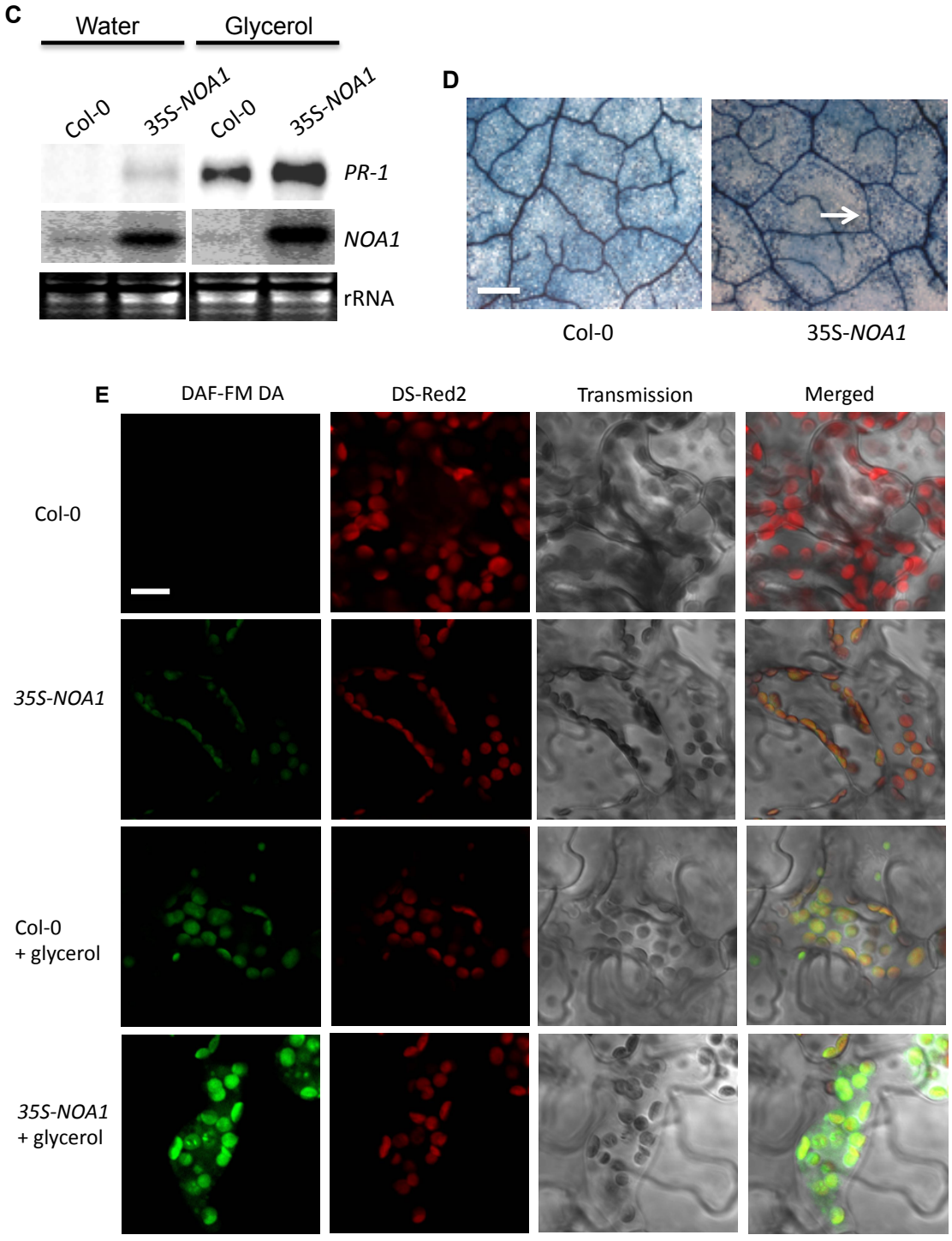

Figure 3.17. Overexpression of *NOA1* potentiates low 18:1-triggered defense phenotypes.

Figure 3.17. Overexpression of *NOA1* potentiates low 18:1-triggered defense phenotypes. (A) Western blot showing NOA1 levels in mock or pathogen (*avrRpt2*)-inoculated Col-0 and *noa1* plants. Leaves were sampled 24 or 48 h post inoculations. Ponceau-S staining of the Western blot was used as the loading control. (B) Western blot showing NOA1 levels in water- or glycerol-treated Col-0 and untreated four-week-old *ssi2*, *ssi2 nia1* and *ssi2 nia2* plants. Plants were treated with glycerol for 24 h prior to sampling. Ponceau-S staining of the Western blot was used as the loading control. (C) RNA gel blot showing transript levels of *PR-1* and *NOA1* genes in water- and glycerol-treated plants. Ethidium bromide staining of rRNA was used as the loading control. (D) Microscopy of glycerol-treated leaves stained with trypan blue 24 h post treatment. Scale bars, 270 microns. Arrow indicates dead cells. (E) Confocal micrograph of DAF-FM DA-stained leaves showing relate NO levels in water- and glycerol-treated plants. Scale bar, 10 μm.

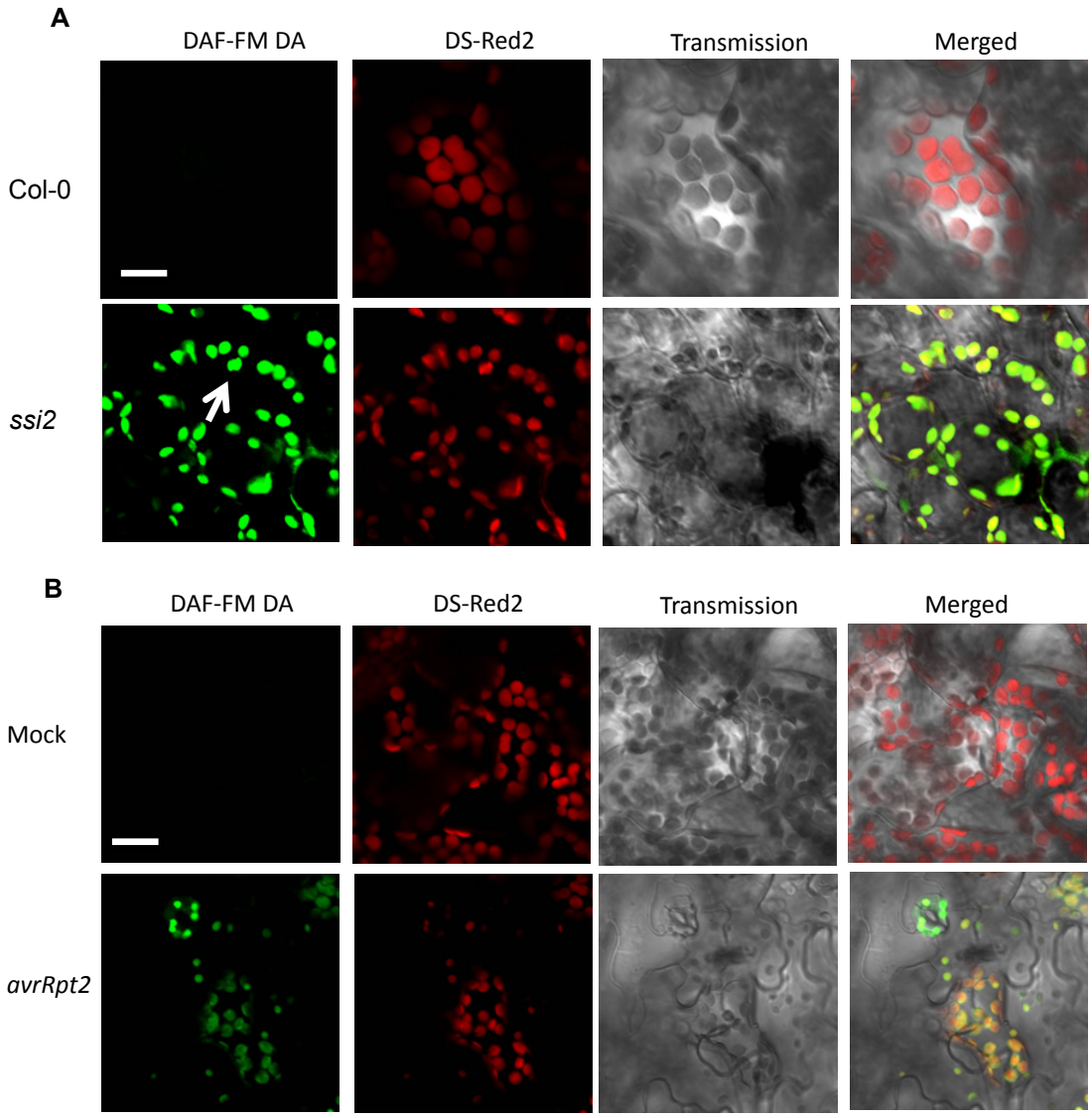

Figure 3.18. Subcellular localization of NO in *ssi2* and *avrRpt2*-inoculated wild-type plants. (A) Confocal micrograph of DAF-FM DA-stained leaves showing subcellular location of NO in wild-type (Col-0), and *ssi2* plants. Scale bar, 10 µm. Chloroplast autofluorescence (red) was visualized using Ds-Red2 channel. Arrow indicates chloroplast. At least ten independent leaves were analyzed in four experiments with similar results. (B) Confocal micrograph showing pathogen-induced NO accumulation in Col-0 plants at 12 hours post inoculation. Plants were inoculated with $MgCl_2$ (mock) or *avrRpt2 Pseudomonas syringae*. Scale bar, 10 µm. At least ten independent leaves were analyzed in four experiments with similar results.

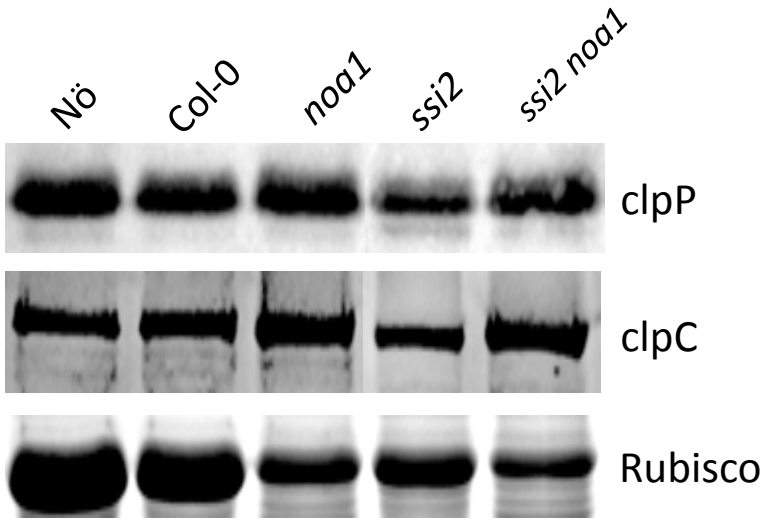

Figure 3.19. Levels of clpC and clpP in *ssi2* plants. Western blot showing levels of clpC, clpP levels in wild-type (*SSI2*), *noa1*, *ssi2* and *ssi2 noa1* plants. Ponceau-S staining of the Western blot was used as the loading control.

A

FABP1	NFEAFMKAIG-LPEFTVGEECE	IITNTMTLGDIVFKRISKR
FABP2	NYDKFMEKMG-VNVFELGVTFN	ELVQTYVYEGVEAKRIFKK
FABP3	NFDDYMKSLG-VGSFKLGVEFD	KLILTLTHGTAVCTRTYEK
FABP4	NFDDYMKEVG-VGSFILGQEFD	KLVVECVMKGVTSTRVYER
FABP5	GFDEYMKELG-VGSCTLGEKFE	KLVVECVMNNVTCTRIYEK
FABP6	NYDEFMKLLG-ISKFTVGKESN	KLVEVSTIGGVTYERVSKR
FABP7	NFDEYMKALG-VGSFQLGEEFD	KMVMTLTFGDVVAVRHYEK
FABP8	NFDDYMKALG-VGSFKLGQEFE	KMVAECKMKGVVCTRIYEK
FABP9	NFEDYMKELG-VNSFKLGEEFD	KMVVECKMNNIVSTRIYEK
NOA1	SHGHMITAVGGNGGYPGGKQFV	KLVDIVDFNGSFLARVRDL

B

Arabidopsis, NOA1	LSHGHMITAVGGNGGYPGGKQ
A. lyrata	LSHGHMITAVGGNGGYSGGKQ
Nicotiana attenuata	LSHGHMITAVGGNGGYSGGKQ
N. benthamiana	LSHGHMITAVGGNGGYSGGKQ
Oryza sativa	LSHGHMITAVGGHGGYPGGKQ
Solanum tuberosum	LSHGHMITAVGGNGGYSGGKQ
Ricinis communis	LSHGHMITAVGGNGGYSGGKQ
Populus trichocarpa	LSHGHMITAVGGNGGYSGGKQ
Hordeum vulgare	LSHGHMVTAVGGHGGYPGGKQ
Vitis vinifera	LSHGQMITAVGGNGGYSGGKQ
Zea mays	LSHGHMVTAVGGHGGYPGGK
Arabidopsis, NOA1	KLVDIVDFNGSFLARVRDL
Nicotiana attenuata	KLVDIVDFNGSFLARVRDL
N. benthamiana	KLVDIVDFNGSFLARVRDL
Solanum tuberosum	KLVDIVDFNGSFLARVRDL
Brassica juncea	KLVDIVDFNGSFLARVRDL
Picea sitchensis	KLVDIVDFNGSFLARVRDL
Oryza sativa	KLVDIVDFNGSFLARVRD
Vitis vinifera	KLVDIVDFNGSFLAHVRDL
Hordeum vulgare	KLVDIVDFNGSFLARIRD
Medicago truncatula	KLVDVVDFNGSFLSRVRDL
Populus trichocarpa	KLVDVVDFNGSFLARLRDL

Figure 3.20. Fatty acid-binding properties of NOA1. (A) Amino acid (aa) alignment of conserved FA binding domains of mammalian FA binding proteins (FABP) and NOA1. The members of the FABP family show 22-73% aa sequence similarity (Zimmerman and Veerkamp 2002). Identical residues are shaded in red. Residues common between NOA1 and most other FABPs are shaded in green. These domains in left and right panels represent aa 151-171 and 193-211 of NOA1 protein, respectively. Sequence alignment was carried out using ClustalW in the Megalign program of the DNASTAR package. (B) Amino acid alignment of putative FA-binding domains of NOA1-like plant proteins.

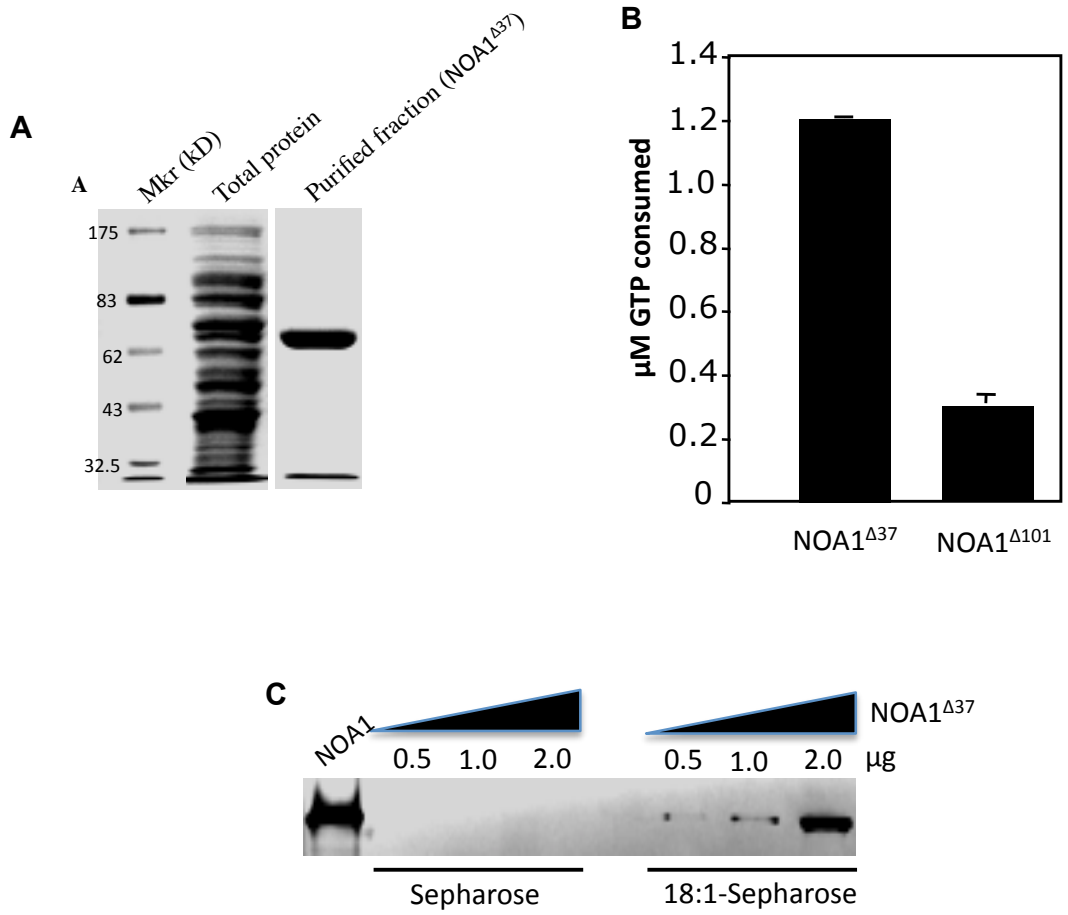

Figure 3.21. N-terminal 37-101 amino acids are critical for NOA1 GTPase activity. (A) SDS-PAGE gel showing NOA1-HIS$^{\Delta 37}$ protein in total and purified fractions. (B) Comparison of GTPase activity of NOA1-HIS lacking N-terminal 37 or 101 amino acids. 100 µM GTP and 2 µM NOA1-HIS were used for the assay and levels of GDP were measured using reverse phase HPLC. (C) 18:1 affinity chromatography carried out using 0.5, 1, or 2 µg of *Escherichia coli* purified NOA1-HIS$^{\Delta 37}$ protein.

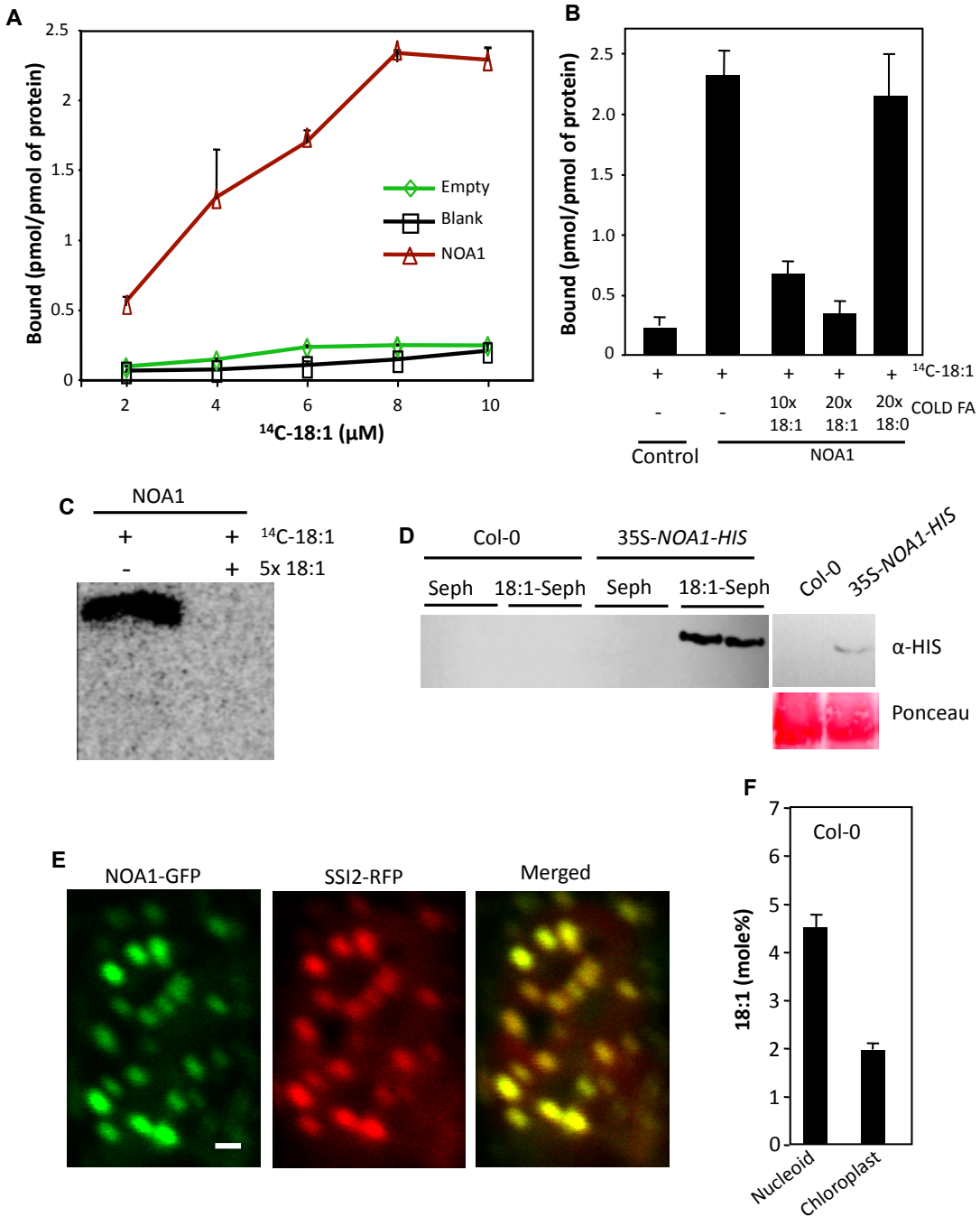

Figure 3.22. **NOA1 binds to 18:1 and co-localizes with SSI2.**

Figure 3.22. **NOA1 binds to 18:1 and co-localizes with SSI2.** (A) 18:1 binding assay carried out using 2 μM purified NOA1, 2 μM total protein extracted from pET28a-transformed *Escherichia coli* (empty), or without any protein (blank). (B) 18:1 binding assay carried out in the presence or absence of 10x and 20x of unlabeled 18:1. 2 μM of NOA1 protein and 8 μM of ^{14}C-18:1 was used for the binding assay. (C) Autoradiograph of NOA1 (2 μM) incubated with 8 μM ^{14}C-18:1 or ^{14}C-18:1 with 5x excess unlabeled 18:1 after electrophoresis on a native PAGE. (D) 18:1 affinity chromatography carried out using total protein extracted from 2 g of Col-0 or 35S-*NOA1-HIS* plants. Left panel shows levels of NOA1 protein in the 35S-*NOA1-HIS* plants prior to affinity chromatography. (E) Confocal micrograph showing co-localization of NOA1-GFP and SSI2-RFP in *Nicotiana benthamiana* plants. Scale bar, 2 μm. (F) Levels of 18:1 in nucleoid versus whole chloroplasts of Col-0 plants.

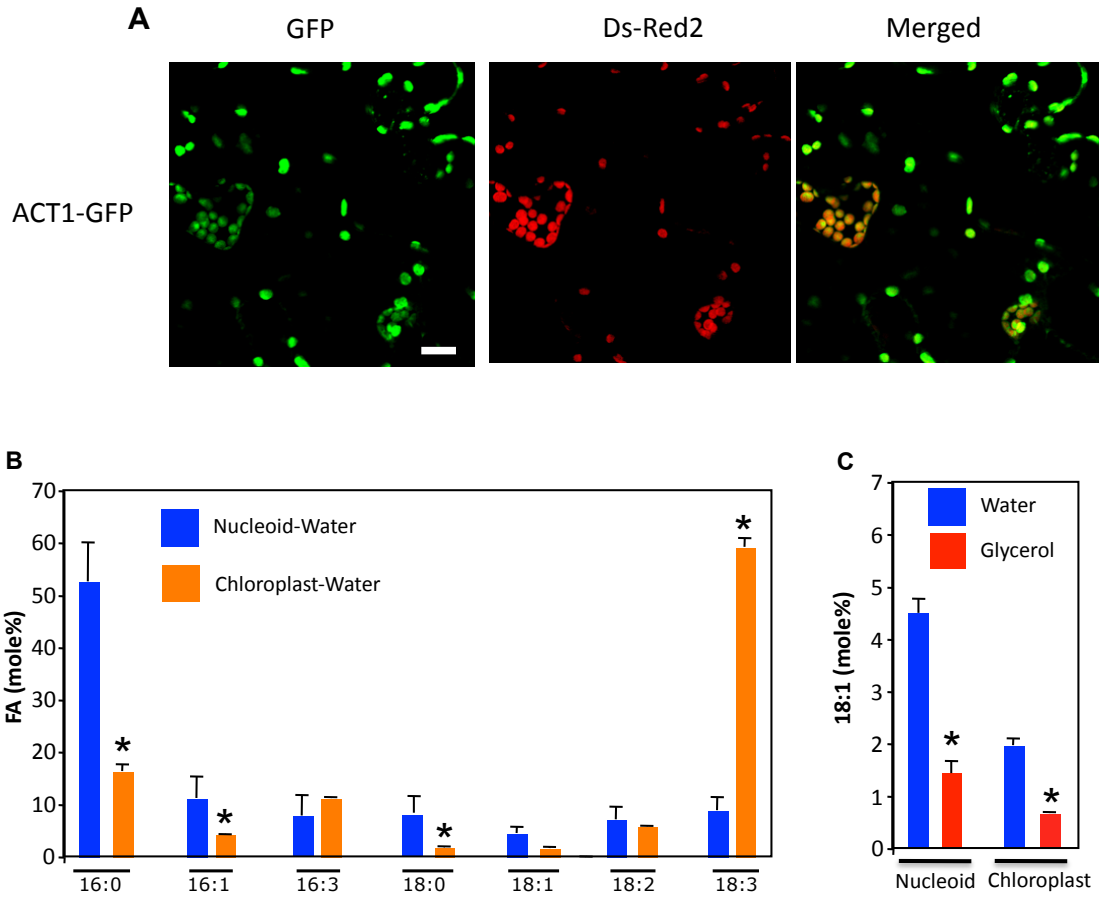

Figure 3.23. Localization of ACT1 and fatty acid analysis of nucleoids. (A) Confocal micrograph showing localization of ACT1-GFP protein in *N. benthamiana*. Scale bar, 10 μm. (B) Fatty acid profile of purified chloroplasts and the nucleoids, which were isolated from plants treated with water or glycerol. Error bars represent SD (n=6). Asterisks denote a significant difference between the FA species present in nucleoids versus chloroplasts (*t* test, P<0.05). (C) 18:1 levels in purified nucleoid and chloroplasts isolated from wild-type (Col-0) plants treated with water or glycerol. Error bars represent SD (n=6). Asterisks denote a significant difference between water- and glycerol-treated samples (*t* test, P<0.05).

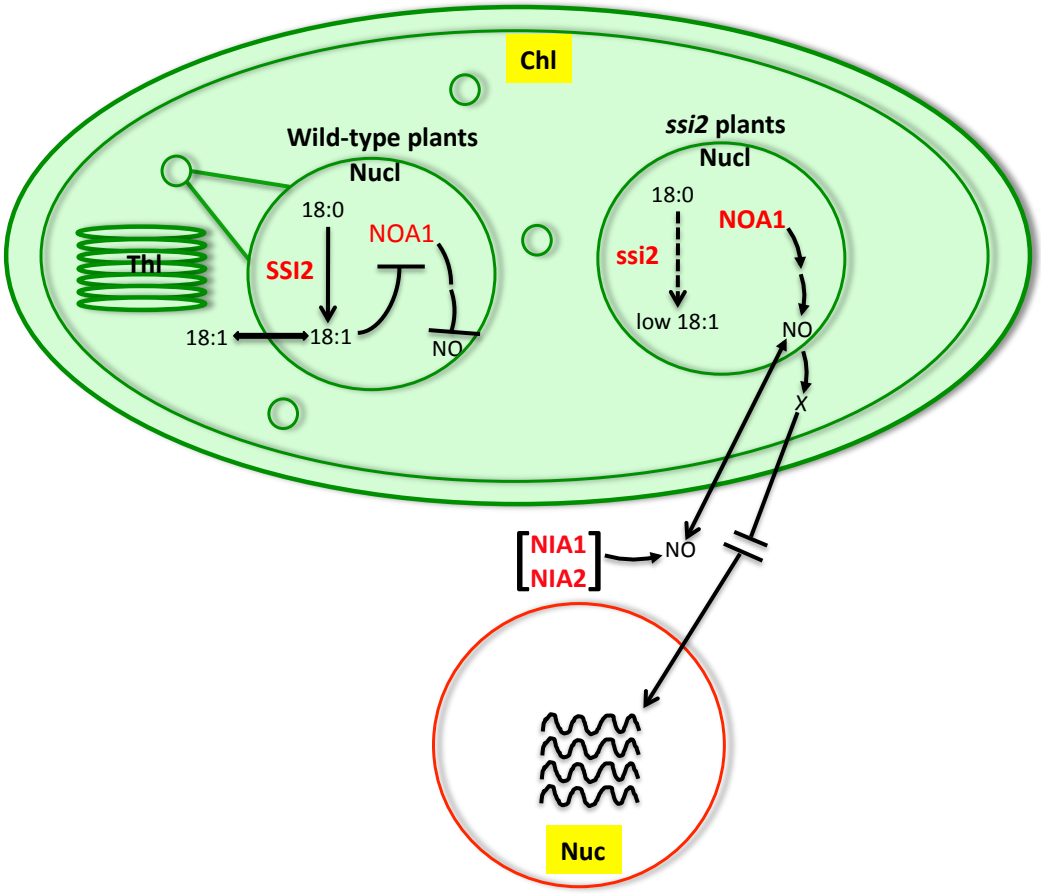

Figure 3.24. A model illustrating 18:1-regulated NO signaling in plants.

Figure 3.24. A model illustrating 18:1-regulated NO signaling in plants. Desaturation of 18:0 to 18:1 is catalyzed by the soluble desaturase SSI2, which is localized in the chloroplastic (Chl, shown as an oval) nucleoids (Nucl, shown as small and big circle inside Chl). 18:1 synthesized in the nucleoids is likely exported to stroma, where it participates in glycerolipid biosynthesis and this reaction is catalyzed by the soluble stromal G3P acyltransferase ACT1. GLY1, a G3P dehydrogenase, which catalyzes biosynthesis of G3P, is also a stromal enzyme (Chanda et al., 2011). 18:1 synthesized in the nucleoids negatively regulates the stability of NOA1, which is also present in the nuceloids. NOA1 levels increase under low 18:1 conditions (due to mutations in *SSI2* or after glycerol application) or in response to pathogen inoculation. This in turn initiates NO biosynthesis in the plastids. A reduction in 18:1 also triggers the increased expression of the extrachloroplastic *NIA1* and *NIA2*, which also contribute to plastidal NO biosynthesis. Mutations in *NIA1*/*NIA2* affect chloroplastic NO production in response to pathogen infection or low 18:1 levels. This suggests that NIA1/NIA2, either feedback regulate NO biosynthesis or that NO made via NIA1/NIA2 enzymes may translocate into chloroplasts. NO produced in response to pathogen infection or low 18:1 triggers nuclear (Nuc) gene expression (indicated by wavy lines). However, NO was not detected in the nucleus, suggesting that NO-mediated nuclear gene expression occurs possibly via unknown intermediate(s) (indicated by X). Alternatively, NO-triggered nuclear gene expression might involve rapid diffusion of NO to the nucleus. NO-mediated increased gene expression results in SA biosynthesis in the chloroplasts, which further potentiates NO-mediated signaling. Thl indicates thylakoids. Enzymes are shown in red. The relative nuclear and chloroplastic sizes are not to scale.

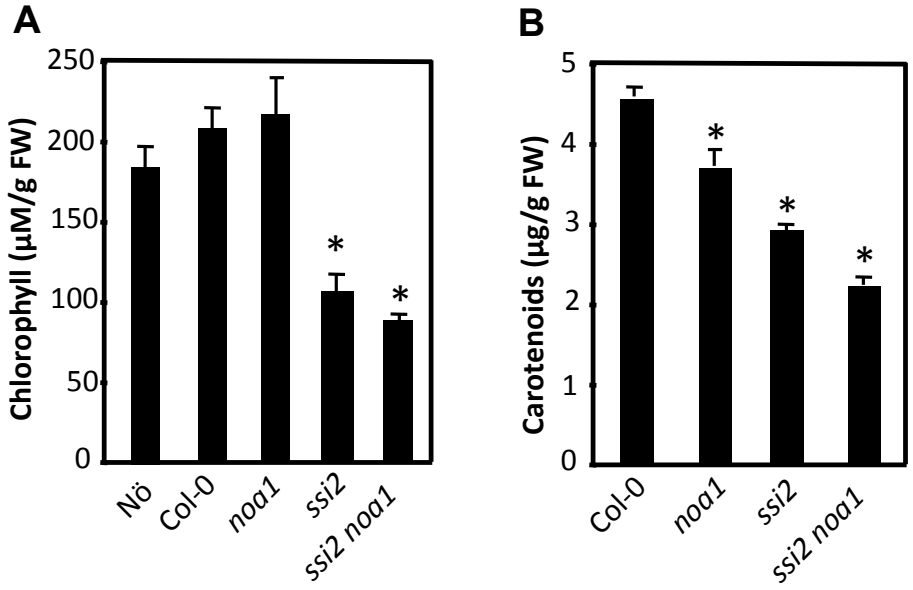

Figure 3.25. Levels of chlorophyll and carotenoids in *ssi2* plants. (A) Levels of chlorophyll in four-week-old soil grown plants. Error bars indicate SD. Asterisks denote a significant difference with wild-type (*t* test, P<0.05, n=4). (B) Levels of carotenoids in four-week-old soil-grown plants. Error bars indicate SD. Asterisks denote a significant difference with wild-type (*t* test, P<0.05, n=4).

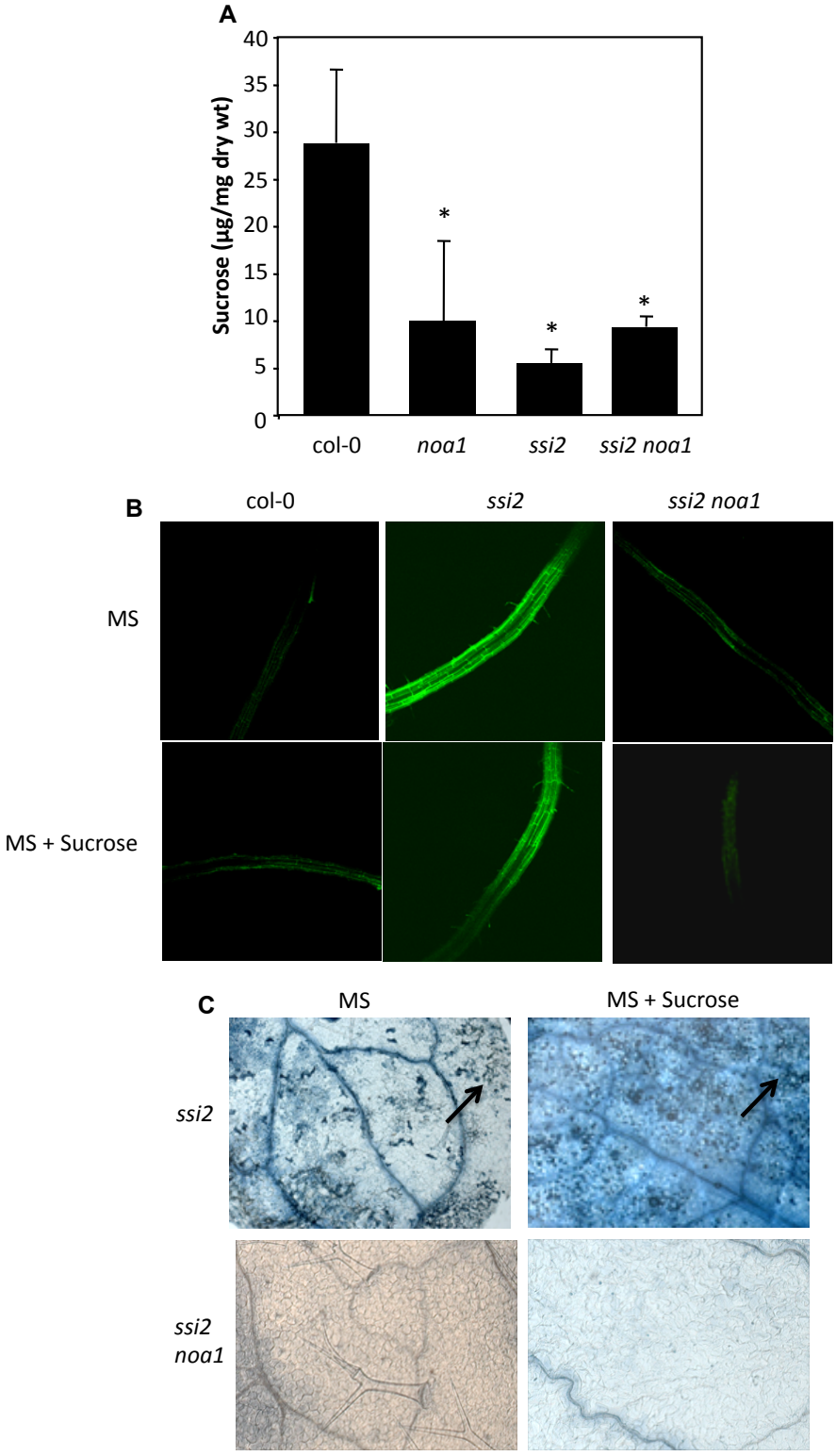

Figure 3.26. Sucrose-grown *ssi2 noa1* plants show wild-type like phenotypes.

Figure 3.26. Sucrose-grown *ssi2 noa1* plants show wild-type like phenotypes. (A) Sucrose levels in wild-type (Col-0), *noa1*, *ssi2* and *ssi2 noa1* plants. Error bars represent SD (n=4). Asterisks denote a significant difference with wild-type (*t* test, $P<0.05$, n=3). (B) Confocal micrograph showing NO-sensitive fluorescent staining of roots. Ten-day-old seedlings were grown with or without sucrose and stained with DAF-FM DA for 15 min. (C) Microscopy of trypan blue-stained leaves obtained from seedling grown on MS medium with or without sucrose. Scale bar, 270 microns. Arrow indicates dead cells.

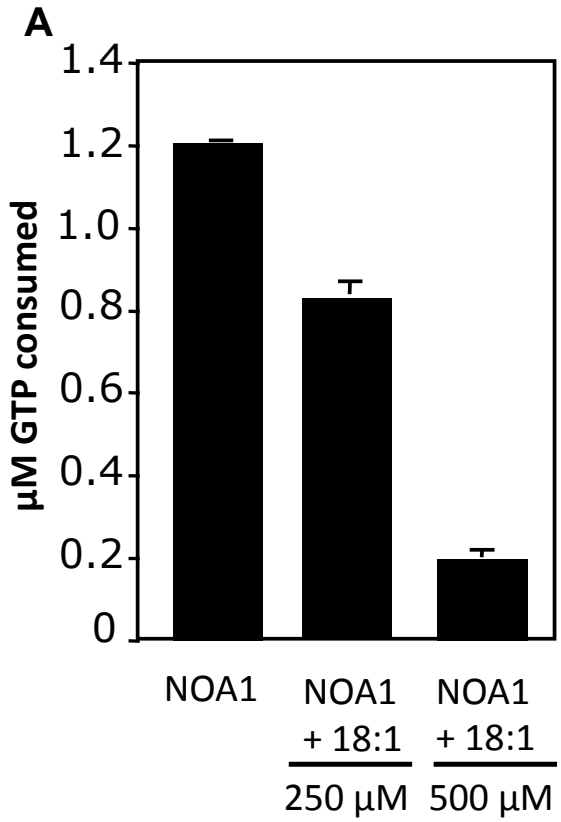

Figure 3.27. GTPase activity in the presence of 18:1. Comparison of GTPase activity of NOA1-HIS lacking N-terminal 37 amino acids in the presence of 250 µM and 500 µM 18:1

Table 3.1. Fold change in transcript levels of genes in *ssi2*, *ssi2 sid2* and *ssi2 act1* plants compared to results from Col-0 (wild-type) plants. Genes showing 2-3, 3-4 and >4-fold activation are marked yellow, orange or red, respectively. Transcriptional profiling was performed using Affymetrix arrays.

Overall_F_ Pvalue	AGI_No	Descriptions	ssi2/Col-0	ssi2 sid2/ Col-0	ssi2 act1/ Col-0	Fold up: SNP
2.65E-06	AT2G15020	hypothetical protein predicted by genscan and genefinder	27.38	117.86	0.23	2.82
0.000185284	AT5G59820	zinc finger protein Zat12 ; supported by full-length cDNA: Ceres:40576.	27.28	16.63	2.23	5.70
2.84E-05	AT1G62300	unknown protein similar to putative DNA-binding protein GI:7268215 from *Arabidopsis thaliana*; supported by cDNA: gi_12658409_gb_ AF331712.1_ AF331712	24.63	10.44	2.99	3.11
1.12567E-05	AT1G26380	hypothetical protein similar to reticuline oxidase-like protein GB:CAB45850 GI:5262224 from *Arabidopsis thaliana*; supported by cDNA: gi_13430839_gb_ AF360332.1_AF360332	19.20	2.66	0.38	16.72
0.000535106	AT3G25610	ATPase II, putative similar to GB:AAD34706 from *Homo sapiens* (Biochem. Biophys. Res. Commun. 257 (2), 333-339 (1999))	18.06	4.86	3.86	1.91
1.70535E-08	AT1G78410	hypothetical protein predicted by genemark.hmm; supported by full-length cDNA: Ceres:157	16.58	4.41	1.40	10.20

Overall_F_ Pvalue	AGI_No	Descriptions	ssi2/Col-0	ssi2 sid2/ Col-0	ssi2 act1/ Col-0	Fold up: SNP
0.007214732	AT2G32030	putative alanine acetyl transferase	16.23	7.52	2.00	2.98
0.000247702	AT1G64780	ammonium transporter, puitative similar to ammonium transporter GI:5880357 from *Arabidopsis thaliana*; supported by cDNA:gi_4324713_gb_AF110771.1_ AF110771	14.91	75.97	0.64	2.84
0.00264441	AT5G01540	receptor-like protein kinase receptor-like protein kinase - *Arabidopsis thaliana*, EMBL:ATLECGENE; supported by cDNA: gi_13605542_gb_AF361597.1_ AF361597	14.24	6.99	0.82	2.08
4.24318E-05	AT1G68620	unknown protein ; supported by cDNA: gi_14335125_gb_AY037242.1	14.14	2.54	0.33	3.23
0.007304582	AT2G15480	putative glucosyltransferase	12.67	3.69	2.12	23.05
0.005796435	AT1G24140	putative metalloproteinase similar to GB:AAB61099	12.65	5.80	1.10	2.76
0.000933283	AT4G34131 /// AT4G34135	glucosyltransferase -like protein immediate-early salicylate-induced glucosyltransferase, *Nicotiana tabacum*, PIR2:T03747; supported by cDNA gi:14334981	12.53	2.44	0.44	15.87
1.46538E-05	AT3G17609	Expressed protein ; supported by full-length cDNA: Ceres: 35429	12.20	20.66	0.41	2.74

Overall_F_ Pvalue	AGI_No	Descriptions	ssi2/Col-0	ssi2 sid2/ Col-0	ssi2 act1/ Col-0	Fold up: SNP
0.000105014	AT4G23260	putative protein receptor protein kinase, *Ipomoea trifida*	12.03	20.91	3.40	2.34
0.000107095	AT1G32940	subtilisin-like serine protease contains similarity to subtilase; SP1 GI:9957714 from *Oryza sativa*	10.24	1.19	0.52	2.24
0.002143897	AT4G27657	Expressed protein ; supported by full-length cDNA: Ceres: 12935.	10.16	7.29	1.84	3.09
0.000224729	AT1G02820	late embryogenis abundant protein, putative similar to late embryogenis abundant protein 5 GI:2981167 from *Nicotiana tabacum;* supported by full-length cDNA: Ceres:96540	9.99	25.94	0.35	2.42
6.86744E-06	AT1G21525	hypothetical protein predicted by genemark.hmm	9.85	3.12	0.51	4.87
0.003225156	AT5G57220	cytochrome P450	9.44	5.32	3.41	2.35
0.000144557	AT4G02330	hypothetical protein similar to pectinesterase	9.40	6.00	3.32	1.93
1.0175E-06	AT5G25930	receptor-like protein kinase - like receptor protein kinase 5, *Arabidopsis thaliana*, PIR:S27756	9.32	3.20	2.55	2.59
0.009297397	AT5G54490	putative protein similar to unknown protein (pir||T05752);supported by full-length cDNA: Ceres:109272	9.12	4.90	0.98	3.75

Overall_F_ Pvalue	AGI_No	Descriptions	ssi2/Col-0	ssi2 sid2/ Col-0	ssi2 act1/ Col-0	Fold up: SNP
0.006336533	AT3G25250	protein kinase, putative contains Pfam profile: PF00069 Eukaryotic protein kinase domain	8.96	4.25	1.21	4.34
3.97556E-06	AT2G30140	putative glucosyltransferase	8.78	3.19	0.64	3.60
0.000602576	AT2G23170	unknown protein	8.51	0.09	0.56	15.71
8.50536E-05	AT2G02990	ribonuclease, RNS1 identical to ribonuclease SP:P42813, GI:561998 from *Arabidopsis thaliana;* supported by full-length cDNA: Ceres:27242.	8.47	3.97	0.95	4.99
0.005768497	AT3G21560	UDP-glucose:indole-3-acetate beta-D-glucosyltransferase, putative similar to UDP-glucose:indole-3-acetate beta-D-glucosyltransferase GB:AAB58497	7.77	18.65	0.85	3.07
1.07408E-05	AT1G71330 /// AT3G13080	putative ABC transporter contains Pfam profile: PF00005 ABC transporter	7.49	3.34	0.37	2.46
0.00010308	AT2G34660	ABC transporter (AtMRP2) identical to GB:AF014960; transports glutathione conjugates; supported by cDNA: gi_2909780_gb_AF020288.1_AF020288	7.35	7.20	1.09	3.13
7.82561E-06	AT5G39050	acyltransferase - like protein Anthocyanin 5-aromatic acyltransferase, *Gentiana triflora,* EMBL:AB010708; supported by cDNA: gi_15450468_gb_AY052335.1	7.23	1.68	1.24	3.58

Overall_F_ Pvalue	AGI_No	Descriptions	ssi2/Col-0	ssi2 sid2/ Col-0	ssi2 act1/ Col-0	Fold up: SNP
0.027909414	AT1G76680 /// AT1G76690	12-oxophytodienoate reductase (OPR2) identical to 12-oxophytodienoate reductase OPR2 GB:AAC78441 *Arabidopsis thaliana*	7.08	4.11	2.49	4.23
0.016476525	AT2G38470	putative WRKY-type DNA binding protein	6.81	6.07	2.11	2.24
3.63985E-07	AT2G41380	putative embryo-abundant protein	6.71	1.17	0.57	21.63
0.000150106	AT3G19660	unknown protein	6.35	0.74	1.00	2.87
0.011259105	AT5G27420	RING-H2 zinc finger protein-like RING-H2 zinc finger protein ATL6 - *Arabidopsis thaliana,* EMBL:AF132016; supported by full-length cDNA: Ceres:106078	6.35	2.98	2.02	2.38
0.0042422	AT1G30410 /// AT1G30420	ABC transporter, putative contains Pfam profile: PF00005: ABC transporter	6.24	2.17	1.95	2.80
2.90007E-05	AT2G36790 /// AT2G36800	putative glucosyl transferase an EST matching the 5 end of this gene (GB:AA605508) was originally described as polyadenylated (GB:AA006321) and is probably transcribed from the opposite strand	6.18	4.26	0.60	10.08
0.034017356	AT2G37970	unknown protein ; supported by cDNA: gi_15451063_gb_AY054612.1	5.77	4.06	0.14	2.42

Overall_F_ Pvalue	AGI_No	Descriptions	ssi2/Col-0	ssi2 sid2/ Col-0	ssi2 act1/ Col-0	Fold up: SNP
0.011548923	AT2G38940 /// AT3G54700	phosphate transporter (AtPT2) identical to GB:U62331	5.73	2.12	0.94	2.41
0.012814322	AT3G12580	heat shock protein 70 identical to heat shock protein 70 GB:CAA05547 GI:3962377 *Arabidopsis thaliana*; supported by cDNA: gi_15809831_ gb_AY054183.1	5.56	5.23	0.47	8.90
0.000145129	AT1G72900	virus resistance protein, putative similar to virus resistance protein GI:558886 from *Nicotiana glutinosa*	5.53	3.66	0.97	4.50
0.027522461	AT4G11280	ACC synthase (AtACS-6); supported by cDNA: gi_16226285_gb_AF428292.1_ AF428292	5.38	2.81	0.34	2.70
1.02936E-05	AT3G59700	serine/threonine-specific kinase lecRK1 precursor, lectin receptor-like	5.37	1.34	0.50	2.52
4.47994E-05	AT2G40140	putative CCCH-type zinc finger protein also an ankyrin-repeat protein	5.34	3.42	1.38	2.08
0.000493712	AT3G21250	unknown protein similar to MRP-like ABC transporter GB:AAC49791 from *Arabidopsis thaliana*	5.32	5.67	1.15	2.04
9.97222E-05	AT1G66090	disease resistance protein, putative similar to disease resistance protein RPP1-WsA *Arabidopsis thaliana* GI:3860163; supported by full-length cDNA.	5.31	6.01	1.84	3.23

Overall_F_ Pvalue	AGI_No	Descriptions	ssi2/Col-0	ssi2 sid2/ Col-0	ssi2 act1/ Col-0	Fold up: SNP
0.038195824	AT2G22500	putative mitochondrial dicarboxylate carrier protein ;supported by full-length cDNA: Ceres:20723	5.28	2.64	1.09	2.40
0.00016076	AT5G54860	putative protein contains similarity to integral membrane protein	5.17	3.13	1.82	2.34
0.000110211	AT3G14620	putative cytochrome P450 similar to GB:Q05047 from *Catharanthus roseus*; supported by cDNA: gi_15529168_ gb_ AY052208.1	5.04	2.97	1.32	2.74
3.4612E-05	AT5G09590	heat shock protein 70 (Hsc70-5) ; supported by cDNA: gi_6746589_gb_ AF217458.1_AF217458	4.93	4.00	1.18	2.18
0.000121362	AT2G38290	putative ammonium transporter	4.91	2.37	3.29	2.05
5.47994E-07	AT1G72910 /// AT1G72930	flax rust resistance protein, putative similar to flax rust resistance protein GI:4588066 from *Linum usitatissimum*; supported by full-length cDNA: Ceres: 2795	4.83	3.13	2.13	2.21
0.000338701	AT1G33110	unknown protein	4.79	5.17	1.27	2.29
0.000414414	AT1G72940	disease resistance protein, putative similar to disease resistance protein GI:9758876 from *Arabidopsis thaliana*	4.78	9.19	1.28	2.84

Overall_F_ Pvalue	AGI_No	Descriptions	ssi2/Col-0	ssi2 sid2/ Col-0	ssi2 act1/ Col-0	Fold up: SNP
0.002179347	AT2G47000	putative ABC transporter related to multi drug resistance proteins and P-glycoproteins	4.77	0.75	0.91	2.60
0.000936673	AT4G05020	coded for by *Arabidopsiss thaliana* cDNA W43435 ; supported by cDNA: gi_ 14532463_gb_AY039856.1	4.75	1.84	0.41	2.67
0.005118574	AT1G19020	Expressed protein ; supported by full-length cDNA: Ceres: 31015.	4.69	1.96	0.88	4.21
0.023524457	AT2G37430	putative C2H2-type zinc finger protein likely a nucleic acid binding protein	4.46	8.90	1.37	16.87
0.00506498	AT1G05680	putative indole-3-acetate beta-glucosyltransferase similar to indole-3-acetate beta-glucosyltransferase GB:AAD32293	4.45	0.96	0.69	12.26
0.00330233	AT1G10370	putative glutathione S-transferase TSI-1 similar to glutathione S-transferase TSI-1 (gi|2190992); similar to ESTs gb|R29860, emb|Z29757, and emb|Z29758; supported by cDNA: gi_11096015_gb_ AF288191.1 _AF288191	4.34	16.12	0.64	3.07
0.001516497	AT3G05360	putative disease resistance protein similar to Cf-2 disease resistance protein GB:AAC15780 from *Lycopersicon pimpinellifolium*	4.30	1.31	0.75	6.41
0.010561956	AT4G21990	PRH26 protein; supported by full-length	4.29	4.19	0.40	3.79

Overall_F_ Pvalue	AGI_No	Descriptions	ssi2/Col-0	ssi2 sid2/ Col-0	ssi2 act1/ Col-0	Fold up: SNP
0.006377861	AT4G23190	serine/threonine kinase - like protein serine/threonine kinase, *Brassica oleracea*	4.26	2.26	1.59	2.15
4.25633E-06	AT2G37710	putative receptor-like protein kinase same as GB:X95909 (polymorphism exists at a GA repeat. We found 6 copies in our sequence whereas only 5 copies exist in GB:X95909)	4.22	1.39	1.34	1.93
0.024583686	AT3G46280	putative protein serine/threonine-specific protein kinase (EC 2.7.1.-) lrrpk, *Arabidopsis thaliana*, PIR:T08975	4.16	1.43	1.94	11.56
0.000506346	AT2G34500	putative cytochrome P450	4.12	0.42	0.36	3.97
1.99601E-09	AT5G22060	Expressed protein ; supported by cDNA: gi_535587_gb_L36113.1_ATHATJ	4.08	2.77	1.16	2.05
0.042798091	AT2G30040	putative protein kinase contains a protein kinase domain profile (PDOC00100)	4.01	3.92	0.47	2.36
0.030170994	AT3G55980	putative protein zinc finger transcription factor (PEI1), *Arabidopsis thaliana*, EMBL:AF050463; supported by cDNA: gi_15810486_gb_AY056282.1	3.94	5.07	1.29	2.12
0.014834257	AT1G21550	unknown protein contains similarity to calcium-binding protein GB:CAB63264 GI:6580549 from *Lotus japonicus*; supported by cDNA:	3.84	4.29	0.57	3.43

Overall_F_ Pvalue	AGI_No	Descriptions	ssi2/Col-0	ssi2 sid2/ Col-0	ssi2 act1/ Col-0	Fold up: SNP
0.024454071	AT5G14730	putative protein predicted protein, *Arabidopsis thaliana*	3.69	3.07	2.38	2.09
0.030303952	AT1G05575	Expressed protein ; supported by full-length cDNA: Ceres: 27081.	3.66	2.73	1.70	2.16
0.00451775	AT3G51450	mucin -like protein hemomucin, *Drosophila melanogaster*, EMBL:DM42014;supported by full-length cDNA: Ceres:38956	3.49	1.24	0.76	1.96
5.34734E-05	AT5G58620	putative protein zinc finger transcription factor, Arabidopsis thaliana, PIR:T49889; supported by cDNA: gi_15809817_gb_AY054176.1	3.44	0.99	0.70	2.49
0.032133768	AT2G39650	unknown protein	3.36	2.71	1.13	2.23
1.19675E-05	AT5G64120	peroxidase (emb|CAA67551.1) ;supported by full-length cDNA: Ceres:23349.	3.24	1.25	0.43	6.58
0.000227806	AT3G09440	heat-shock protein (At-hsc70-3) identical to (At-hsc70-3) (cytosolic Hsp70) GB:CAA76606 *Arabidopsis thaliana*; supported by cDNA: gi_15292924_gb_ AY050896.1	3.24	3.40	0.32	3.52
0.018867815	AT5G47070	protein serine threonine kinase-like	3.23	1.47	1.21	2.06
0.001437115	AT2G23420	unknown protein	3.19	4.25	0.77	2.13

Overall_F_ Pvalue	AGI_No	Descriptions	ssi2/Col-0	ssi2 sid2/ Col-0	ssi2 act1/ Col-0	Fold up: SNP
0.019176309	AT4G37370	cytochrome P450 - like protein cytochrome P450, *Glycyrrhiza echinata*, AB001379;supported by full-length cDNA: Ceres:253698	3.15	0.52	0.57	10.89
0.013364443	AT4G13180	short-chain alcohol dehydrogenase like protein short-chain alcohol dehydrogenase -*Picea abies*, PIR2:S34678;supported by full-length cDNA: Ceres:748	3.09	1.35	0.63	6.18
5.77021E-06	AT3G07720	unknown protein similar to hypothetical protein GB:S33464 *Arabidopsis thaliana*; supported by cDNA: gi_14517447_gb_ AY039559.1	2.99	2.24	0.70	2.79
0.000898647	AT2G43620	putative endochitinase	2.82	0.77	0.16	2.30
0.021872447	AT1G63720	hypothetical protein similar to putative protein GB:CAA18164 *Arabidopsis thaliana*; supported by cDNA: gi_13878144_gb_AF370335.1_AF370335	2.79	1.39	1.10	2.55
0.004030357	AT5G38530	tryptophan synthase beta chain	2.66	1.59	0.67	2.32
0.000326773	AT5G56030	HEAT SHOCK PROTEIN 81-2 (HSP81-2) (sp|P55737)	2.52	3.09	0.59	2.20
0.00808353	AT4G01870	predicted protein of unknown function similar to bacterial tolB proteins but unclear if T7B11.13 is involved in viral transport	2.50	0.66	0.54	28.67

Overall_F_ Pvalue	AGI_No	Descriptions	ssi2/Col-0	ssi2 sid2/ Col-0	ssi2 act1/ Col-0	Fold up: SNP
0.004756472	AT4G19880	putative protein various predicted proteins	2.47	1.49	2.45	2.37
0.00129253	AT1G23010	unknown protein similar to *Bacillus* spore coat protein, CotA, GB:BAA22774	2.45	2.64	1.32	3.84
0.000235824	AT4G02940	hypothetical protein similar to *Arabidopsis thaliana* hypothetical protein T13L16.2, GenBank accession number 2708738	2.37	1.25	0.83	2.42
8.61634E-05	AT5G56000 /// AT5G56010	heat shock protein (emb|CAA72514.1)	2.34	2.78	0.56	1.99
0.006021863	AT1G28600	lipase, putative contains Pfam profile: PF00657 Lipase/Acylhydrolase with GDSL-like motif;supported by full-length cDNA: Ceres:37307	2.33	1.77	0.60	2.52
0.037721901	AT3G20590 /// AT3G20600	non-race specific disease resistance protein, putative contains non-consensus CT donor splice site at exon 1; potential pseudogene; similar to non-race specific disease resistance protein GB:AAB95208 *Arabidopsis thaliana*	2.32	1.54	1.86	2.26
Overall_F_	**AGI_No**	**Descriptions**	**ssi2/Col-0**	**ssi2 sid2/**	**ssi2 act1/**	**Fold up:**

Pvalue				Col-0	Col-0	SNP
0.001079335	AT3G23240	ethylene response factor 1 (ERF1) identical to ethylene response factor 1 GB:AAD03544 from *Arabidopsis thaliana*;supported by full-length cDNA: Ceres:21068	2.27	0.99	0.53	3.24
5.40735E-05	AT5G04950	nicotianamine synthase (dbj|BAA74589.1)	2.26	2.40	0.29	3.31
0.014191344	AT1G71100	putative ribose 5-phosphate isomerase similar to ribose 5-phosphate isomerase GB:6677767 from *Mus musculus*; supported by full-length cDNA: Ceres:3116.	2.20	1.40	1.94	2.21
0.039704729	AT4G24160	putative protein CGI-58 protein - Homo sapiens,PID:g4929585	2.19	1.76	0.87	4.88
0.004028164	AT4G33040	putative protein AT.I.24, Arabidopsis thaliana, gb:U63815;supported by full-length cDNA: Ceres:4868	2.18	1.55	0.37	1.99
Overall_F_ Pvalue	**AGI_No**	**Descriptions**	**ssi2/Col-0**	**ssi2 sid2/**	**ssi2 act1/**	**Fold up:**

				Col-0	Col-0	SNP
0.048664429	AT5G24660	putative protein similar to unknown protein (emb CAB62461.1);supported by full-length cDNA: Ceres:268701.	2.16	1.06	0.17	2.50
0.005677623	AT1G55920	serine acetyltransferase identical to GB:CAA84371 from *Arabidopsis thaliana* (Eur. J. Biochem. 227 (1-2), 500-509 (1995)); supported by cDNA: gi_926938_gb_L42212.1_ATHSAT1G	2.12	1.44	0.76	2.68
0.00198018	AT1G51700	dof zinc finger protein identical to dof zinc finger protein *Arabidopsis thaliana* GI:3608261; supported by cDNA: gi_3608260_dbj_AB017564.1_AB017564	2.09	3.22	1.64	2.09
0.008735653	AT5G51830	fructokinase 1; supported by cDNA: gi_13878052_gb_AF370289.1_AF370289	2.07	0.55	0.78	3.38

Table 3.2. Transcript levels of *NOA1*, *NIA1*, *NIA2* and *PR-1* in response to pathogen infections or exogenous application of SA. These data were obtained from the *Arabidopsis* gene expression browser (www.expressionbrowser.com; Zhang et al. 2010[a]). T and C indicate treatment and control, respectively.

Experiment: Pseudomonas syringae pv tomato avrRpm1 infiltration for 24 hr: Plants were infiltrated with $1x10^8$ cfu/ml *Pseudomonas syringae pv tomato avrRpm1*, 2 leaves per plant, 8 plants pooled, harvested after 24h.

Name	T	C	Fold Change	p-value
AT2G14610 (PR-1)	6739	660	10.19	0.0036
AT1G77760 (NIA1)	471	408	1.15	0.273
AT1G37130 (NIA2)	8336	4734	1.76	0.0123
AT3G47450 (NOA1)	130	253	-1.94	0.0012

Experiment: SA treatment vs. Control: plant defense signal salicylic acid (SA)

Name	T	C	Fold Change	p-value
AT2G14610 (PR-1)	3983	102	38.82	6.71E-5
AT1G77760 (NIA1)	8472	7695	1.1	0.4652
AT1G37130 (NIA2)	9797	9814	-1.0	0.9713
AT3G47450 (NOA1)	187	282	-1.5	0.0497

Experiment: *Pseudomonas syringae pv tomato* DC3000 infection 24 hr: Plants were inoculated by vacuum infiltration with *Pseudomonas syringae pv. tomato* strain DC3000 bacteria at a concentration of 10^6 cfu/ml. Inoculated leaf tissue from at least 15 plants was collected for RNA isolation.

Name	T	C	Fold Change	p-value
AT2G14610 (PR-1)	954	374	2.55	0.5541
AT1G77760 (NIA1)	1229	86	14.25	0.0837
AT1G37130 (NIA2)	3699	3149	1.17	0.4509
AT3G47450 (NOA1)	72	105	-1.44	0.2196

CHAPTER 4

Role of DIR1 in G3P mediated systemic acquired resistance

Introduction

The plastidal glycerolipid biosynthesis is initiated upon acylation of glycerol-3-phosphate (G3P) with 18:1, which leads to the formation of lysophosphatidic acid (Lyso PA) (Figure 1). 18:1 in turn is derived from 18:0, via the activity of soluble stearoyl-acyl carrier protein desaturases (described in chapter 3). As shown in chapter 3, 18:1 levels are important regulators of plant defense signaling. Characterization of *ssi2* suppressor mutants has shown that the altered defense-related phenotypes are the result of the reduction in the levels of the unsaturated FA, 18:1, which causes induction of several resistance (*R*) genes (Chandra-Shekara et al., 2007; Venugopal et al., 2009; Xia et al., 2009; Mandal et al., 2012). Restoration of 18:1 levels, via mutations in *ACT1*, *GLY1* or *ACP4*, normalizes *R* gene expression in *ssi2* plants. The low 18:1-mediated induction of *R* gene expression and the associated defense signaling can also be suppressed by simultaneous mutations in *EDS1* and the genes governing SA biosynthesis (*SID2*, *EDS5*) (Venugopal et al., 2009). Furthermore, the functional redundancy between EDS1 and SA likely masks the requirement for EDS1 by several coiled coil (CC)- nucleotide binding site (NBS)- leucine rich repeat (LRR) proteins, previously thought to function independently of EDS1.

The results shown in this chapter were published in the following journals:

1. Chanda B*, Xia Y*, Mandal MK, Yu K, Sekine KT, Gao QM, Selote D, Hu Y, Stromberg A, Navarre D, Kachroo A, Kachroo P. 2011. Glycerol-3-phosphate is a critical mobile inducer of systemic immunity in plants. *Nat. Genet*. **43** (5): 421-429. “Copyright (2011) Nature Publishing Group, U.S.A” (* Contributed equally).
2. Mandal MK, Chanda B, Xia Y, Yu K, Sekine KT, Gao QM, Selote D, Hu Y, Stromberg A, Navarre D, Kachroo A, Kachroo P. 2011. Glycerol-3-phosphate and

systemic immunity. *Plant Signaling & Behavior*. **6** (11). "Copyright (2011) Landes Bioscience, U.S.A". www.landesbioscience.com.

The plastidal 18:1 levels are regulated via the chloroplastic glycerol-3-phosphate (G3P) pool and vice-versa (Kachroo et al., 2004). However, 18:1 and G3P appear to function distinctly in defense signaling. For example, G3P levels are important for basal defense against the hemibiotrophic fungus, *Colletotrichum higginsianum* (Chanda et al., 2008). Genetic mutations affecting G3P synthesis in Arabidopsis enhance susceptibility to *C. higginsianum*. Conversely, plants accumulating increased G3P show enhanced resistance. More recently, we demonstrated roles for G3P in *R*-mediated defense leading to systemic acquired resistance (SAR) (Chanda et al., 2011). *R*-mediated defense against the avirulent bacterial pathogen *Pseudomonas syringae* is associated with a rapid increase in G3P levels within 6 h of inoculation with avirulent bacteria. The accumulation of G3P in the infected and systemic tissues precedes the accumulation of other metabolites known to be essential for SAR. Compromised SAR in G3P-deficient mutants defective in G3P dehydrogenase or glycerol kinase activities was restored by exogenous application of G3P, thus arguing a role for G3P in SAR. This was further supported by the fact that exogenous G3P induced SAR in the absence of the primary pathogen in both Arabidopsis and soybean (Chanda et al., 2011). To determine the molecular mechanism underlying G3P-conferred SAR, I evaluated the role of the lipid transfer protein (LTP) encoded by DIR1, which acts as a positive regulator of SAR (Chanda et al., 2011).

Results and Discussion

DIR1 does not bind G3P

To characterize the role of DIR1, the mature protein lacking the N-terminal transit peptide was expressed as an epitope-tagged fusion in *Escherichia coli* and purified using affinity chromatography (Figure 4.1A). Infiltration of DIR1-His_6 protein into *dir1* plants restored SAR (Chanda et al., 2011), indicating that the recombinant protein was biologically functional. The fact that the lipid transfer-like DIR1 protein along with G3P,

a precursor for all lipid biosynthesis, induces strong SAR raised the possibility that DIR1 might directly associate with G3P. To test this, I carried out i*n vitro* binding assays wherein 250 μg of DIR1 protein was equilibrated in a dialysis bag (3.5 kD cut off) at 4°C in 10 mM Tris-HCl, pH 7.5, containing 1mM azide and 3 μM ^{14}C-G3P (American Radiolabel Co., MO-USA). After overnight equilibration, the dialysis bag was immersed in 10 mM Tris-HCl, pH 7.5 and 10 μl aliquots were removed from the bag after 24 h and quantified using a liquid scintillation analyzer (1900-TR, Thermo Scientific, IL-USA). This assay did not detect binding between DIR1 and G3P (Figure 4.1B). To gain a different perspective regarding this result, I carried out in-gel binding assay in which 20 μg of DIR1 protein was bound to 20 μl of Ni-NTA beads (Qiagen Inc., CA), washed three times with 10 mM potassium phosphate buffer and incubated with 8 μM of ^{14}C-G3P for 30 min at room temperature. The beads were washed three times with 10 mM potassium phosphate buffer. One half of the beads was quantified using liquid scintillation and the other half was run on a 12% native gel and autoradiographed using a Typhoon PhosphorImager. No binding between G3P and DIR1 was detected using in-gel binding assays (data not shown).

G3P and DIR1 are dependent on each other for translocation into distal tissues

Next, I investigated if G3P facilitated the translocation of DIR1 to distal tissues by monitoring the movement of full-length DIR1 tagged with green fluorescent protein (GFP) in *Nicotiana benthamiana* plants infiltrated with water or G3P. The transiently-expressed DIR1-GFP migrated as a doublet (Fig. 4.2A), possibly corresponding to the full-length and the mature protein lacking the predicted 25 amino acids (aa) N-terminal transit peptide. Interestingly, both bands translocated to the distal tissues in the presence of G3P, but not of water (Fig. 4.2A). Unlike DIR1-GFP, G3P did not promote the translocation of GFP to the distal tissues (Fig. 4.2A). Microscopic examination detected only low levels of fluorescence in the distal leaves of G3P-infiltrated plants, likely due to low levels of the DIR1-GFP protein translocating to distal tissues. Notably, DIR1-GFP was present in both soluble and microsomal fractions of extracts from infiltrated leaves (Fig. 4.2B). Interestingly, in the infiltrated leaves, DIR1-GFP localized to the nuclear envelope (Fig. 4.2C), endoplasmic reticulum (ER) (Fig. 4.2D, Fig. 4.2E) and

plasmodesmata (Fig. 4.2F). The symplastic localization of DIR1-GFP was further confirmed by plasmolysis of plant cells transiently expressing DIR1-GFP (Fig. 4.2G) and protoplasts prepared from stable transgenic plants expressing DIR1-GFP under the 35S promoter (Fig. 4.2H). Likewise, the GFP fused to DIR1 signal peptide localized to the ER, rather than the typical cytoplasmic and nuclear location of GFP (Fig. 4.2I, Fig. 4.2J). These results suggest that the symplastic movement of DIR1 is likely critical for SAR, and supported the observations that G3P and DIR1 are interdependent for translocation to systemic tissues. However, these findings do not explain how a lipid transfer-like protein might associate with the phosphorylated sugar G3P, to move systemically. Analysis of G3P in the leaf extracts showed that it was derivatized into an unknown compound before/during translocation (Chanda et al., 2011). Thus, it is likely that the G3P derivative has a lipid moiety via which it associates with DIR1 for transfer.

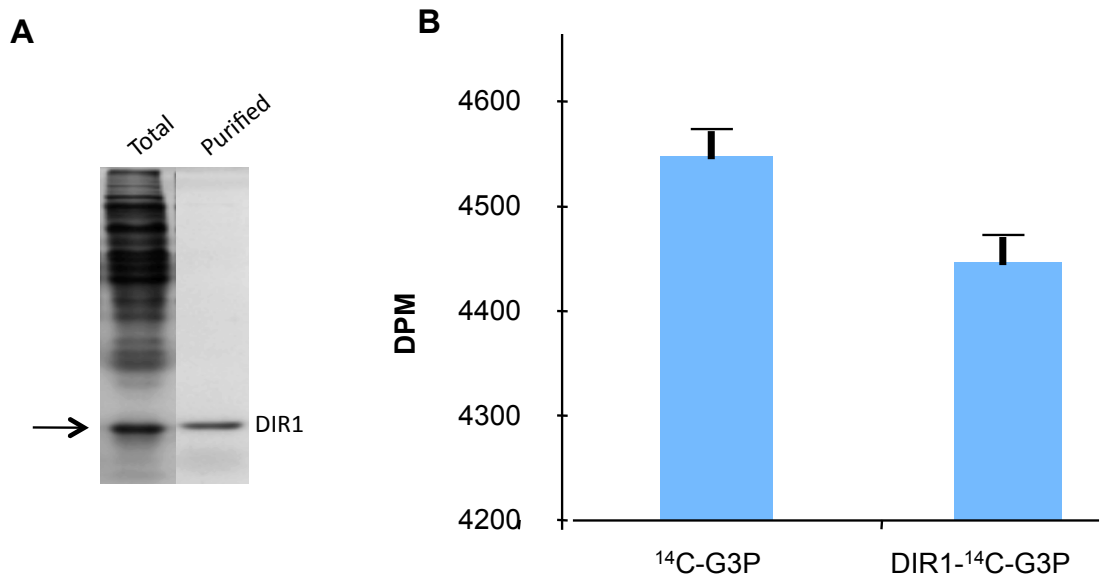

Figure 4.1. DIR1 expression and binding to ^{14}C-G3P.

(A) SDS-PAGE gel showing DIR1-His_6 protein (marked by arrow) in total and purified fractions. (B) *In vitro* binding assay carried out using purified DIR1-HIS_6 protein and labeled ^{14}C-G3P. In this assay 3 µM ^{14}C-G3P was incubated with or without DIR1-HIS_6 protein and 10 µl aliquots were removed after 24 h and quantified using a liquid scintillation analyzer.

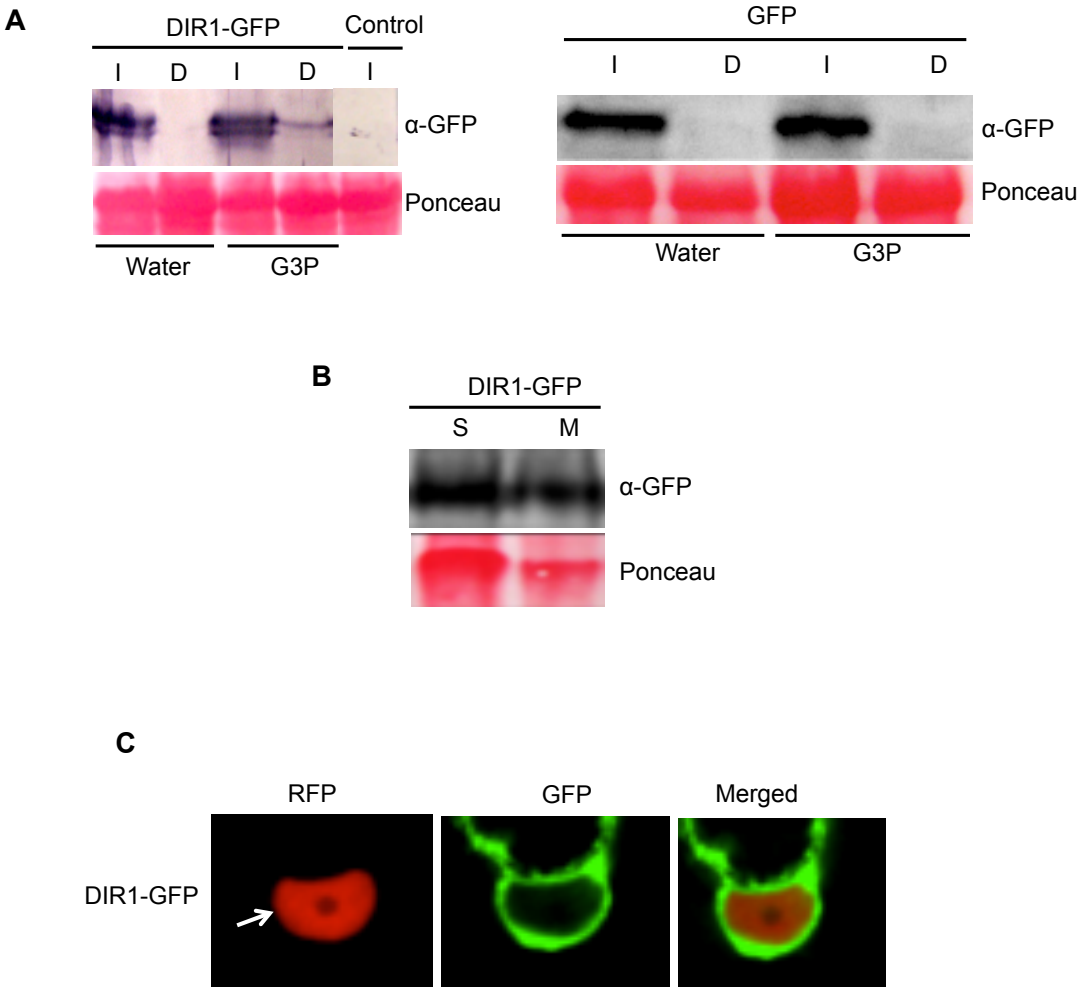
A
DIR1-GFP
Control
I
D
I
D
I
α-GFP
Ponceau
Water
G3P
GFP
I
D
I
D
α-GFP
Ponceau
Water
G3P
B
DIR1-GFP
S
M
α-GFP
Ponceau
C
RFP
GFP
Merged
DIR1-GFP

D

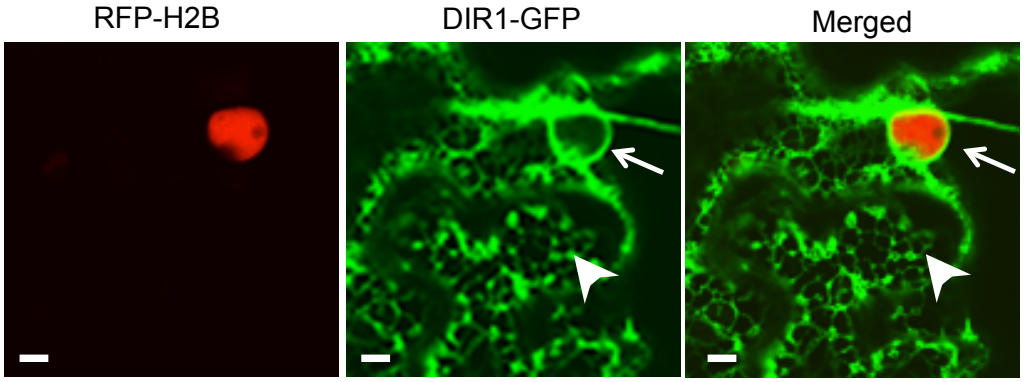
RFP-H2B
DIR1-GFP
Merged

E

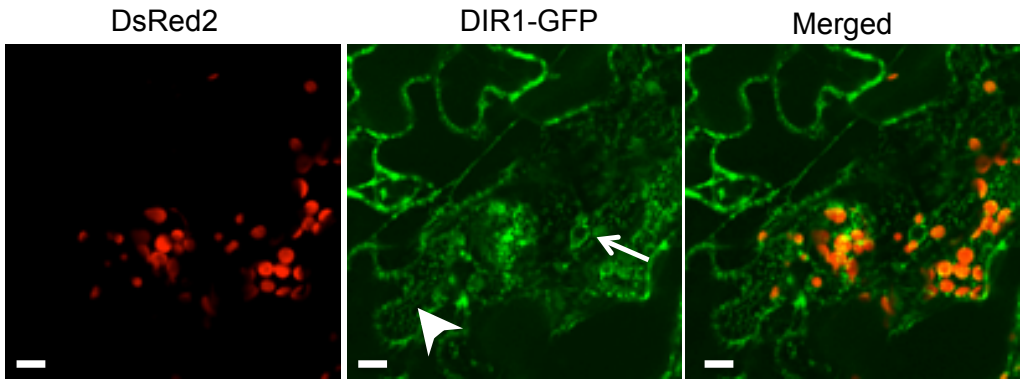
DsRed2
DIR1-GFP
Merged

F

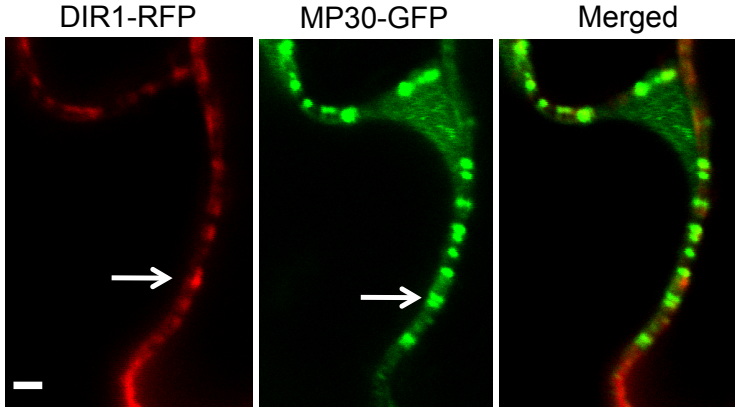
DIR1-RFP
MP30-GFP
Merged

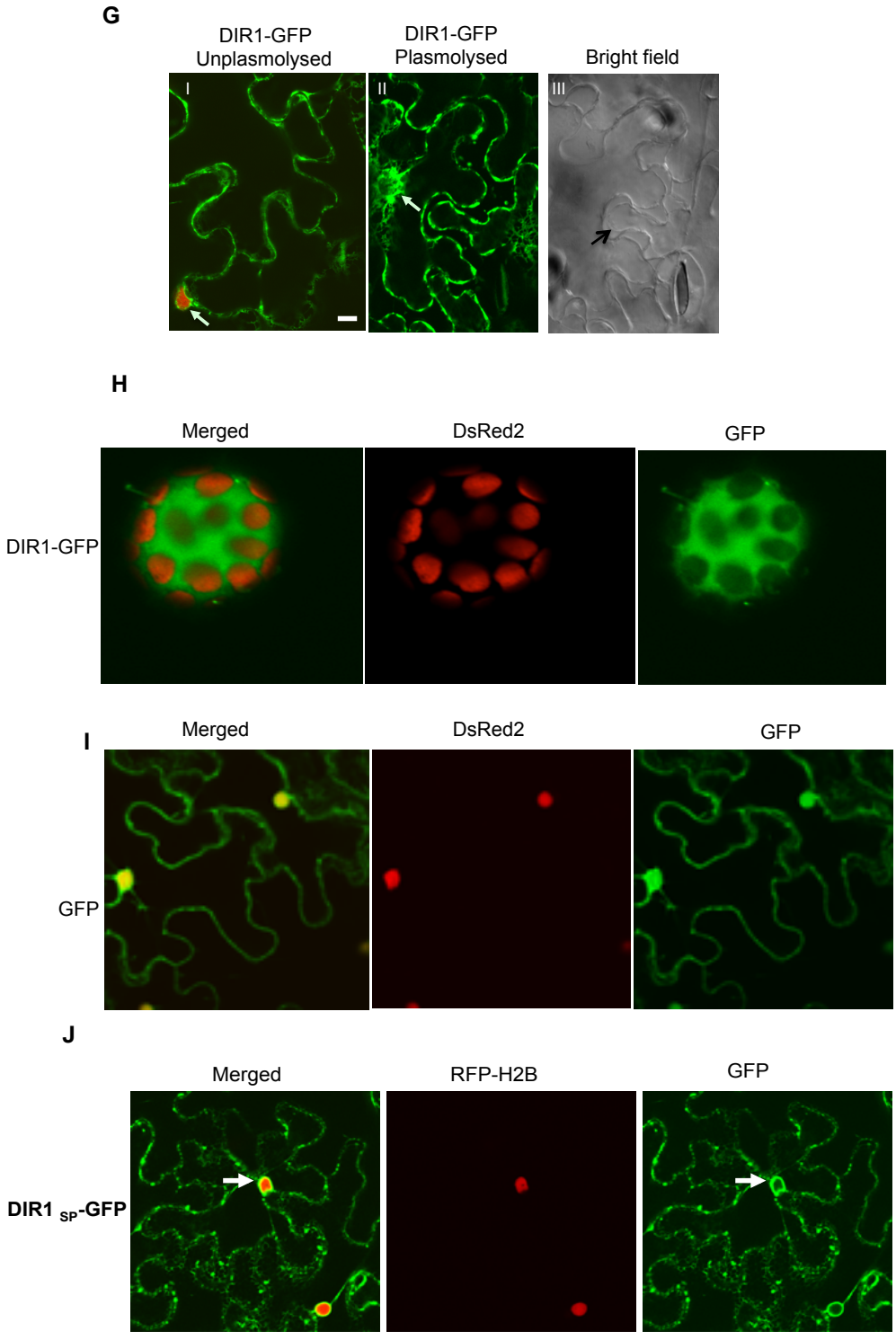

Figure 4.2. DIR1-GFP is a symplastic protein and dependent on G3P for its translocation into distal tissues.

Figure 4.2. DIR1-GFP is a symplastic protein and dependent on G3P for its translocation into distal tissues.

(A) Immunoblot showing GFP levels in infiltrated (I) and distal (D) tissues of *Nicotiana benthamiana* plants that were treated with water or G3P. Control indicates untreated wild-type plants. (B) DIR1-GFP levels in soluble (S) and microsomal (M) fractions of *N. benthamiana* plants. (C) Confocal micrographs showing localization of DIR1-GFP in *Nicotiana benthamiana* plants expressing RFP-tagged nuclear histone protein H2B. Arrow indicates nucleus. **(**D) Confocal micrographs showing localization of DIR1-GFP in *N. benthamiana* plants expressing RFP-ER. Scale bar, 5 μM. Arrow and arrowhead indicates nucleus and ER, respectively. (E) Confocal micrographs showing localization of DIR1-GFP in transgenic *Arabidopsis*. Scale bar, 5μM. (F) Confocal micrographs showing co-localization of DIR1-RFP and Tobacco Mosaic Virus movement protein (MP) 30-GFP in *Nicotiana benthamiana* plants. The punctate fluorescence signals indicated by arrows are plasmodesmata. Scale bar, 5 μM. (G) Confocal images showing subcellular localization of DIR1-GFP in *Nicotiana benthamiana* plants plasmolysed with 0.8 M mannitol,. The left panel (I) shows fluorescence of untreated cell, the middle panel (II) shows fluorescence of plasmolysed cells, and the right panel (III) shows corresponding transmission images of the plasmolysed cells. White arrows indicate nucleus. Black arrow indicates the plasma membrane where it is pulled away from the cell wall. Scale bars, 5 μM. (H) Confocal micrographs showing localization of DIR1-GFP in protoplast prepared from transgenic plants expressing DIR1-GFP under the 35S promoter. Scale bar, 2 μM. (I) Confocal micrographs showing localization of GFP in *N. benthamiana* plants expressing RFP-tagged nuclear histone protein H2B, Scale bar, 5 μM. (J) Confocal micrographs showing localization of SP_{DIR1}-GFP in *N. benthamiana* plants expressing RFP-tagged nuclear histone protein H2B, Scale bar, 5 μM. Arrow and arrowhead indicates nucleus and ER, respectively.

REFERENCES

1. Aronsson H, Jarvis P. 2002. A simple method for isolating import-competent Arabidopsis chloroplasts. *FEBS lett* **529**: 215-220.
2. Attaran E, Zeier TE, Griebel T, Zeier J. 2009. Methyl salicylate production and jasmonate signaling are not essential for systemic acquired resistance in Arabidopsis. *Plant Cell*. **21**: 954–971.
3. Axtell, M.J. and Staskawicz, B.J. 2003. Initiation of RPS2-specified disease resistance in Arabidopsis is coupled to the AvrRpt2-directed elimination of RIN4. *Cell*. **112**, 369–377.
4. Balcerczyk A, Soszynski M, Bartosz G. 2005. On the specificity of 4-amino-5-methylamino-2',7'-difluorofluorescein as a probe for nitric oxide. *Free Rad Biol Med* **39**: 327-335.
5. Besson-Bard A, Pugin A, Wendehenne D. 2008. New insights into nitric oxide signaling in plants. *Annu Rev Plant Biol* **59**: 21-39.
6. Bloj B, Zilversmit DB. 1977. Rat liver proteins capable of transferring phosphatidylethanolamine. Purification and transfer activity for other phospholipids and cholesterol. *J. Biol. Chem*. **252**:1613–1619.
7. Boller T, He SY. 2009. Innate immunity in plants: an arms race between pattern recognition receptors in plants and effectors in microbial pathogens. *Science.* **324**:742–744.
8. Calvo AM, Hinze LL, Gardner HW, Keller NP. 1999. Sporogenic effect of polyunsaturated fatty acids on development of *Aspergillus* spp. *Appl Environ Microbiol* **65**: 3668–3673.
9. Cammue BP, Thevissen K, Hendriks M, Eggermont K, Goderis IJ, Proost P, Van Damme J, Osborn RW, Guerbette F, Kader JC. 1995. A potent antimicrobial protein from onion seeds showing sequence homology to plant lipid transfer proteins. *Plant Physiol*. **109**:445-455.
10. Carvalho AO, Gomes VM. 2007. Role of plant lipid transfer proteins in plant cell physiology: a concise review. *Peptides*. **28**:1144–1153.

11. Chanda B, Venugopal SC, Kulshrestha S, Navarre DA, Downie B, Vaillancourt L, Kachroo A, Kachroo P. 2008. Glycerol-3-phosphate levels are associated with basal resistance to the hemibiotrophic fungus *Colletotrichum higginsianum* in *Arabidopsis*. *Plant Physiol*. **147**: 2017–2029.
12. Chanda B, Xia Y, Mandal MK, Yu K, Sekine K-T, Gao Q-M, Selote D, Hu Y, Stromberg A, Navarre D, Kachroo A, Kachroo P. 2011. Glycerol-3-phosphate is a critical mobile inducer of systemic immunity in plants. *Nature Genet* **43**: 421-427.
13. Chandra-Shekara AC, Gupte M, Navarre D, Raina S, Raina R, Klessig A, Kachroo P. 2006. Light-dependent hypersensitive response and resistance signaling against Turnip Crinkle Virus in Arabidopsis. *Plant J* **45**: 320-334.
14. Chandra-Shekara AC, Venugopal SC, Barman SR, Kachroo A, Kachroo P. 2007. Plastidial fatty acid levels regulate resistance gene-dependent defense signaling in Arabidopsis. *Proc Natl Acad Sci USA*. **104**: 7277-7282.
15. Chaturvedi R, Krothapalli K, Makandar R, Nandi A, Sparks AA, Roth MR, Welti R, Shah J. 2008. Plastid omega3-fatty acid desaturase-dependent accumulation of a systemic acquired resistance inducing activity in petiole exudates of Arabidopsis thaliana is independent of jasmonic acid. *Plant J*. **54**:106–117.
16. Clay NK, Adio AM, Denoux C, Jander G, Ausubel FM. 2009. Glucosinolate metabolites required for an Arabidopsis innate immune response. *Science.* **323**: 95–101.
17. Cohn J, Sessa G, Martin GB. 2001. Innate immunity in plants. *Curr. Opin. Immunol.* **13**:55–62.
18. Conrath U. 2006. Systemic acquired resistance. *Plant Signal Behav*. **4**:179–184.
19. Davda RK, Stepniakowski KT, Lu G, Ullian E, Goodfriend TL, Egan BM. 1995. Oleic acid inhibits endothelial nitric oxide synthase by a protein kinase C-independent mechanism. *Hypertension* **26**: 764-770.
20. Delladonne M, Xia Y, Dixon RA, Lamb C. 1998. Nitric oxide functions as a signal in plant disease resistance. *Nature* **394**: 585-588.
21. Dempsey DA, Shah J, Klessig DF. 1999. Salicylic acid and disease resistance in plants. *Crit. Rev. Plant Sci.* **18***:* 547–575.
22. Denys A, Hichami A, Khan NA. 2001. Eicosapentaenoic acid and

docosahexaenoic acid modulate MAP kinase .ERK1/ERK2. signaling in human T cells. *J Lipid Res* **42**: 2015–2020.

23. Desikan R, Griffiths R, Hancock J, Neill S. 2002. A new role for an old enzyme: nitrate reductase-mediated nitric oxide generation is required for abscisic acid-induced stomatal closure in *Arabidopsis thaliana*. *Proc Natl Acad Sci USA* **99**: 16314-16318.
24. Dong X. 2001. Genetic dissection of systemic acquired resistance. *Current Opinion in Plant Biology*. 4: 309-314.
25. Durner J, Wendehenne D, Klessig DF. 1998. Defense gene induction in tobacco by nitric oxide, cyclic GMP and cyclic ADP-ribose. *Proc Natl Acad Sci USA* **95**: 10328-10333.
26. Durrant, WE, Dong X. 2004. Systemic acquired resistance. *Annu. Rev. Phytopathol.* **42**: 185–209.
27. Flor HH. 1971. Current status of the gene-for-gene concept. *Annu. Rev. Plant Pathol.* **9**:275–96.
28. Foissner I, Wendehenne D, Langebartels C, Durner J. 2000. *In vivo* imaging of an elicitor-induced nitrix oxide burst in tobacco. *Plant J* **23**: 817-824.
29. Furuhashi M, Hotamisligil GS. 2008. Fatty acid-binding proteins: role in metabolic diseases and potential as drug targets. *Nature Rev Drug Discov* **7**: 489-503.
30. Garcia-Olmedo F, Molina A, Segura A, Moreno M. 1995. The defensive role of nonspecific lipid-transfer proteins in plants. *Trends Microbiol.* **3**(2):72- 74.
31. Gas E, Flores-Pe´rez U, Sauret-Gueto S, Gas E, Jarvis P, Rodrı´guez-Concepcio´na M. 2008. A mutant impaired in the production of plastome-encoded proteins uncovers a mechanism for the homeostasis of isoprenoid biosynthetic enzymes in Arabidopsis plastids. *Plant Cell* **20**: 1303-1315.
32. Gechev TS, Hille J**.** 2005. Hydrogen peroxide as a signal controlling plant programmed cell death. *J Cell Biol* **168:** 17–20
33. Guerzoni ME, Lanciotti R, Cocconcelli PS. 2001. Alteration in cellular fatty acid composition as a response to salt, acid, oxidative and thermal stresses in Lactobacillus helveticus. Microbiology **147**: 2255-64

34. Guo FQ, Okamoto M, Crawford NM. 2003. Identification of a plant nitric oxide synthase gene involved in hormonal signaling. *Science* **302**: 100-103.
35. Hammerschmidt S, Schiller J, Kuhn H, Meybaum M, Gessner C, Sandvoss T, Arnold K, Wirtz H. 2003. Influence of tidal volume on pulmonary NO release, tissue lipid peroxidation and surfactant phospholipids. *Biochim Biophys Acta.* **1639:**17-26.
36. He Y, Tang R-H, Hao Y, Stevens RD, Cook CW, Ahn SM, Jing L, Yang Z, Chen L, Guo F, Fiorani F, Jackson RB, Crawford NM, Pei Z-M. 2004. Nitric oxide represses the Arabidopsis floral transition. *Science* **305**: 1968-1971.
37. Hotamisligil, G. S. 2006. Inflammation and metabolic disorders. Nature **444**: 860–867.
38. Iba K. 2002. Acclimative response to temperature stress in higher plants: approaches of gene engineering for temperature tolerance. *Ann Rev Plant Biol* **53**: 225–245.
39. Jayaraj J, Punja ZK. 2007. Combined expression of chitinase and lipid transfer protein genes in transgenic carrot plants enhances resistance to foliar fungal pathogens. *Plant Cell Rep.* **26**(9): 1539-1546.
40. Jeong SY, Rose A, Meier I. 2003. MFP1 is a thylakoid-associated, nucleoid-binding protein with a coiled-coil structure. *Nucl Acid Res* **31**: 5175-5185.
41. Jung HW, Tschaplinkski TJ, Wang L, Glazebrook J, Greenberg, JT. 2009. Priming in systemic plant immunity. *Science* **324**: 89–91.
42. Kachroo A, Kachroo P. 2009. Fatty acid derived signals in plant defense. *Annu Rev Phytopath* **47**: 153-176.
43. Kachroo A, Lapchyk L, Fukushigae H, Hildebrand D, Klessig D, Kachroo P. 2003a. Plastidal fatty acid signaling modulates salicylic acid- and jasmonic acid-mediated signaling in the Arabidopsis *ssi2* mutant. *Plant Cell* **15**: 2952-2965.
44. Kachroo A, Shanklin J, Lapchyk L, Whittle E, Hildebrand D, Kachroo P. 2007. The Arabidopsis stearoyl-acyl carrier protein-desaturase family and the contribution of leaf isoforms to oleic acid synthesis. *Plant Mol Biol* **63**: 257-271.

45. Kachroo A, Venugopal SC, Lapchy, L, Falcone D, Hildebrand D, Kachroo P. 2004. Oleic acid levels regulated by glycerolipid metabolism modulate defense gene expression in Arabidopsis. *Proc Natl Acad Sci USA.* **101**: 5152-5157.
46. Kachroo P, Kachroo A, Lapchyk L, Hildebrand D, Klessig DF. 2003b. Restoration of defective cross talk in *ssi2* mutants: role of salicylic acid, jasmonic acid, and fatty acids in SSI2-mediated signaling. *Mol. Plant Microbe Interact* **16**: 1022–1029.
47. Kachroo P, Shanklin J, Shah J, Whittle E, Klessig D. 2001. A fatty acid desaturase modulates the activation of defense signaling pathways in plants *Proc Natl Acad Sci USA.* **98**: 9448-94453.
48. Kachroo P, Venugopal SC, Navarre DA, Lapchyk L, Kachroo A. 2005. Role of salicylic acid and fatty acid desaturation pathways in ssi2-mediated signaling. *Plant Physiol* **139**: 1717-1735.
49. Kader JC, Julienne M, Vergnolle C. 1984. Purification and characterization of a spinach leaf protein capable of transferring phospholipids from liposomes to mitochondria or chloroplasts. *Eur J Biochem.***139**(2):411-416.
50. Kader JC. 1996. Lipid-transfer proteins in plants. *Annu Rev Plant Phys.* **47**:627-654.
51. Kader JC. 1997. Lipid-transfer proteins: A puzzling family of plant proteins. *Trends Plant Sci.* **2**(2):66-70.
52. Kalyanaraman B. 2004. Nitrated lipids: a class of cell-signaling molecules. *Proc Natl Acad Sci USA*.**101:**11527-11528.
53. Kamp HH, Wirtz KWA, Van Deenen LL. 1973. Some properties of phosphatidylcholine exchange protein purified from beef liver. *Biochim. Biophys. Acta*. **318**:313–325.
54. Kim Y, Nakatomi R, Akagi T, Hashikawa T, Takahashi R. 2005. Unsaturated fatty acids induce cytotoxic aggregate formation of amyotrophic lateral sclerosis-linked superoxide dismutase 1 mutants. *J Biol Chem* **280**: 21515-21521.
55. Kristensen AK, Brunstedt J, Nielsen KK, Roepstorff P, Mikkelsen JD. 2000. Characterization of a new antifungal non-specific lipid transfer protein(nsLTP) from sugar beet leaves. *Plant Sci.* **155**(1):31-40.

56. Kunst L, Browse J, Somverville C. 1988. Altered regulation of lipid biosynthesis in a mutant of Arabidopsis deficient in chloroplast glycerol-3-phosphate acyltransferase activity. *Proc Natl Acad Sci USA* **85**: 4134-4147.

57. Laloi C, Apel K, Danon A**.** 2004. Reactive oxygen signalling: the latest news. *Curr Opin Plant Biol* **7:** 323–328.

58. Lancaster JR Jr. 1996. Diffusion of free nitrix oxide. *Methods Enzymol* **268**: 31-50.

59. Lee LY, Gelvin SB. 2008. T-DNA binary vectors and systems. *Plant Physiol* **146**: 325–332.

60. Levine A, Tenhaken R, Dixon R, Lamb C**.** 1994. H_2O_2 from the oxidative burst orchestrates the plant hypersensitive disease resistance response. *Cell* **79:** 583–593.

61. Lightner J, James DW Jr, Dooner HK, Browse J. 1994. Altered body morphology is cause by increased stearate levels in a mutant of *Arabidopsis*. *Plant J* **6**: 401-412.

62. Lindermayr C, Saalbach G and Durner J. 2005. Proteomic identification of *S*-nitrosylated proteins in *Arabidopsis thaliana*. *Plant Physiol*. **137** 921–930.

63. Mackey D, Belkhadir Y, Alonso JM, Ecker JR, and Dangl, JL. 2003. Arabidopsis RIN4 is a target of the type III virulence effector AvrRpt2 and modulates RPS2-mediated resistance. *Cell* **112**: 379–389.

64. Maldonado AM, Doerner P, Dixon RA, Lamb CJ, Cameron RK. 2002. A putative lipid transfer protein involved in systemic resistance signaling in Arabidopsis. *Nature* **419**: 399–403.

65. Mandal MK**,** Chandra-Shekara AC, Jeong RD, Yu K, Zhu S**,** Chanda B**,** Navarre D, Kachroo A, Kachroo P. 2012**.** Oleic acid-dependent modulation of NITRIC OXIDE ASSOCATED 1 protein levels regulate nitric oxide-mediated signaling in plant defense. *Plant Cell* (Accepted).

67. Mandal MK**,** Chanda B, Xia Y**,** Yu K, Sekine K, Gao Q, Selote D, Navarre D, Kachroo A, Kachroo P. Plant Signaling & Behavior. 2011**.** Glycerol-3-phosphate in systemic signaling.

66. Mármol F, Sánchez J, López D, Martínez N, Mitjavila MT, Puig-Parellada P. 2009. Oxidative stress, nitric oxide and prostaglandin E2 levels in the gastrointestinal tract of aging rats. *J Pharm Pharmacol*. **61**:201–206.
67. Martin GB, Bogdanove AJ, Sessa G. 2003. Understanding the functions of plant disease resistance proteins. *Annu Rev Plant Biol* **54:** 23–61
68. Martin K, Kopperud K, Chakrabarty R, Banerjee R, Brooks R, Goodin MM. 2009. Transient overexpression in *Nicotiana benthamiana* fluorescent marker lines provide enhanced definition of protein localization, movement and interactions in planta. *Plant J* **59**: 150-162.
69. McHale L, Tan X, Koehl P, Michelmore RW**.** 2006. Plant NBS-LRR proteins: Adaptable guards. *Genome Biol*. **7,** 212.
70. Mensink RP, Zock PLA, Kester DM, Katan MB. 2003. Effects of dietary fatty acids and carbohydrates on the ratio of serum total to HDL cholesterol and on serum lipids and apolipoproteins: A meta-analysis of 60 controlled trials. *Am. J. Clin. Nutr.* **77** 1146–1155.
71. Molina A, Olmedo GF. 1997. Enhanced tolerance to bacterial pathogens caused by the transgenic expression of barley lipid transfer protein LTP2. *Plant J.* **12:** 669–675.
72. Moreau M, Lee GI, Wang Y, Crane BR, Klessig DF. 2008. AtNOS/AtNOA1 is a functional Arabidopsis thaliana cGTPase and not a nitric-oxide synthase. *J Biol Chem* **283**: 32957-32967.
73. Nandi A, Welti R, Shah, J. 2004. The Arabidopsis thaliana dihydroxyacetone phosphate reductase gene suppressor of fatty acid desaturase deficiency1 is required for glycerolipid metabolism and for the activation of systemic acquired resistance. *Plant Cell.* **16**: 465–477.
74. Nawrath C, Métraux JP. 1999. Salicylic acid induction–deficient mutants of Arabidopsis express PR-2 and PR-5 and accumulate high levels of camalexin after pathogen inoculation. *Plant Cell* **11:** 1393–1404.
75. Ongena M, Duby F, Rossignol F, Fauconnier ML, Dommes J, Thonart P. 2004. Stimulation of the lipoxygenase pathway is associated with systemic resistance

induced in bean by a nonpathogenic Pseu-domonas strain. Mol. Plant-Microbe Interact. **17**:1009–18

76. Parani M, Rudrabhatla S, Myers R, Weirich H, Smith B, Leaman DW Goldman SL. 2004. Microarray analysis of nitric oxide responsive transcripts in Arabidopsis. *Plant Biotech J* **2**: 359-366.
77. Parcy F. 2005. Flowering: a time for integration. *Int J Dev Biol* 49: 585-593.
78. Park SW, Kaimoyo E, Kumar D, Mosher S, Klessig DF. 2007. Methyl salicylate is a critical mobile signal for plant systemic acquired resistance. *Science* **318**:113–116.
79. Pastorello EA, Farioli L, Pravettoni V, Ortolani C, Ispano M, Monzaet M. 1999. The major allergen of peach (Prunus persica) is a lipid transfer protein. *J. Allergy Clin. Immunol.* **103**: 520–526.
80. Peters Jr T, Taniuchi H, Anfinsen Jr CB. 1973. Affinity chromatography of serum albumin with fatty acids immobilized on agarose. *J Biol Chem* **248**: 2447-2451.
81. Rasmussen JT, Borchers T, Knudsen J. 1990. Comparison of the binding affinities of acyl-CoA-binding protein and fatty-acid-binding protein for long-chain acyl-CoA esters. *Biochem J* **265**: 849-855.
82. Ree K, Gehl B, Chehab EW, Tsai Y-C, Braam J. 2011. Nitric oxide accumulation in Arabidopsis is independent of NOA in the presence of sucrose. *Plant J* doi: 10.1111/j.1365-313X.2011.04680.x.
83. Rodriguez-Concepcion, M. 2004. The MEP pathway: A new target for the development of herbicides, antibiotics and antimalarial drugs. Bentham Science Publishers. **10**: 2391-2400.
84. Rollo CD, Czyzewska E, Borden JH. 1994. Fatty acid necromones for cochroaches. *Naturwissenschaften* **81**: 409–410.
85. Routaboul J-M, Fischer SF, Browse J. 2000. Trienoic fatty acids are required to maintain chloroplast function at low temperatures. *Plant Physiol* 124: 1697–1705.
86. Ryals JA, Neuenschwander UH, Willits MG, Molina A, Steiner HY, Hunt MD.1996. Systemic Acquired Resistance. *Plant Cell*. **10**:1809–1819.

87. Shah J, Kachroo P and Klessig DF. 1999. The Arabidopsis ssi1 mutation restores pathogenesis-related gene expression in npr1 plants and renders defensin gene expression salicylic acid depen-dent. *Plant Cell*. **11**: 191–206.
88. Shanklin J, Cahoon, EB. 1998. Desaturation and related modifications of fatty acids. *Annu Rev Plant Physiol Plant Mol Biol* **49**: 611-641.
89. Shanklin J, Somverville C. 1991. Stearoyl-acyl-carrier-protein desaturase from higher plants is structurally related to the animal and fungal homologs. *Proc Natl Acad Sci USA* **88**: 2510-2514.
90. Smith AF, Tsuchida K, Hanneman E, Suzuki TC, Wells MA. 1992. Isolation, characterization, and cDNA sequence of two fatty acid binding proteins from the midgut of *Manduca sexta* larvae. *J Biol Chem* **267**: 380-384.
91. Sun J, Zhang X, Broderick M, Fein H. 2003. Measurement of nitric oxide production in biological systems by using Griess reaction assay. *Sensor* **3**:276-284.
92. Terras FRG, Goderis IJ, Vanleuven F, Vanderleyden J, Cammue BPA, Broekaert WF. 1992. *In vitro* Antifungal Activity of a Radish (*Raphanus sativus L*) Seed Protein Homologous to Nonspecific Lipid Transfer Proteins. *Plant Physiol.* **100**(2):1055-1058.
93. Tre´panier M, Be´card G, Moutoglis P, Willemot C, Gagne´ S, et al. 2005. Dependence of arbuscular- mycorrhizal fungi on their plant host for palmitic acid synthesis. Appl. Environ. Microbiol. **71**:5341–47
94. Truman W, Bennett MH, Kubigsteltig L, Turnbull C, Grant M. 2007. Arabidopsis systemic immunity uses conserved defense signaling pathways and is mediated by jasmonates. *Proc Natl Acad Sci USA*. **104**: 1075–1080.
95. Upchurch RG. 2008. Fatty acid unsaturation, mobilization, and regulation in the response of plants to stress. *Biotechnol Lett* **30**: 967–977.
96. Van der Biezen EA, Jones JDG. 1998. Plant disease-resistance proteins and the gene-for-gene concept. *Trends Biochem. Sci.* **23**:454–56.
97. Venugopal SC, Jeong RD, Mandal MK, Zhu S, Chandra-Shekara AC, Duroy N, Kachroo A, Kachroo P. 2009. Enhanced disease susceptibility 1 and salicylic acid act redundantly to regulate resistance gene expression and low oleate-induced defense signaling. *PLOS Genetics* **5**: e1000545.

98. Vernooiji B, Friedrich L, Morse A, Reist R, Kolditz-Jawhar R, Ward E, Kessmann H, Ryals J. 1994. Salicylic acid is not the translocated signal responsible for inducing systemic acquired resistance. *Plant Cell*. **6**: 959–965.

99. Wendehenne D, Pugin A, Klessig DF. 2001. Nitric oxide: comparative synthesis and signaling in animal and plant cells. *Trends Plant Sci* **6**: 177-183.

100. Wildermuth MC, Dewdney J, Wu G, Ausubel FM. 2001. Isochorismate synthase is required to synthesize salicylic acid for plant defence. *Nature* **414,** 562–565

101. Wilson ID, Neill SJ, Hancock JT .2008. Nitric oxide synthesis and signaling in plants. *Plant Cell Environ* **31**: 622-631.

102. Wilson RA, Calvo AM, Chang PK, Keller NP. 2004. Characterization of the *Aspergillus parasiticus* delta12-desaturase gene: a role for lipid metabolism in the Aspergillus-seed interaction. *Microbiol* **150**: 2881–2888.

103. Wu FH, Shen SC, Lee LY, Lee SH, Chan MT, Lin CS. 2009. Tape–Arabidopsis Sandwich – a simpler Arabidopsis protoplast isolation method. *Plant Methods*. **5***:* 10.

104. Xia Y, Gao Q-M, Navarre D A, Hildebrand D, Kachroo A, Kachroo P. 2009. An intact cuticle in distal tissues is essential for the induction of systemic acquired resistance in plants *Cell Host & Microbe*. **5**: 151-165.

105. Yamada M. 1992. Lipid Transfer Proteins in Plants and Microorganisms. *Plant Cell Physiol.* **33**(1):1-6.

106. Yamauchi Y, Furutera A, Seki K, Toyoda Y, Tanaka K, Sugimoto Y. 2008. Malondialdehyde generated from peroxidized linolenic acid causes protein modification in heat-stressed plants. *Plant Physiol Biochem* **46**: 786–793.

107. Yeats TH, Rose JKC. 2008. The biochemistry and biology of extracellular plant lipid-transfer proteins (LTP's). *Protein Sci.* **17**: 191–198.

108. Zeidler D, Zahringer U, Gerber I, Dubery I, Hartung T, Bors W, Hutzler P, Durner J. 2004. Innate immunity in Arabidopsis thaliana: Lipopolysaccharides activate nitric oxide synthase (NOS) and induce defense genes. *Proc Natl Acad Sci USA* **101**: 15811-15816.

109. Zemojtel T, Penzkofer T, Dandekar T, Schultz J. 2004. A novel conserved family of nitric oxide synthase? *Trends Biochem Sci* **29**:224-226.

110. Zhang D-X, Nagabhyru P, Schardl CL.2009. Regulation of a chemical defense against herbivory produced by symbiotic fungi in grass plants. *Plant Physiol* **150**: 1072-1082.

111. Zhang M, Zhang Y, Liu L, Yu L, Tsang S, Tan J, Yao, W, Kang MS, An Y, Fan X. 2010. Gene Expression Browser: large-scale and cross experiment microarray data integration, management, search & visualization. *BMC*

1. *Bioinformatics* **11**: 433.

112. Zimmerman AW, Veerkamp JH. 2002. New insights into the structure and function of fatty acid-binding proteins. *Cell Mol Life Sci* **59**: 1096-1116.

APPENDIX-A

LIST OF ABBREVIATIONS

Acronym/ abbreviation	Expansion
16:0	Palmitic acid
18:0	Stearic acid
18:1	Oleic acid
18:2	Linoleic acid
18:3	Linolenic acid
BiFC	Bi-molecular fluorescence complementation
BSA	Bovine serum albumin
BTH	Benzo[1,2,3]thiadiazole-7-carbothioic Acid *S*-Methyl Ester
$CaCl_2$	Calcium chroride
CAPS	Cleaved Amplified Polymorphic Sequences
Co-IP	Co-immunoprecipitation
DAF-FM DA	3-Amino, 4-aminomethyl-2′,7′-difluorofluorescein Diacetate
DAPI	4',6-diamidino-2-phenylindole
dATP	Deoxyribo adenosine triphosphate
dCAPS	Derived Cleaved Amplified Polymorphic Sequences
dCTP	Deoxyribo cytosine triphosphate
DEPC	Diethyl pyrocarbonate
DGDG	Digalactosyldiacylglycerol
DIR1	Defective in induced resistance 1
DMSO	Dimethyl sulfoxide
DNA	Deoxyribonucleic acid
dNTP	Deoxyribo nucleic triphosphate
DPI	Days post inoculation
DPT	Days post treatment
DTT	Dithiothreitol

EDTA	Ethylene diamine tetra acetic acid
EGTA	Ethylene glycol tetraacetic acid
ER	Endoplasmic reticulum
EtBr	Ethidium bromide
FABP	Fatty acid binding protein
g/mg/µg/ng	Gram/ milligram/ microgram/ nanogram
G3P	Glycerol-3-phosphate
GFP	Green fluorescent protein
GTP	Guanosine triphosphate
h/min/sec	Hours/minutes/seconds
K_2HPO_4	Potassium phosphate, dibasic
KCl	Potassium chloride
KH_2PO_4	Potassium phosphate, monobasic
KOH	Potassium hydroxide
L/mL/µL	Liter/ milliliter/ microliter
LB	Luria-Bertani
LTP	Lipid transfer protein
M/mM/µM	Molar/millimolar/ micromolar
$MgCl_2$	Magnesium chloride
MGDG	Monogalactosyldiacylglycerol
MOPS	3-(N-morpholino)propanesulfonic acid
MS	Murashige and skoog
MS media	Murashige & Skoog media
Na_2HPO_4	Sodium hydrogen phosphate
Na_2HPO_4	Sodium hydrogen phosphate
NaCl	Sodium chloride
NaN_3	Sodium azide
NaOAc	Sodium acetate
NaOH	Sodium hydroxide
NO	Nitric oxide

NOA1	Nitric oxide associated 1
^{o}C	Degree centigrade
PBS	Phosphate buffered saline
PC	Phosphatidylcholine
PCR	Polymerase chain reaction
PE	Phosphatidylethaloamine
PFD	Photon flux density
PG	Phosphatidylglycerol
PI	Phosphatidylinositol
PR-1	Pathogenesis related 1
PR-2	Pathogenesis related 2
PS	Phosphatidylserine
R	Resistant or resistance
RFP	Red fluorescent protein
Rh	Relative humidity
RNA	Ribonucleic acid
SA	Salicylic acid
SAG	Salicylic acid glucoside
SAR	Systemic acquired resistance
SD	Standard deviation
SDS	Sodiumdodecyl sulfate
SSC	Sodium chloride, sodium citrate
TBE	Tris- borate/ EDTA electrophoresis buffer
TE	TRIS-EDTA
TRIS	Hydroxymethyl Aminomethane
Wt	Wild-type
µM	Micron meter

VITA

Mihir Kumar Mandal

EDUCATION:

2001-2003: M.S. (Molecular Biology & Biotechnology), G. B. Pant University of Agriculture &Technology, Pantnagar, Uttaranchal, India.

1997-2001: B.S. (Agricultural Sciences, Plant Breeding & Genetics), Assam Agricultural University, India.

RESEARCH EXPERIENCE

2003-2006: Junior Research Fellow at National Institute of Plant Genome Research, Jawaharlal Nehru University Campus, New Delhi, India.

PUBLICATIONS:

(i) **Mandal MK,** Chandra-Shekara AC, Jeong RD, Yu K, Zhu S**,** Chanda B**,** Navarre D, Kachroo A, Kachroo P. (**2012).** Oleic acid-dependent modulation of NITRIC OXIDE ASSOCATED 1 protein levels regulate nitric oxide-mediated signaling in plant defense. ***Plant Cell***, in press.

(ii) **Mandal MK,** Chanda B, Xia Y**,** Yu K, Sekine K, Gao Q, Selote D, Navarre D, Kachroo A, Kachroo P. (**2011).** Glycerol-3-phosphate in systemic signaling. ***Plant Signaling & Behavior***, **6**: 1871-1874.

(iii) Chanda B, Xia Y, **Mandal MK,** Yu K, Sekine K, Gao Q, Selote D, Hu Y, Stromberg, A, Navarre D, Kachroo A, Kachroo P. (**2011).** Glycerol-3-phosphate a

critical mobile inducer of systemic immunity in plants. ***Nature Genetics***, **43**: 421-427.

(iv) Ashraf N, Ghai D, Barman P, Basu S, Nagaraju G, **Mandal MK**, Chakraborty N, Datta A, Chakraborty S. (**2009).** Comparative analyses of genotype dependent expressed sequence tags and stress responsive transcriptome of chickpea wilt illustrates predicted and unexpected genes and novel regulators of plant immunity. ***BMC Genomics***, **10**: 415.

(v) Venugopal SC, Jeong RD, **Mandal MK**, Zhu S, Chandra-Shekara AC, Xia Y, Hersh M, Stromberg AJ, Navarre D, Kachroo A, Kachroo P. **(2009)**. Enhanced disease susceptibility 1 and salicylic acid act redundantly to regulate resistance gene-mediated signaling. ***PLoS Genetics***, **5**:e1000545.

(vi) **Mandal MK**, Pandey D, Purwar S, Singh US, Kumar A. (**2006)**. Influence of jasmonic acid as potential activator of induced resistance against karnal bunt in developing spikes of wheat. ***J Biosci***, **31**: 607–616.

MEMBERSHIP:

- International Society for Molecular Plant-Microbe Interactions (**IS-MPMI**), since 2008

- American Society of Plant Biologists (**ASPB**), since 2008

- American Phytopathological Society (**APS**), since 2009

PROFESSIONAL AWARDS AND HONORS:

- **2012,** Received Myrle E. and Verle D. Nietzel Visiting Distinguished Faculty Award by University of Kentucky.
- **2011,** Scientific image selected as the cover picture of The EMBO Journal, Vol. **30** (2011).
- **2011,** Awarded travel grant by ASPB to attend the annual meeting**.**
- **2010,** Awarded travel grant by University of Kentucky Graduate School.
- **2010,** Awarded travel grant by University of Kentucky Graduate School.
- **2009,** Awarded travel grant by University of Kentucky Graduate School.
- **2006-2012,** Graduate Research Assistant, Department of Plant Pathology, University of Kentucky.
- **2003-2006,** Awarded Junior Research Fellowship by Council of Scientific and Industrial Research, Government of India.
- **2001-2003**, Awarded M.S. fellowship by Department of Biotechnology, Government of India.
- **1997-2001**, Awarded merit scholarship during B.S. by Assam Agricultural University.

PROFESSIONAL SERVICE:

- Member of the University of Kentucky Graduate Student Congress (2009-2011).